AD-A190 033 OPTIMAL CONTROL AND IDENTIFICATION OF SPACE STRUCTURES (U) CALIFORNIA UNIV LOS ANGELES SCHOOL OF ENGINEERING AND APPLIED SCIENCE J S GIBSON 21 DEC 87 1/1

UNCLASSIFIED AFOSR-TR-88-0173 AFOSR-84-0309 F/G 22/2 NL

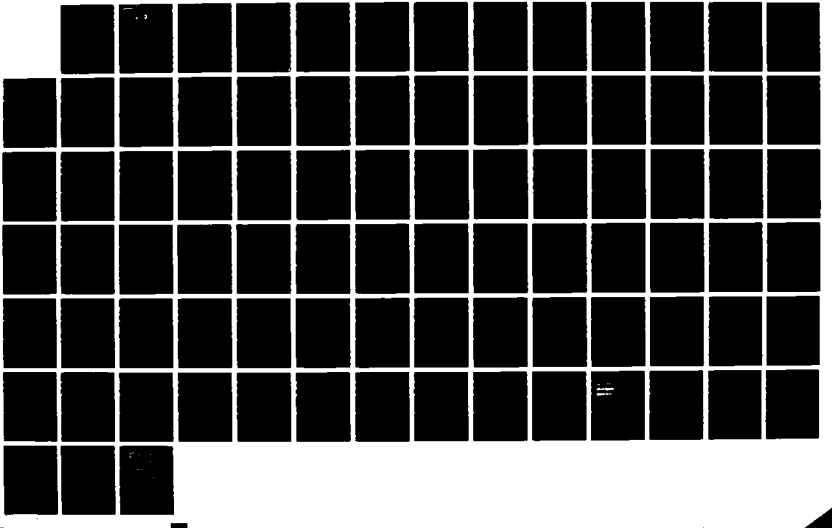

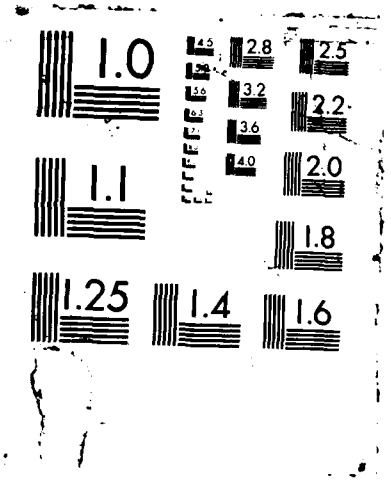
1.0
1.1
1.25
1.4
1.6
1.8
2.0
2.2
2.5
2.8
3.2
3.6
4.0

UNCLASSIFIED DTIC FILE COPY

SECURITY CLASSIFICATION OF THIS PAGE

REPORT DOCUMENTATION PAGE

Form Approved OMB No. 0704-0188

AD-A190 033 DTIC ELECTE FEB 29 1988 S D

1b. RESTRICTIVE MARKINGS	
2b. DECLASSIFICATION/DOWNGRADING SCHEDULE	3. DISTRIBUTION/AVAILABILITY OF REPORT approved for public release; distribution unlimited.
4. PERFORMING ORGANIZATION REPORT NUMBER(S)	5. MONITORING ORGANIZATION REPORT NUMBER(S) AFOSR.TR. 88-0173
6a. NAME OF PERFORMING ORGANIZATION University of California	6b. OFFICE SYMBOL (If applicable)
6c. ADDRESS (City, State, and ZIP Code) School of Engineering and Applied Science Los Angeles, California 90024	7a. NAME OF MONITORING ORGANIZATION AFOSR
8a. NAME OF FUNDING/SPONSORING ORGANIZATION AFOSR	8b. OFFICE SYMBOL (If applicable) NM
8c. ADDRESS (City, State, and ZIP Code) BLDG 410 Bolling AFB, Washington DC 20332	7b. ADDRESS (City, State, and ZIP Code) Building 410 Bolling AFB, Wahington DC 20332-0448
	9. PROCUREMENT INSTRUMENT IDENTIFICATION NUMBER AFOSR-84-0309
	10. SOURCE OF FUNDING NUMBERS

PROGRAM ELEMENT NO.	PROJECT NO.	TASK NO	WORK UNIT ACCESSION NO.
61102f	2304	A1	

11. TITLE (Include Security Classification)
Optimal Control and Indentification of Space Structures

12. PERSONAL AUTHOR(S)
J.S. Gibson

13a. TYPE OF REPORT	13b. TIME COVERED	14. DATE OF REPORT (Year, Month, Day)	15. PAGE COUNT
Final	FROM 15 Aug 84 TO 14/Dec 87	21 December 1987	

16. SUPPLEMENTARY NOTATION

17. COSATI CODES			18. SUBJECT TERMS (Continue on reverse if necessary and identify by block number)
FIELD	GROUP	SUB-GROUP	

19. ABSTRACT (Continue on reverse if necessary and identify by block number)

The focus of this research was to develop theoretical and computational tools for optimal control and adaptive parameter identification and control and adaptive parameter systems, primarily large flexible space structures Approximations results for optimal control of infinite-dimensional systems were drived along with numerical results. Also developed was an approximation theory for discrete-time optimal regulator problems, which included problems with flexible structures as a particular example.

20. DISTRIBUTION/AVAILABILITY OF ABSTRACT ☐ UNCLASSIFIED/UNLIMITED ☐ SAME AS RPT ☐ DTIC USERS	21. ABSTRACT SECURITY CLASSIFICATION
22a. NAME OF RESPONSIBLE INDIVIDUAL JAMES M CROWLEY	22b. TELEPHONE (Include Area Code) 767-5025 / 22c. OFFICE SYMBOL NM

DD Form 1473, JUN 86 Previous editions are obsolete. SECURITY CLASSIFICATION OF THIS PAGE

UNCLASSIFIED

FINAL REPORT AFOSR-TR- 88-0173

AFOSR GRANT 840309

OPTIMAL CONTROL AND IDENTIFICATION OF SPACE STRUCTURES

November 30, 1987

J.S. Gibson, Principal Investigator
Mechanical, Aerospace and Nuclear Engineering
University of California,
Los Angeles 90024

This research has dealt with optimal control and adaptive parameter identification and control of distributed systems, with primary application to large flexible space structures. The research has developed both mathematical theory and numerical methods for design of control laws and compensators for complex distributed systems like large space platforms and antennas. Approximation theory that serves as the basis for computer aided design of control systems involving partial and functional differential equations has been an especially improtant part of this research project. Also, variable-order adaptive parameter estimators and adaptive controllers have been developed for distributed systems, and the parameter estimators (lattice filters) have been applied to both numerical simulations and experimental structures.

Approximation in Optimal Control of Distributed Systems

In optimal control of distributed systems, we have studied control problems for infinite dimensional systems with quadratic performance criteria. These problems require the solution of

infinite dimensional Riccati operator equations, which must be solved numerically by large-order approximations. Approximation theory and numerical results for continuous-time optimal control are given in [1,2,16].

We have collaborated with Professor I. Gary Rosen to develop approximation theory and numerical methods for discrete-time infinite dimensional optimal regulator problems and to demonstrate the practical implications of the theory and the usefulness of the numerical methods on several examples, involving flexible structures, diffusion processes and time-delay systems [3,4,5,6,15]. In these numerical examples, we have discovered important relationships between the length of the sampling interval (the time step) and the numerical condition of the approxomating finite-dimensional discrete-time control problems.

In connection with optimal control of flexible space structures, we have investigated integrated control-structure design, by which we mean simultaneous optimal design of structure and controller. We have combined structural weight and robustness with respect to modelling errors in an overall objective functional for integrated control-structure optimization. This results in a nonlinear programming problem whose solution we have demonstrated in several numerical examples [7,8,16,17].

Adaptive Parameter Identification and Control of Distributed Systems

Another area of primary interest in this project has been adaptive parameter identification and adaptive control of distributed systems. We have studied the application of modern least-square identification schemes to infinite dimensional systems, and our most important results concern lattice filters for estimating coefficients in infinite dimensional autoregressive-moving average (ARMA) models [9,10,11,12,15].

Because lattice filters are recursive in order as well as in time, they permit the order of the model to vary adaptively as either more structural modes are excited or as higher frequency modes are damped out while lower modes remain excited. We have developed a vector-channel lattice filter [10,15], which is an extension of previous lattice filters and which is important for applications with several measurements from the same structure. With experimental data from a large and very flexible grid at the NASA Langley Research Center, we have demonstrated the effectiveness of lattice filters for adaptive identification and prediction of flexible structures [11].

We have begun developing approximation theory that will predict the performance of lattice filters with structures having various types of damping [12]. We expect such theory to be important in both adaptive identification and adaptive control of large space structures.

Also, we have incorporated our adaptive parameter estimators into variable-order adaptive control algorithms for flexible space structrues. Our main application so far has been to robotic manipulators with flexible links [13,14,18,19]. We plan to develop similar control algorithms for large flexible platforms and antennas with structure similar to the flexible grid on which [11] is based.

REFERENCES

RESEARCH PAPERS

1. J.S. Gibson and A. Adamian, "Approximation Theory for LQG Optimal Control of Flexible Structures," submitted to SIAM J. Control and Optimization.

2. J.S. Gibson and I.G. Rosen, "Shifting the Closed-loop Spectrum in the Optimal Linear-quadratic Regulator Problem for Hereditary Systems," IEEE Trans. Automatic Control, Vol. AC-32, No.9, September 1987, pp. 831-836.

3. J.S. Gibson and I.G. Rosen, "Numerical Approximation for the Infinite-Dimensional Discrete-Time Optimal Linear-Quadratic Regulator Problem," to appear in SIAM J. Control and Optimization.

4. J.S. Gibson and I.G. Rosen, "Computational Methods for Discrete-time Compensators for Distributed Systems," Invited Paper, Conference on Control and Identification of Distributed Systems, Vorau, Austria, July 1986.

5. J.S. Gibson and I.G. Rosen, "Approximation of Discrete-time LQG Compensators for Distributed Systems with Boundary Input and Unbounded Measurement," to appear in Automatica.

6. J.S. Gibson and I.G. Rosen, "Approximation in Discrete-time Boundary Control of Flexible Structures," 26th IEEE Conference on Decision and Control, Los Angeles, CA, December 1987.

7. A. Adamian and J.S. Gibson, "Sensitivity Optimization for Integrated Control/Structure Design and Robustness," submitted to Automatica.

8. J.S. Gibson and M. Navid, "Integrated Structural and Control System Design Optimization," submitted to AIAA Journal on Guidance, Control and Dynamics.

9. J.S. Gibson and F. Jabbari, "An ARMA Model for a Class of Distributed Parameter Systems," Invited Paper, IEEE Conference on Decision and Control, Las Vegas, Nevada, December 1984.

10. F. Jabbari and J.S. Gibson, "Vector-channel Lattice Filters and Identification of Flexible Structures," to appear in IEEE Trans. Automatic Control.

11. F. Jabbari and J.S. Gibson, "Adaptive Identification of Flexible Structures by Lattice Filters," AIAA

Conference on Guidance, Control and Dynamics, Monterey, CA, August 1987.

12. J.S. Gibson and F. Jabbari, "A Digital Input-output Model for Trace-class Systems," submitted to J. Math. Anal. Appl.

13. Y.-P. Yang and J.S. Gibson, "Adaptive Control of a Robotic Manipulator with a Flexible Link," in preparation, to be submitted for journal publication (based on Reference 18).

14. Y.-K. Kim and J.S. Gibson, "Adaptive Control of a Manipulator with a Sliding Flexible Link," in preparation, to be submitted for journal publication (based on Reference 19).

PHD DISSERTATIONS

15. F. Jabbari, Lattice Filters and Adaptive Identification of Flexible Structures, PhD Dissertation, UCLA, 1986.

16. A. Adamian, Integrated Control/Structure Design and Robustness, PhD Dissertation, UCLA, 1986.

17. M. Navid, Integrated Structural and Control System Design Optimization, PhD Dissertation, UCLA, 1986.

18. Y.-P. Yang, Adaptive Control of Robotic Manipulators with Flexible Links, PhD Dissertation, UCLA, 1987.

19. Y.-K. Kim, "Adaptive Control of a Manipulator with a Sliding Flexible Link," PhD Dissertation, UCLA, to be completed in January 1988.

NOTE: References 5, 6, 10 and 11 are contained in the following Appendix. Copies of the other completed research papers and the dissertations 15, 16 and 17 have been sent to AFOSR previously. Final drafts of References 13, 14, 18 and 19 will be sent to AFOSR upon completion.

APPENDIX

Approximation of Discrete-Time LQG Compensators for Distributed Systems with Boundary Input and Unbounded Measurement†

J.S. Gibson*
Department of Mechanical,
Aerospace and Nuclear Engineering
University of California, Los Angeles
Los Angeles, CA 90024

and

I.G. Rosen**
Department of Mathematics
University of Southern California
Los Angeles, CA 90089

(*)This research was supported in part by the Air Force Office of Scientific Research under contract No. AFOSR-84-0309.

(**)This research was supported in part by the Air Force Office of Scientific Research under contract No. AFOSR-84-0393.

(†)Part of this research was carried out while the authors were visiting scientists at the Institute for Computer Applications in Science and Engineering (ICASE), NASA, Langley Research Center, Hampton, VA, 23665 which is operated under NASA contracts No. NAS1-17070 and No. NAS1-18107.

ABSTRACT

We consider the approximation of optimal discrete-time linear quadratic Gaussian (LQG) compensators for distributed parameter control systems with boundary input and unbounded measurement. Our approach applies to problems that can be formulated in a state space on which both the discrete-time input and output operators are continuous. Approximating compensators are obtained via application of the LQG theory and associated approximation results for infinite dimensional discrete-time control systems with bounded input and output. Numerical results for spline and modal approximation schemes used to compute optimal compensators for a one dimensional heat equation with either Neumann or Dirichlet boundary control and pointwise measurement of temperature are presented and discussed.

1. Introduction

In this paper we develop an approximation theory for the computation of optimal discrete-time linear quadratic Gaussian (LQG) compensators (combined feedback control law and state estimator) for distributed parameter systems with boundary input or control and unbounded output or measurement. In a continuous time setting, boundary input typically results in an unbounded input operator. That is, the system's input operator maps the control input into a space larger than the state space in which the open-loop system is usually formulated. In the discrete-time case, on the other hand, for a wide class of distributed systems, the resulting input operator is bounded on the usual underlying state space. An unbounded output, or measurement, operator has domain smaller than the usual open-loop state space.

For continuous time systems, Pritchard and Salamon (1987) have established an abstract semigroup theoretic framework for treating the linear quadratic regulator problem (control only) for infinite dimensional systems with unbounded input and output operators. Their approach is based upon a weak or distributional formulation of the Riccati equations which characterize the optimal feedback control laws in an appropriate dual space . Curtain (1984) provides a procedure for the design of finite dimensional compensators for parabolic systems with unbounded control and observation. In (Curtain and Salamon, 1986) a finite dimensional compensator design procedure for a wider class of infinite dimensional systems with unbounded input (but bounded output) including hereditary systems with control delays and partial differential systems with boundary control is developed. Lasiecka and Triggiani have looked at linear regulator problems for parabolic (1983a, 1987a) and hyperbolic (1983b, 1986) systems with boundary control and obtained, among other things, global and local regularity results for the optimal controls and state trajectories. In (Lasiecka and Triggiani, 1987b) Galerkin approximations and an associated convergence theory for closed-loop solutions to regulator problems for parabolic systems with Dirichlet boundary input are studied. A more complete survey of the boundary control literature including references to some of the poineering work in this area can be found in (Pritchard and Salamon, 1987).

In our treatment here, we consider the discrete-time problem (i.e. piecewise constant input and sampled output). Our interest in the discrete-time or digital formulation is motivated by 1) the fact that it represents a more accurate or realistic description of how the linear-quadratic theory for distributed systems would actually be applied in practice, and by 2) how the boundedness of the discrete-time input operator in the usual underlying state space facilitates the development of an approximation theory which can simultaneously handle both unbounded input and unbounded output. Our approach is based upon an application of the theory we developed earlier in (Gibson and Rosen, 1985 and 1986) for the approximation of optimal discrete-time LQG compensators for infinite dimensional systems with bounded input and output. Our results are applicable to boundary control systems in which a restriction of the state transition operator and the discrete-time input operator are bounded on a space on which the output operator is bounded as well. To illustrate our approach, in this paper we describe in detail the application of our theory to a one dimensional heat equation with either Neumann or Dirichlet boundary control and pointwise measurement of temperature. Elsewhere (see Gibson and Rosen, 1987) we have applied our results to develop approximation schemes for the computation of optimal LQG compensators for flexible structures (i.e. Euler-Bernoulli beams) with shear force input at the boundary and a pointwise measurement of strain.

An outline of the remainder of the paper is as follows. In Section 2 we describe an abstract framework for the study of boundary control systems and their discrete-time formulation. In Section 3 we review the LQG theory for infinite dimensional discrete-time systems and associated abstract approximation results. In the fourth section, we discuss spline and modal subspace based approximation schemes for the heat equation example. Section 5 contains some concluding remarks.

2. The Boundary Control System and its Discrete-Time Formulation

We employ a semigroup theoretic formulation that has been used previously for a class of abstract boundary control systems. See, for example, (Curtain and Salamon, 1986). Let W,V and H be Hilbert spaces with W and V densely and continuously embedded in H. We

consider boundary control systems of the form

(2.1) $\dot{w}(t) = \Delta w(t), \qquad t > 0$

(2.2) $w(0) = w_0$

(2.3) $\Gamma w(t) = v(t), \qquad t \geq 0$

(2.4) $y(t) = Cw(t), \qquad t \geq 0$

where $\Delta \in \mathfrak{L}(W,H)$, the boundary input operator Γ is an element in $\mathfrak{L}(W,R^m)$ and the output operator C is an element in $\mathfrak{L}(V,R^p)$. Note that the operator Δ need not be the Laplacian. Our choice of Δ to denote a general, most often differential, operator satisfying the conditions set forth below is consistent with the notation used in earlier treatments of boundary control systems elsewhere in the literature.

We assume that 1) Γ is surjective and its null space, $\mathfrak{N}(\Gamma) = \{\varphi \in W: \Gamma\varphi = 0\}$, is dense in H, 2) the operator $\mathcal{A}$, defined to be the restriction of the operator Δ to $\mathfrak{N}(\Gamma)$, is a closed operator on H and has non-empty resolvent set and 3) for each $T > 0$, all $w_0 \in W$, and $v \in C^1(0,T; R^m)$ with $\Gamma w_0 = v(0)$, there exists a unique $w \in C([0,T]; W) \cap C^1([0,T]; H)$ which depends continuously on w_0 and v and which satisfies (2.1) - (2.3) for each $t \in [0,T]$. It then follows (see Hille and Phillips, 1957) that the operator $\mathcal{A} : \text{Dom}(\mathcal{A}) \subset H \to H$ given by $\mathcal{A}\varphi = \Delta\varphi$ for $\varphi \in \text{Dom}(\mathcal{A}) = \mathfrak{N}(\Gamma)$ is the infinitesimal generator of a $\mathcal{C}_0$ semigroup, $\{\mathcal{T}(t) : t \geq 0\}$, of bounded linear operators on H.

Define the space Z as the dual of $\text{Dom}(\mathcal{A}^*)$ where the norm on $\text{Dom}(\mathcal{A}^*)$ is taken to be the graph Hilbert space norm associated with the operator $\mathcal{A}^*$. Then H is densely and continuously embedded in Z and $\{\mathcal{T}(t) : t \geq 0\}$ can be uniquely extended to a $\mathcal{C}_0$ semigroup of bounded linear operators on Z. Its generator is the extension of the operator $\mathcal{A}$ to an the operator $\hat{\mathcal{A}}$ in $\mathfrak{L}(H,Z)$ given by $(\hat{\mathcal{A}}\varphi)(\psi) = \langle\varphi, \mathcal{A}^*\psi\rangle_H$ for $\varphi \in H$ and $\psi \in \text{Dom}(\mathcal{A}^*)$.

Since Γ was assumed to be a surjection, it has a right inverse. Let $\Gamma^+ : R^m \to W$ be any right inverse of Γ. Since $\text{Dom}(\Gamma^+) = R^m$, we have $\Gamma^+ \in \mathfrak{L}(R^m, W)$. For $v \in R^m$, we define $\mathfrak{B} \in \mathfrak{L}(R^m, Z)$ by $\mathfrak{B}v = (\Delta - \hat{\mathcal{A}})\Gamma^+ v$. If Γ_1^+ and Γ_2^+ are two distinct right inverses of Γ then $\mathfrak{R}(\Gamma_1^+ - \Gamma_2^+) \subset \mathfrak{N}(\Gamma)$. Since $\hat{\mathcal{A}}$ coincides with Δ on $\mathfrak{N}(\Gamma)$, it follows that the operator $\mathfrak{B}$ is

well defined. It can be shown (see Curtain and Salamon, 1986) that for each $w_0 \in H$ and $v \in L_2(0,T; R^m)$ there exists a unique $w \in C([0,T]; H) \cap H^1(0,T; Z)$ which depends continuously on w_0 and v and which satisfies

$$\dot{w}(t) = \mathcal{A}w(t) + \mathcal{B}v(t), \quad t > 0$$
$$w(0) = w_0$$

in Z. The function w is given by

$$(2.5) \quad w(t) = \mathcal{T}(t)w_0 + \int_0^t \mathcal{T}(t-s)\,\mathcal{B}v(s)ds, \quad t \geq 0$$

and is referred to as a weak solution to the boundary control system (2.1) - (2.3).

The discrete-time formulation of (2.1) - (2.4) is found by considering piecewise-constant controls of the form

$$(2.6) \quad v(t) = u_k, \quad t \in [k\tau, (k+1)\tau), \quad k = 0,1,2,...$$

where τ denotes the length of the sampling interval. Let $w_k = w(k\tau)$, $k = 0,1,2,...$ where $w(\cdot)$ is the unique weak solution to (2.1) - (2.3) given by (2.5) corresponding to $w_0 \in H$ and input v given by (2.6). (We note that with piecewise constant input of the form (2.6), the solution w is in fact a strong solution on each subinterval $[k\tau, (k+1)\tau]$.) For each $k = 0,1,2,...$ define $z_k \in C([k\tau, (k+1)\tau]; H)$ by $z_k(t) = w(t) - \Gamma^+ u_k$, $t \in [k\tau, (k+1)\tau]$. Then

$$\begin{aligned}
\dot{z}_k(t) = \dot{w}(t) &= \mathcal{A}w(t) + \mathcal{B}u_k \\
&= \mathcal{A}z_k(t) + (\mathcal{A} + \mathcal{B}\Gamma)\Gamma^+ u_k \\
&= \mathcal{A}z_k(t) + \Delta\,\Gamma^+ u_k, \quad t \in (k\tau, (k+1)\tau], \\
z_k(k\tau) &= w_k - \Gamma^+ u_k .
\end{aligned}$$

Therefore

$$w_{k+1} = z_k((k+1)\tau) + \Gamma^+ u_k$$
$$= \mathcal{T}(\tau)(w_k - \Gamma^+ u_k) + \int_0^\tau \mathcal{T}(s)\,\Delta\,\Gamma^+ u_k\,ds + \Gamma^+ u_k$$
$$= \mathcal{T}(\tau) w_k + (I - \mathcal{T}(\tau))\,\Gamma^+ u_k + \int_0^\tau \mathcal{T}(s)\Delta\Gamma^+ u_k ds,$$

or

$$w_{k+1} = Tw_k + Bu_k, \quad k = 0,1,2,...$$
$$w_0 \in H$$

where $T \in \mathcal{L}(H)$ and $B \in \mathcal{L}(R^m, H)$ are given by $T = \mathcal{T}(\tau)$ and $B = (I - \mathcal{T}(\tau))\,\Gamma^+ + \int_0^\tau \mathcal{T}(s)\Delta\Gamma^+ ds$ respectively.

We note that as in the case of the continuous-time input operator $\mathcal{B}$, the discrete-time input operator B is well defined and does not depend upon a particular choice for Γ^+. Indeed if B_1 and B_2 are the input operators which correspond to the choices Γ_1^+ and Γ_2^+ then for $u \in R^m$ we have

$$(B_1 - B_2)u = (I - \mathcal{T}(\tau))(\Gamma_1^+ - \Gamma_2^+)u + \int_0^\tau \mathcal{T}(s)\Delta\,(\Gamma_1^+ - \Gamma_2^+)uds.$$

But $(\Gamma_1^+ - \Gamma_2^+)u \in \mathcal{N}(\Gamma) = \mathrm{Dom}(\mathcal{A})$ and therefore

$$\int_0^\tau \mathcal{T}(s)\Delta(\Gamma_1^+ - \Gamma_2^+)uds = \int_0^\tau \mathcal{T}(s)\,\mathcal{A}(\Gamma_1^+ - \Gamma_2^+)\,uds$$

$$= \int_0^\tau \frac{d}{ds}\,\mathcal{T}(s)(\Gamma_1^+ - \Gamma_2^+)uds = (\mathcal{T}(\tau) - I)(\Gamma_1^+ - \Gamma_2^+)\,u\,.$$

In addition, if Γ^+ is chosen so that $\mathcal{R}(\Gamma^+) \subset \mathcal{N}(\Delta)$, B takes on the particularly simple form $B = (I - \mathcal{T}(\tau))\Gamma^+$. It is worth noting that a simple calculation reveals that

$$B = \int_0^\tau \mathcal{T}(s)\,\mathcal{B}ds$$

in agreement with the standard technique for obtaining the discrete or sampled time formulation of a continuous time system in either a finite dimensional or bounded input setting.

It is our intention here to apply the approximation theory we developed earlier in (Gibson and Rosen, 1986) for the design of optimal discrete-time LQG compensators for infinite dimensional systems with bounded input and output operators. We therefore require the additional assumptions that 4) $T = \mathcal{T}(\tau) \in \mathcal{L}(V)$ and 5) $\mathcal{R}(\Gamma^+) \subset V$. Although not all boundary control systems we might formulate would satisfy these conditions, there are many interesting and important systems which do (see, for example, Section 4 below and Gibson and Rosen, 1987). In this case, the control system (2.1) - (2.4) takes the form

$$w_{k+1} = Tw_k + Bu_k, \quad k = 0,1,2,... \tag{2.7}$$

$$w_0 \in V \tag{2.8}$$

$$y_k = Cw_k, \quad k = 0,1,2,... \ . \tag{2.9}$$

3. LQG Theory for Infinite Dimensional Discrete-Time Systems and Finite Dimensional Approximation

3.1. The Infinite Dimensional Probelm

The discrete-time linear-quadratic regulator problem for the boundary control system (2.1) - (2.3) is:

Find $u^* = \{u^*_k\}_{k=0}^{\infty} \in \ell_2(0, \infty; R^m)$ which minimizes the quadratic performance index

$$J(u) = \sum_{k=0}^{\infty} \langle Qw_k, w_k \rangle_V + u_k^T Ru_k$$

where $Q \in \mathcal{L}(V)$ is self-adjoint and nonnegative, R is a symmetric positive definite m×m matrix and the state $w = \{w_k\}_{k=0}^{\infty}$ evolves according to the recurrence (2.7), (2.8).

An optimal control exists for each initial condition w_0 if and only if the operator algebraic Riccati equation

$$\Pi = T^*(\Pi - \Pi B(R + B^*\Pi B)^{-1}B^*\Pi)T + Q \ . \tag{3.1}$$

has a bounded nonnegative, self-adjoint solution Π. In this case, the optimal control has the feedback form $u_k = -Fw_k$ where $F = (R + B^* \Pi B)^{-1} B^* \Pi T$. A control (sequence) u is admissible for the initial condition w_0 if the corresponding J(u) is finite. If there exists an admissible control for each initial condition, then (3.1) has a bounded nonnegative, self-adjoint solution. If each admissible control for each initial condition drives the state to zero asymptotically, then there exists at most one bounded nonnegative, self-adjoint solution to (3.1). The optimal trajectory $w^* = \{w^*_k\}_{k=0}^{\infty}$ evolves according to $w^*_k = S^k w_0$, $k = 0,1,2,...$, where the closed loop state transition operator $S \in \mathcal{L}(V)$ is $S = T - BF$. If Q is coercive, then S has spectral radius less than one and is uniformly exponentially stable. From the finite dimensionality of the control space we obtain

$$u^*_k = - \langle f, w^*_k \rangle_V , \quad k = 0,1,2,... \tag{3.2}$$

where $f = (f_1, f_2, ..., f_m)^T \in \times_{j=1}^{m} V$ is called the optimal functional feedback control gain.

The results stated here for the optimal linear-quadratic regulator problem are summarized from (Gibson and Rosen, 1985).

When only a finite dimensional measurement $y = \{y_k\}_{k=0}^{\infty}$ of the infinite dimensional state w is available (recall (2.9)), a state estimator or observer is required. For a given input sequence u and corresponding output sequence y, the optimal LQG estimator is

$$\hat{w}_{k+1} = T\hat{w}_k + Bu_k + \hat{F}\{y_k - C\hat{w}_k\}, \quad k = 0,1,2,... \tag{3.3}$$

$$\hat{w}_0 \in V \tag{3.4}$$

where the optimal estimator or observer gain $\hat{F} \in \mathcal{L}(R^p, V)$ is $\hat{F} = T \hat{\Pi} C^* (\hat{R} + C \hat{\Pi} C^*)^{-1}$ with $\hat{\Pi} \in \mathcal{L}(V)$ the minimal, self-adjoint, nonnegative solution (if one exists) to the operator algebraic Riccati equation

$$\hat{\Pi} = T(\hat{\Pi} - \hat{\Pi} C^* (\hat{R} + C \hat{\Pi} C^*)^{-1} C \hat{\Pi}) T^* + \hat{Q} . \tag{3.5}$$

Since $\hat{F} \in (R^p, V)$, it has the representation

$$\hat{F}y = \hat{f}^T y \ , \quad y \in R^p$$

where $\hat{f} = (f_1, f_2, ..., f_p)^T \in \times_{j=1}^{p} V$ is called the optimal functional observer gain. The operator $\hat{Q} \in \mathcal{L}(V)$ is self-adjoint, nonnegative and the p×p matrix $\hat{R}$ is symmetric, positive definite.

In a stochastic setting, the operator $\hat{Q}$ and the matrix $\hat{R}$ are, respectively, the covariance operator and covariance matrix for uncorrelated, zero-mean, stationary, Gaussian white noise processes that force the state and corrupt the measurement. In this case, if $\hat{Q}$ is trace class, (3.3), (3.4) is the infinite dimensional analog of the discrete-time Kalman-Bucy filter. In a strictly deterministic setting, $\hat{Q}$ and $\hat{R}$ are assumed to be determined via engineering design criteria such as stability margins, robustness of the closed-loop system, etc.

Replacing operators in the control problem with the adjoints of the appropriate operators in the estimator problem yields the usual duality between the LQG optimal control and estimator problems. Hence sufficient conditions for existence and uniqueness of solutions of (3.5) and the closed-loop estimator stability properties are analogous to the results for the control problem. In particular, if $e_k = \hat{w}_k^* - w_k$, then $e_k = \hat{S}^k e_0$, k = 0, 1,2, ..., where $\hat{S} = T - \hat{F}C$, and a sufficient condition for $\hat{S}$ to be uniformly exponentially stable is that $\hat{Q}$ be coercive.

The optimal LQG compensator consists of the state estimator in (3.3) and (3.4) and the control law

(3.6) $$\hat{u}_k^* = -F \hat{w}_k^* , \ k = 0,1,2,...$$

The resulting closed-loop system is given by

$$\mathcal{W}_k = \mathcal{A}^k \mathcal{W}_0, \quad k = 0,1,2,...$$

where $\mathcal{W}_k = (w_k, \hat{w}^*_k)^T$ with $\{w_k\}^*_{k=0}$ the state trajectory that results from the input (3.6) and $\mathcal{A} \in \mathcal{L}(V \times V)$ is

$$\mathcal{A} = \begin{bmatrix} T & -BF \\ \hat{F}C & T-BF-\hat{F}C \end{bmatrix} .$$

It is easy to show that the spectrum of $\mathcal{A}$ is given by $\sigma(\mathcal{A}) = \sigma(S) \cup \sigma(\hat{S})$, so that the stability of the closed-loop plant-compensator system is determined by the stability of the plant with full state feedback and the stability of the estimator error.

3.2. Approximation

For each N = 1,2,..., let V_N be a finite dimensional subspace of V and let P_N be a bounded linear mapping from V onto V_N (for example, the orthogonal projection with respect to either the V or H inner product). Let T_N, Q_N, $\hat{Q}_N \in \mathfrak{L}(V_N)$, $B_N \in \mathfrak{L}(R^m, V_N)$ and $C_N \in \mathfrak{L}(V_N, R^p)$ and set

$$F_N = (R + B_N^* \Pi_N B_N)^{-1} B_N^* \Pi_N T_N$$

and

$$\hat{F}_N = T_N \hat{\Pi}_N C_N^* (\hat{R} + C_N \hat{\Pi}_N C^*_N)^{-1}$$

where Π_N and $\hat{\Pi}_N$ are the minimal, self-adjoint, nonnegative solutions (assuming that they exist) to the finite dimensional operator algebraic Riccati equations

$$\Pi_N = T_N^* (\Pi_N - \Pi_N B_N (R + B_N^* \Pi_N B_N)^{-1} B_N^* \Pi_N) T_N + Q_N \tag{3.7}$$

and

$$\hat{\Pi}_N = T_N (\hat{\Pi}_N - \hat{\Pi}_N C_N^* (\hat{R} + C_N \hat{\Pi}_N C_N^*)^{-1} C_N \hat{\Pi}_N) T_N^* + \hat{Q}_N \tag{3.8}$$

respectively. The approximating optimal compensator is given by

$$\hat{u}^*_{N,k} = -F_N \hat{w}^*_{N,k} , k = 0,1,2,..$$

where $\hat{w}^*_N = \{\hat{w}^*_{N,k}\}_{k=0}^{\infty}$ is determined according to the approximating observer

$$\hat{w}^*_{N,k+1} = T_N \hat{w}^*_{N,k} + B_N \hat{u}^*_{N,k} + \hat{F}_N(y^*_{N,k} - C_N \hat{w}^*_{N,k}), \quad k = 0,1,2...$$
$$\hat{w}^*_{N,0} = P_N \hat{w}_0 \in V_N .$$

The measurements y^*_N are given by $y^*_{N,k} = Cw_{N,k}$, $k = 0,1,2,...$ where

$$w_{N,k+1} = Tw_{N,k} - B\hat{u}^*_{N,k}, \quad k = 0,1,2,...$$
$$w_{N,0} = w_0 .$$

The resulting closed-loop system is given by $\mathcal{W}_{N,k} = \mathcal{A}_N^k \mathcal{W}_{N,0}$, $k = 0,1,2,...$ where $\mathcal{W}_{N,k} = (w_{N,k}, \hat{w}^*_{N,k})^T$ and $\mathcal{A}_N \in \mathfrak{L}(V \times V_N)$ is given by

$$\mathcal{A}_N = \begin{bmatrix} T & -BF_N \\ \hat{F}_N C & T_N - B_N F_N - \hat{F}_N C \end{bmatrix} . \tag{3.9}$$

Let $S_N = T_N - B_N F_N$ and $\hat{S}_N = T_N - \hat{F}_N C_N$ and assume that $P_N \to I$ strongly on V as $N \to \infty$. Assume further that $T_N P_N \to T$, $T^*_N P_N \to T^*$, $Q_N P_N \to Q$ and $\hat{Q}_N P_N \to \hat{Q}$ strongly on V and that $B_N \to B$ and $C_N P_N \to C$ in norm as $N \to \infty$. If the pairs (T_N, B_N) and (T^*_N, C^*_N) are uniformly exponentially stabilizable and the pairs (T_N, Q_N) and $(T^*_N, \hat{Q}_N)$ are detectable (see Kwakernaak and Sivan, 1972) then there exist unique, self-adjoint, nonnegative solutions Π_N and $\hat{\Pi}_N$ to the algebraic Riccati equations (3.1) and (3.5). If Π_N and $\hat{\Pi}_N$ are bounded from above uniformly in N, then $\Pi_N P_N$ and $\hat{\Pi}_N P_N$ converge weakly to Π and $\hat{\Pi}$, respectively, as $N \to \infty$.

If, in addition, S_N and $\hat{S}_N$ are uniformly exponentially stable, uniformly with respect to N, then $\Pi_N P_N$ and $\hat{\Pi}_N P_N$ converge strongly. Weak convergence of $\Pi_N P_N$ to Π yields strong convergence of $F_N P_N$ to F and $S_N P_N$ to S. If $\Pi_N P_N$ converges strongly then $F_N P_N \to F$ in

norm. Weak convergence of $\hat{\Pi}_N P_N$ to $\hat{\Pi}$ yields weak convergence of $\hat{F}_N$ to $\hat{F}$ and $\hat{S}_N P_N$ to $\hat{S}$. When $\hat{\Pi}_N P_N \to \hat{\Pi}$ strongly, then $\hat{F}_N \to \hat{F}$ in norm and $\hat{S}_N P_N \to \hat{S}$ strongly in V as $N \to \infty$. Finally, if $\mathcal{P}_N$ is the mapping of V×V onto $V \times V_N$ given by $\mathcal{P}_N(w_1, w_2) = (w_1, P_N w_2)$, then $\Pi_N P_N \to \Pi$ weakly or strongly is sufficient to conclude that $\mathcal{A}_N \mathcal{P}_N \to \mathcal{A}$ weakly or strongly depending only upon whether $\hat{\Pi}_N P_N \to \hat{\Pi}$ weakly or strongly as $N \to \infty$. Under appropriate additional hypotheses on the spectral properties of the open-loop system and on the approximation scheme, it is possible to show that $\mathcal{A}_N \mathcal{P}_N$ converges to $\mathcal{A}$ in norm. (We have been able to obtain such a result only for modal approximations.) Norm convergence of the closed-loop state transition operators is sufficient to conclude that uniform exponential stability of $\mathcal{A}$ implies uniform exponential stability of $\mathcal{A}_N$ for all N sufficiently large (see Gibson and Rosen 1986).

In practice, the finite dimensional approximating subspaces V_N are often constructed using any of a number of common finite element bases, e.g. polynomial and hermite spline functions, mode shapes, orthogonal polynomials, etc. For the discrete-time boundary control systems of interest to us here, the approximations to T and B, T_N and B_N, are obtained by approximating the continuous time semigroup, $\{\mathcal{T}(t) : t \geq 0\}$, by a semigroup of bounded linear operators on V_N, $\{\mathcal{T}_N(t): t \geq 0\}$. In fact it is the infinitesimal generator $\mathcal{A}$ of the semigroup $\{\mathcal{T}(t): t \geq 0\}$ that is approximated by a bounded linear operator $\mathcal{A}_N$ on V_N with $\{\mathcal{T}_N(t): t \geq 0\}$ then being defined by $\mathcal{T}_N(t) = \exp(\mathcal{A}_N t)$, $t \geq 0$. With $T_N = \mathcal{T}_N(\tau)$ and $B_N = (I - \mathcal{T}_N(\tau))P_N\Gamma^+ + \int_0^\tau \mathcal{T}_N(s)P_N\Delta\Gamma^+ ds$, the required convergence can usually be proved using the Trotter-Kato semigroup approximation result (see (Kato, 1966) and (Pazy, 1983)). The approximations to Q, $\hat{Q}$ and C, Q_N, $\hat{Q}_N$ and C_N, respectively, typically are taken to be $Q_N = P_N Q$, $\hat{Q}_N = P_N \hat{Q}$ and $C_N = CP_N$.

Let $\{\varphi_j^N\}_{j=1}^{n_N}$ denote a basis for V_N and set $\Phi^N = (\varphi_1^N, \varphi_2^N, \ldots, \varphi_{n_N}^N)^T \in \prod_{j=1}^{n_N} V_N$.

Adopting the convention that [L] denotes the matrix representation with respect to the basis $\{\varphi_j^N\}_{j=1}^{n_N}$ for a linear operator L with domain and/or range in V_N, we find that $[F_N] = (R + [B_N]^T \Theta^N [B_N])^{-1}[B_N]^T \Theta^N [T_N]$ and $[\hat{F}_N] = [T_N]\hat{\Theta}^N[C_N]^T(\hat{R} + [C_N]\hat{\Theta}^N[C_N]^T)^{-1}$ where Θ^N and $\hat{\Theta}^N$ are the unique, symmetric, nonnegative solutions to the $n_N \times n_N$ matrix algebraic Riccati equations

(3.10) $$\Theta^N = [T_N]^T (\Theta^N - \Theta^N[B_N](R + [B_N]^T \Theta^N[B_N])^{-1}[B_N]^T \Theta^N)[T_N] + M^N[Q_N]$$

and

(3.11) $$\hat{\Theta}_N = [T_N](\hat{\Theta}^N - \hat{\Theta}^N[C_N]^T(\hat{R} + [C_N]\Theta^N[C_N]^T)^{-1}[C_N]\Theta^N)[T_N]^T + [\hat{Q}_N](M^N)^{-1} .$$

The matrix M^N is the $n_N \times n_N$ Gram matrix $<\Phi^N, (\Phi^N)^T>_V$.

If $\hat{w}^*_{N,k} = (\Phi^N)^T \hat{W}^*_{N,k}$ with $\hat{W}^*_{N,k} \varepsilon R^{n_N}$, then $\hat{u}^*_{N,k} = -[F_N] \hat{W}^*_{N,k}$, $k = 0,1,2,...$ with

$$\hat{W}^*_{N,k+1} = [T_N] \hat{W}^*_{N,k} + [B_N] \hat{u}^*_{N,k} + [\hat{F}_N]\{\hat{y}^*_{N,k} - [C_N] \hat{W}^*_{N,k}\}, \quad k = 0,1,2,...$$

$$\hat{W}^*_{N,0} = (M^N)^{-1} <\Phi^N, \hat{w}_0>_V .$$

The approximating optimal functional feedback control gain, $f^N = (f^N_1, f^N_2,..., f^N_m)^T \varepsilon \times_{j=1}^{m} V_N$ are given by $f^N = [F_N](M^N)^{-1}\Phi^N$ and the approximating optimal functional observer gain $\hat{f}^N = (\hat{f}^N_1, \hat{f}^N_2,..., \hat{f}^N_p)^T \varepsilon \times_{j=1}^{p} V_N$ by $\hat{f} = [\hat{F}_N]^T\Phi^N$. If $\Pi_N P_N \rightarrow \Pi$ weakly (strongly) then $f^N_i \rightarrow f_i$, $i = 1,2,..., m$ weakly (strongly) in V. If $\hat{\Pi}_N P_N \rightarrow \hat{\Pi}$ weakly (strongly) then $f^N_i \rightarrow f_i$, $i = 1,2,..., p$ weakly (strongly) in V. If the injection $V \subset H$ is compact, then $f^N_i \rightarrow f_i$, $i = 1,2,..., m$ and $\hat{f}^N_i \rightarrow \hat{f}_i$, $i = 1,2,...,p$ strongly in H if $\Pi_N P_N$ and $\hat{\Pi}_N P_N$ converge only weakly.

4. Examples and Numerical Results

We consider the one-dimensional heat equation

(4.1) $$\frac{\partial w}{\partial t}(t,x) = a \frac{\partial^2 w}{\partial x^2}(t,x), \qquad 0 < x < 1, \qquad t > 0,$$

where $a > 0$, with the homogeneous Dirichlet boundary condition ,

$$(4.2) \qquad w(t,0) = 0, \quad t > 0,$$

and either the Neumann boundary control

$$(4.3) \qquad \frac{\partial w}{\partial x}(t,1) = v(t), \qquad t > 0,$$

or the Dirichlet boundary control

$$(4.4) \qquad w(t, 1) = v(t), \quad t > 0,$$

where $v \in L_2(0, \infty)$. For output we take a temperature measurement

$$(4.5) \qquad y(t) = w(t, \zeta), \qquad t \geq 0,$$

at some fixed point $\zeta \in (0, 1)$. Initial conditions for these systems have the form

$$(4.6) \qquad w(0, x) = w_0(x), \qquad 0 \leq x \leq 1$$

where $w_0 \in L_2(0, 1)$.

Although the two control systems above appear to be similar, they are, in fact, quite different and must be treated separately. We begin with the more straight forward of the two, Neumann boundary control. Let $H = L_2(0, 1)$, $V = H^1_L(0, 1) = \{\varphi \in H^1(0, 1) : \varphi(0) = 0\}$ and $W = H^2(0, 1) \cap H^1_L(0, 1)$. With H endowed with the usual L_2 inner product, V with the inner product $\langle \varphi, \psi \rangle_V = \int_0^1 D\varphi\, D\psi$ and W with the inner product $\langle \varphi, \psi \rangle_W = \sum_{j=1}^{2} \int_0^1 D^j \varphi\, D^j \psi$, we have the continuous and dense embeddings $W \subset V \subset H \subset V' \subset W'$. Define $\Delta \in \mathfrak{L}(W, H)$, $\Gamma \in \mathfrak{L}(W, R^1)$ by $\Delta \varphi = a D^2\varphi$, $\Gamma\varphi = D\varphi(1)$ and $C\varphi = \varphi(\zeta)$ respectively. With these definitions the boundary

control system (4.1) - (4.3), (4.5), (4.6) has the form (2.1) - (2.4). The operator $\mathcal{A}$: Dom $(\mathcal{A}) \subset H \to H$ is given by $\mathcal{A}\varphi = a D^2\varphi$ for $\varphi \in \{\varphi \in H^2(0, 1): \varphi(0) = D\varphi(1)) = 0\}$. It is densely defined, negative definite, self-adjoint and it is the infintesimal generator of a uniformly exponentially stable analytic semigroup $\{\mathcal{T}(t): t \geq 0\}$ of bounded, self-adjoint linear operators on H. Also, $\{\mathcal{T}(t): t \geq 0\}$ is a uniformly exponentially stable, analytic semigroup of bounded, self-adjoint operators on V with generator $\tilde{\mathcal{A}}$ given by $\tilde{\mathcal{A}}\varphi = \mathcal{A}\varphi$ for $\varphi \in \{\varphi \in H^3(0, 1): \varphi(0) = D\varphi(1) = D^2\varphi(0) = 0\}$. Choosing $\Gamma^+ \in \mathfrak{L}(R^1, W)$ as $(\Gamma^+u)(x) = xu$ for $x \in [0, 1]$, we have $\mathcal{R}(\Gamma^+) \subset V$, $\mathcal{R}(\Gamma^+) \subset \mathcal{D}(\Delta)$ and that conditions 1) -5) given in Section 2 are satisfied. For the optimal control and estimator problems, we take $Q = qI$, $\hat{Q} = \hat{q} I$, $R = r$ and $\hat{R} = \hat{r}$ where I is the identity on V, $q, \hat{q} \geq 0$ and $r, \hat{r} > 0$. The uniform exponential stability of the semigroup $\{\mathcal{T}(t): t \geq 0\}$ on V implies that the algebrai Riccati equations (3.1) and (3.5) admit unique bounded, nonnegative, self-adjoint solutions Π and $\hat{\Pi}$ respectively. The optimal control (3.2) takes the form

$$u_k^* = -\int_0^1 Df\, Dw_k^*, \qquad k = 0,1,2,... \tag{4.7}$$

where the optimal functional feedback control gain f and the optimal functional observer gain $\hat{f}$ are elements in $H_L^1(0,1)$.

We construct an approximation scheme using a linear spline based Ritz-Galerkin approach. For each $N = 1,2,...$, $\{\varphi_j^N\}_{j=0}^N$ denotes the usual linear spline or "hat" functions defined on the interval [0,1] with respect to the uniform mesh $\{0, 1/N, 2/N,...,1\}$. We discard the element centered at $x = 0$, φ_0^N, set $V_N = \text{span}\,\{\varphi_j^N\}_{j=1}^N$ and choose P_N to be the orthogonal projection of V onto V_N with respect to the V inner product. Hence V_N is an N dimensional subspace of V.

For $\varphi \in \text{Dom}(\mathcal{A})$, $|\mathcal{A}\varphi|_H \geq a|\varphi|_V \geq a|\varphi|_H$ and therefore $0 \in \rho(\mathcal{A})$ and $\mathcal{A}^{-1}: H \to \text{Dom}(\mathcal{A})$ satisfies $|\mathcal{A}^{-1}\varphi|_V \leq a^{-1}|\varphi|_H$ for $\varphi \in H$. We define $\mathcal{A}_N: V_N \to V_N$ as the inverse of the operator $\mathcal{A}_N^{-1} = P_N\mathcal{A}^{-1}$ restricted to V_N. The operator $-\mathcal{A}_N^{-1}$ is positive definite because $\langle \mathcal{A}_N^{-1}\varphi_N, \varphi_N\rangle_V = -a^{-1}|\varphi_N|_H^2$ for $\varphi_N \in V_N$, and it is self-adjoint since $\langle \mathcal{A}_N^{-1}\varphi_N, \psi_N\rangle_V = \langle P_N\mathcal{A}^{-1}\varphi_N, \psi_N\rangle_V = \langle \mathcal{A}^{-1}\varphi_N, \psi_N\rangle_V = a^{-1}\langle \varphi_N, \psi_N\rangle_H$. Hence the operator $\mathcal{A}_N$ is well defined and self-adjoint. For $\varphi_N \in V_N$ and $\psi_N = \mathcal{A}_N\varphi_N$, the estimate

$$< \mathcal{A}_N\varphi_N,\varphi_N>_V = < \psi_N,\mathcal{A}_N^{-1}\psi_N>_V = -a^{-1}|\psi_N|_H^2$$
$$\leq -a|\mathcal{A}^{-1}\psi_N|_V^2 \leq -a\,|P_N\mathcal{A}^{-1}\psi_N|_V^2 = -a|\mathcal{A}_N^{-1}\psi_N|_V^2$$
$$= -a\,|\varphi_N|_V^2$$

implies that $\mathcal{A}_N$ is the infinitesimal generator of a $\mathcal{C}_0$ semigroup $\{\mathcal{T}_N(t) : t \geq 0\}$ of bounded, self-adjoint linear operators on V_N satisfying $|\mathcal{T}_N(t)| \leq e^{-a\,t}$, $t \geq 0$.

It can be shown that $a<\varphi , \psi>_V = <(-\mathcal{A})^{1/2}\varphi, (-\mathcal{A})^{1/2}\psi>_H$. It then follows that the matrix representation for the operator $\mathcal{A}_N$ with respect to the basis $\{\varphi_j^N\}_{j=1}^{n_N}$ is $[\mathcal{A}_N] = -a< \varphi_i^N, \varphi_j^N>_H^{-1} < \varphi_i^N, \varphi_j^N>_V$. This agrees with the system matrix derived by a standard Ritz-Galerkin finite element approach. Note that even though $\mathcal{A}_N$ is defined to be the inverse of the operator $P_N(\mathcal{A})^{-1}$ restricted to the space V_N, computing its matrix representation does not require either $\mathcal{A}^{1/2}$ or $\mathcal{A}^{-1}$ explicitly. In general, the same approach can be used to obtain an operator representation for the Ritz Galerkin approximation to any self-adjoint coercive operator.

Let $\mathcal{I}_N$ denote the interpolation operator from V onto V_N defined by $(\mathcal{I}_N\varphi)(j/N) = \varphi(j/N)$, j = 1, 2,..., N. Then for $\varphi \in W$, elementary approximation properties of linear interpolatory spline functions (see (Schultz, 1971)) imply

$$|(P_N - I)\varphi|_V \leq |(\mathcal{I}_N - I)\varphi|_V \leq \frac{1}{N\pi}\,|D^2\varphi|_H$$

and therefore, since W is dense in V, that $P_N \to I$ strongly on V as $N\to\infty$. Also, it follows that $\mathcal{A}_N^{-1} = P_N\mathcal{A}^{-1} \to \mathcal{A}^{-1}$ strongly on V as $N\to\infty$. If we define $T_N = \mathcal{T}_N(\tau)$, then the Trotter-Kato approximation theorem yields that $T_NP_N \to T$ strongly on V as $N\to\infty$ and, since $T^* = T = \mathcal{T}(\tau)$ and $T_N^* = T_N = \mathcal{T}_N(\tau)$ that $T_N^*P_N \to T^*$ strongly on V as $N\to\infty$.

Since $\mathcal{R}(\Gamma^+) \subset V_N$ (recall that $(\Gamma^+u)(x) = ux$, $0 \leq x \leq 1$), we define the approximating input operators B_N by $B_N = (I - \mathcal{T}_N(\tau))\Gamma^+$ and set $Q_N = qI$, $\hat{Q}_N = \hat{q}\,I$ and $C_N = C$. The strong convergence of P_N to the identity and T_NP_N to T together with the finite dimensionality of the domain of B and the range of C are sufficient to conclude that $Q_NP_N \to Q$, $\hat{Q}_NP_N \to \hat{Q}$ strongly on V and that $B_N \to B$ and $C_NP_N \to C$ in norm as $N \to \infty$.

The uniform exponential stability of the semigroups $\{\mathcal{T}_N(t) : t \geq 0\}$ implies

(4.8) $$|T_N^k|_V = |(T_N^*)^k|_V \le r^k, \quad k = 0,1,2,...$$

with $r = e^{-a\tau} < 1$. Consequently the pairs (T_N, B_N) and (T_N, C_N^*) are uniformly exponentially stabilizable and the pairs (T_N, Q_N) and $(T_N, \hat{Q}_N)$ are detectable. It follows that there exist unique self-adjoint, nonnegative solutions Π_N and $\hat{\Pi}_N$ to the finite dimensional algebraic Riccati equations (3.7) and (3.8) respectively. The uniform exponential bound (4.8) with $r < 1$ imples that the zero control yields a uniform upper bound for Π_N and $\hat{\Pi}_N$ and therefore the uniform exponential stability of $S_N = T_N - B_N F_N$ and $\hat{S}_N = T_N - \hat{F}_N C_N$. We conclude that $\Pi_N P_N$ and $\hat{\Pi}_N P_N$ converge strongly in V to Π_N and $\hat{\Pi}_N$, respectively ,and that $F_N P_N$ and $\hat{F}_N$ converge to F and $\hat{F}$ in norm as $N \to \infty$. The approximating optimal functional feedback control and observer gains, f_N and $\hat{f}_N$, converge respectively to f and $\hat{f}$ in the H^1 norm as $N \to \infty$.

In implementing the approximation scheme just outlined above, eigenvector decomposition of the associated Hamiltonian matrix was used to solve the matrix algebraic Riccati equations (3.10) and (3.11) (see Pappas, et. al., 1980). The required matrix exponentials also were computed using eigenvalue/eigenvector decomposition. All calculations were carried out via Fortran codes on an IBM PC AT. We set $a = \sqrt{.1}$, $q = \hat{q} = r = \hat{r} = 1.0$, $\xi = \sqrt{2}/2$ and $\tau = .01$ and obtained the functional gains plotted in Figs. 4.1 and 4.2. We plot f_N and $\hat{f}_N$ as well as Df_N and $D\hat{f}_N$ to exhibit the H^1 convergence. We note that Df (or Df_N) appears as the feedback kernel in the optimal control law (4.7).

We also simulated the operation of the closed-loop system with an approximating compensator. Using a 20 mode model for the infinite dimensional system and N = 12, we computed the closed-loop spectrum of the approximating compensator (i.e. the eigenvalues of the operator $\mathcal{A}_N$ given by (3.9) with N = 12). These eigenvalues along with the first 20 open-loop eigenvalues (i.e. the first 20 eigenvalues of the operator $T = \mathcal{T}(\tau)$) and the approximating closed-loop control and observer eigenvalues are tabulated in Table 4.1 below. Table 4.1 reveals that the last seven open-loop eigenvalues remain essentially unchanged in the closed-loop system-i.e. these modes are neither controlled nor observed by the finite dimensional compensator. Also, as one would expect, $\sigma(\mathcal{A}_N)$ consists essentially of the union of $\sigma(S_N)$, $\sigma(\hat{S}_N)$ and the eigenvalues corresponding to the

uncontrolled/unobserved modes of the open-loop system.

It is worth noting that the scheme we have outlined above for the Neumann boundary control problem is the same scheme that one would ordinarily use if the problem were formulated in the space H - i.e. if the output operator C was bounded on $L_2(0,1)$ (see Gibson and Rosen, 1986). This is possible primarily because the space $V = H^1_L(0,1)$ is the natural energy space for the underlying homogeneous or open-loop system. Consequently, the inherent self-adjointness and coercivity in the problem is preserved when it is formulated in the stronger space. In the case of Dirichlet boundary control, the situation is quite different.

For the Dirichlet boundary control system (4.1), (4.2), (4.4) - (4.6), we choose the spaces H, V and W and their corresponding inner products to be the same as they were in the Neumann case. The operators $\Delta \in \mathcal{L}(W,H)$ and $C \in \mathcal{L}(V,R^1)$ also remain unchanged, however now we have $\Gamma \in \mathcal{L}(W,R^1)$ given by $\Gamma\varphi = \varphi(1)$. It then follows that the operator $\mathcal{A} : \mathrm{Dom}(\mathcal{A}) \subset H \to H$ is given by $\mathcal{A}\varphi = aD^2\varphi$ for $\varphi \in H^2(0,1) \cap H^1_0(0,1)$. It is well known that $\mathcal{A}$ is densely defined, negative definite and self-adjoint and that it is the infinitesimal generator of the uniformly exponentially stable analytic semigroup $\{\mathcal{T}(t) : t \geq 0\}$ of bounded, self-adjoint linear operators on H. However this time the operators $\mathcal{T}(t)$ for $t > 0$ are neither self-adjoint nor a semigroup on V. Indeed, since $\mathcal{R}(\mathcal{T}(t)) \subset H^1_0(0,1)$ for all $t > 0$ and $H^1_0(0,1)$ is a closed proper subspace of $H^1_L(0,1)$, $\mathcal{T}(t)$ is not strongly continuous in the V-norm at $t = 0$. (The fact that our general framework requires $\Gamma\Gamma^+ = 1$ and $\mathcal{R}(\Gamma^+) \subset V$ precludes our choosing V to be $H^1_0(0,1)$.) On the other hand, $\{\mathcal{T}(t) : t \geq 0\}$ an analytic semigroup implies (see Pazy, 1983) that there exists a constant $\mu > 0$ for which $|\mathcal{A}\mathcal{T}(t)|_H \leq \mu t^{-1}$ for $t > 0$. Consequently, if we define $T = \mathcal{T}(\tau)$, then it follows that $T \in \mathcal{L}(V)$ and moreover, that

$$|T^k\varphi|^2_V = -a^{-1}\langle \mathcal{A}\mathcal{T}(k\tau)\varphi, \mathcal{T}(k\tau)\varphi\rangle \leq a^{-1}\,|\mathcal{A}\mathcal{T}(k\tau)\varphi|_H\,|\mathcal{T}(k\tau)\varphi|_H$$

$$\leq \frac{\mu e^{-ak\tau}}{ak\tau}\,|\varphi|^2_H \leq \frac{\mu e^{-ak\tau}}{ak\tau}\,|\varphi|^2_V$$

for $k = 1,2,...$ and $\varphi \in V$. We have therefore

$$(4.9) \qquad |T^k|_V = |(T^*)^k|_V \le Mr^k, \ k = 0,1,2,...$$

where $M > 0$ and $r < 1$.

We again choose $\Gamma^+ \in \mathfrak{L}(R^1,W)$ as $(\Gamma^+u)(x) = xu$ for $x \in [0,1]$. Then $\mathfrak{R}(\Gamma^+) \subset \mathfrak{N}(\Delta)$ and we have reformulated the boundary control system (4.1), (4.2), (4.4) - (4.6) in the general form of (2.1) - (2.4) and conditions 1) - 5) are satisfied.

We formulate the optimal control problem with the performance index

$$J(u) = \sum_{k=0}^{\infty} q \langle w_k , w_k \rangle_H + ru_k^2$$

where $q \ge 0$ and $r > 0$. That is, we take Q to be the bounded, self-adjoint nonnegative operator on $H_L^1(0,1)$ given by $(Q\varphi)(x) = q \int_0^x \int_y^1 \varphi(z)dzdy$ and R to be r. For the estimator problem we set $\hat{Q} = \hat{q} I$ and $\hat{R} = \hat{r}$ with $\hat{q} \ge 0$ and $\hat{r} > 0$.

The uniform exponential bound (4.9) implies the existence of unique, nonnegative, self-adjoint solutions Π and $\hat{\Pi}$ to the algebraic Riccati equations (3.1) and (3.5). The optimal control is again of the form (4.7) with the optimal functional gains f and $\hat{f}$ in H_L^1.

The fact that $\{\mathcal{T}(t) : t \ge 0\}$ is not a semigroup on V precludes the use of a semigroup - theoretic approach to approximation. We therefore employ modal subspaces and approximate the open-loop state transition operator T directly as a bounded linear operator on V.

For each $N = 1,2,...$ let $V_N = \text{span } \{\varphi_j\}_{j=0}^N$ where for $x \in [0,1]$, $\varphi_0(x) = x$ and $\varphi_j(x) = \sin j\pi x$, $j = 1,2,...,N$. Let p_N denote the orthogonal projection of $H = L_2(0,1)$ onto span $\{\varphi_j\}_{j=1}^N$ and let P_N denote the orthogonal projection of V onto V_N. Using the fact that $V = H_0^1(0,1) \oplus \varphi_0$, it is not difficult to see that $P_N\varphi = \varphi(1)\varphi_0 + p_N(\varphi - \varphi(1)\varphi_0)$ for $\varphi \in V$ and hence, via elementary properties of Fourier series (see Tolstov, 1962), that $|(P_N - I)\varphi|_V = |(p_N - I)(\varphi - \varphi(1)\varphi_0)|_V \to 0$ as $N \to \infty$ for each $\varphi \in V$.

We define $T_N \in \mathfrak{L}(V_N)$ by $T_N = P_NT$. Then, since $\mathfrak{R}(T) = \mathfrak{R}(\mathcal{T}(\tau)) \subset H_0^1(0,1)$,

for $\psi_N = \sum_{j=0}^{N} \psi_N^j \varphi_j \in V_N$ we have

$$T_N \psi_N = P_N T \psi_N = P_N \mathcal{T}(\tau)\psi_N = p_N \mathcal{T}(\tau)\psi_N = \mathcal{T}(\tau) p_N \psi_N = \sum_{j=1}^{N} \{ \frac{2(-1)^j}{j\pi} \psi_N^0 + \psi_N^j \} e^{-aj^2\pi^2\tau} \varphi_j .$$

It follows that $T_N^* = P_N T^*$, $|T_N^k|_V = |(T_N^*)^k|_V \le Mr^k$, $k = 0,1,2,\ldots$ with $M > 0$ and $r < 1$ independent of N, and that

$$\begin{aligned} |(T_N P_N - T)\varphi|_V &\le |(P_N T P_N - P_N T)\varphi|_V + |(P_N - I)T\varphi|_V \\ &\le Mr|(P_N - I)\varphi|_V + |(P_N - I)T\varphi|_V \to 0 \end{aligned}$$

as $N \to \infty$ for $\varphi \in V$. Similarly, $T_N^* P_N \to T^*$ strongly on V as $N \to \infty$.

The approximating input, output, and state penalization operators B_N, C_N, Q_N and $\hat{Q}_N$ take the form

$$B_N u = (I - T_N)\Gamma^+ u = \varphi_0 u + \sum_{j=1}^{N} \frac{2(-1)^j}{j\pi} e^{-aj^2\pi^2\tau} \varphi_j u ,$$

$C_N = C, Q_N = qP_N Q$ and $\hat{Q}_N = \hat{q} I$. Reasoning as we did in the Neumann case, the approximating algebraic Riccati equations (3.7) and (3.8) admit unique, nonnegative, self-adjoint solutions Π_N and $\hat{\Pi}_N$ respectively, $\Pi_N P_N \to \Pi$ and $\hat{\Pi}_N P_N \to \hat{\Pi}$ strongly on V and $F_N P_N \to F$ and $\hat{F}_N \to \hat{F}$ in norm as $N \to \infty$. The approximating functional feedback control and observer gains f_N and $\hat{f}_N$ converge to f and $\hat{f}$ respectively, strongly in H^1 as $N \to \infty$.

With $a = 1.0$, $q = \hat{q} = r = 1.0$, $\hat{r} = 5.0$, $\xi = \sqrt{2}/2$ and $\tau = .01$ and the scheme outlined above we obtained the approximating optimal functional feedback control and observer gains plotted in Figs. 4.3 and 4.4 below. The first 12 open-loop and the approximating closed-loop control and observer eigenvalues for $N = 12$ are tabulated in Table 4.2.

Table 4.2 reveals an interlacing of the closed-loop control and open-loop eigenvalues. That is, the closed-loop control eigenvalues (i.e. the elements in the spectrum of S) are alternately more and less stable than the corresponding open-loop eigenvalues. We also have observed this phenomenon in other numerical studies we are carrying out involving LQG boundary control for flexible

structures. In additon, in the Dirichlet boundary control system discussed above, if Q is chosen as the identity operator on $V = H^1_L(0,1)$, virtually all of the closed-loop control eigenvalues are less stable than the corresponding open-loop eigenvalues. It is clear that this non-standard behavior results from the presence of the one dimensional subspace represented by $\mathfrak{R}(\Gamma^+)$. Indeed, the behavior of the closed-loop spectrum in the case of Neumann boundary control is as would be expected. We feel that what we are seeing can most likely be explained via infinite dimensional analogs of existing results relating the asymptotic properties of the closed-loop spectrum of a linear regulator and the zeros of the corresponding open-loop transfer function (see Kwakernaak and Sivan, 1972 and Harvey and Stein, 1978). However, as of yet, we have been unable to establish this conjecture satisfactorily and we consider it to be beyond the scope of this paper, which is primarily concerned with approximation. We leave it as an interesting open question.

5. Concluding Remarks

We have developed a framework for the finite dimensional approximation of optimal discrete-time LQG compensators for distributed parameter systems with boundary input and unbounded measurement. Our theory applies to the class of boundary control problems which can be formulated in a state space in which both the discrete-time input and output operators are continuous. We have used a functional analytic treatment to develop a convergence theory and have demonstrated the feasibility of our approach via examples involving either the Neumann or Dirichlet boundary control of a one dimensional heat equation with point measurement of temperature. We have shown that while both problems outwardly appear to be quite similar, they in fact require very different approaches to approximation. Also in the Dirichlet case the observed behavior of the resulting closed-loop spectrum is, in some ways unexpected and its explanation remains open.

Finally, we have been looking at the application of our schemes to LQG problems for flexible structures with boundary inputs and unbounded measurement and systems with control and/or observations delays. We have been considering vibration suppression for cantilevered beams via shear or moment inputs at the free end and pointwise observation of strain or acceleration. These studies are currently underway with the results to be reported elsewhere.

Acknowledgment: The authors would like to gratefully acknowledge Mr. Milton Lie of the Department of Mathematics at the University of Southern California for his assistance in carrying out the computations reported on in this paper.

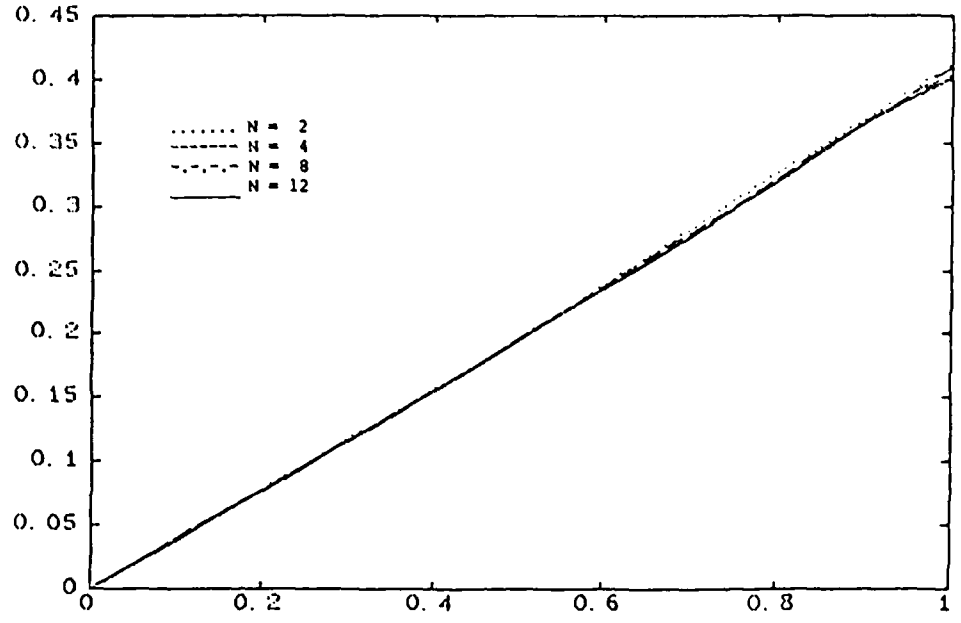

Neumann boundary control; approximating optimal functional feedback control gain, f_N.

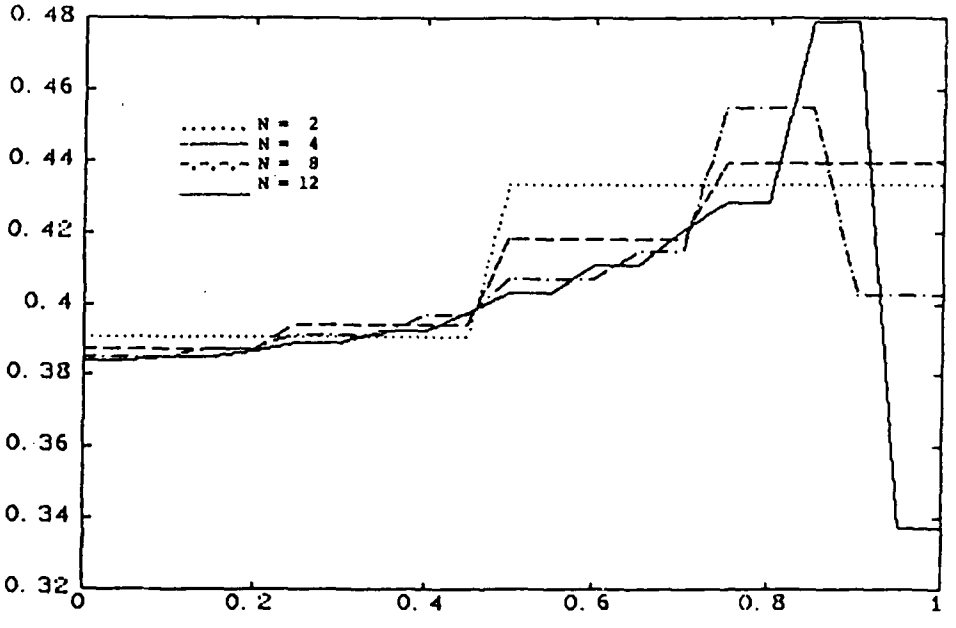

Neumann boundary control; first derivative of approximating optimal functional feedback control gain, Df_N.

Figure 4.1

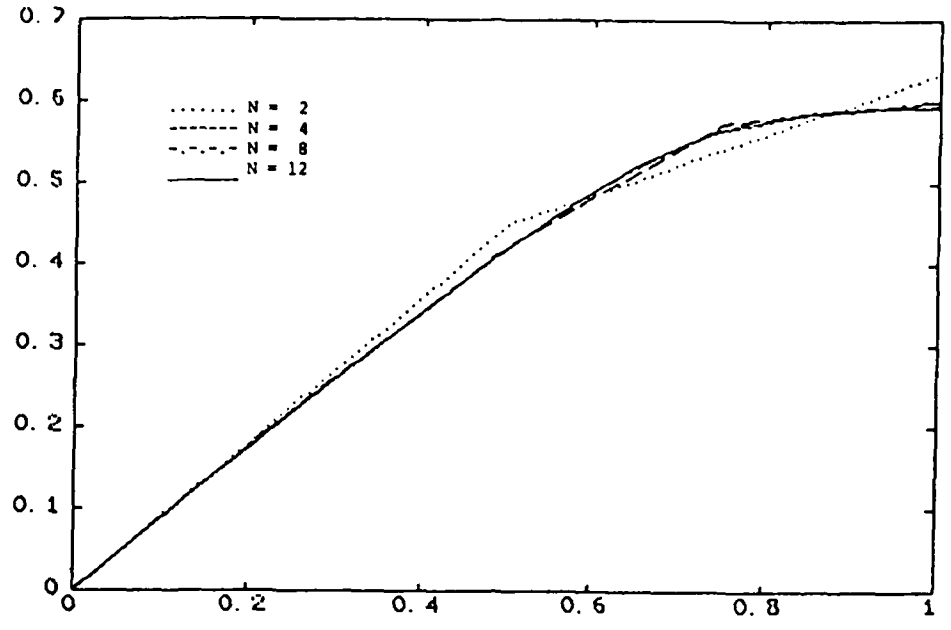

Neumann boundary control; approximating optimal functional observer gain, $\hat{f}_N$.

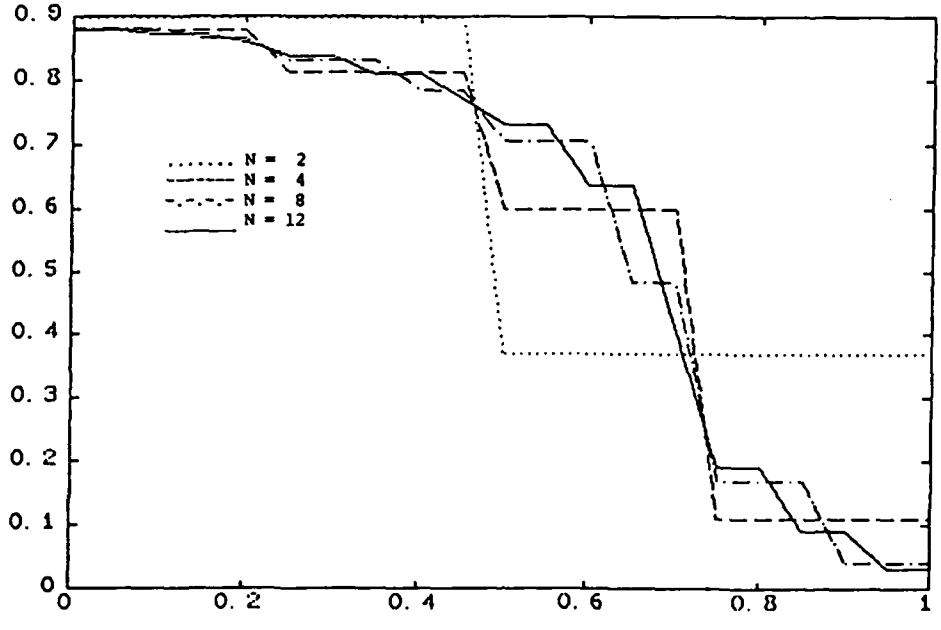

Neumann boundary control; first derivative of approximating optimal functional observer gain, $D\hat{f}_N$.

Figure 4.2

	Open-Loop	$\sigma(\mathcal{A}_{12})$	$\sigma(S_{12})$	$\sigma(\hat{S}_{12})$
1	.9975	.9968	.9968	
2	.9780	.9780		.9778
		.9769	.9768	
3	.9402	.9408		.9387
		.9371	.9371	
4	.8861	.8872		
		.8778	.8775	.8798
5	.8188	.8194		
		.7982	.7985	.7998
6	.7419	.7414		
		.7026	.7019	.7030
7	.6590	.6573		
		.5960	.5921	.5946
8	.5740	.5718		
		.4891	.4769	.4804
9	.4901	.4875		
		.4433		.4412
10	.4104	.4041		
		.3675	.3675	.3682
11	.3368	.3341		
		.2772	.2763	.2768
12	.2711	.2705		
		.2145	.2129	.2133
13	.2139	.2134		
		.1811	.1811	.1816
14	.1655	.1663		
15	.1255	.1260		
16	.0934	.0933		
17	.0681	.0677		
18	.0482	.0483		
19	.0341	.0340		
20	.0235	.0236		

Neumann boundary control; simulation results

Table 4.1

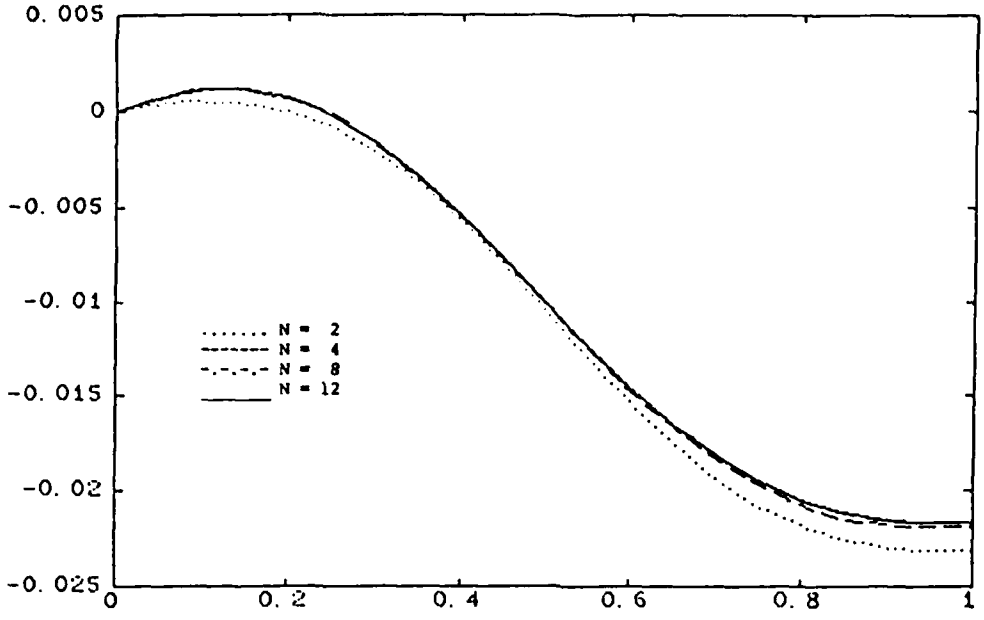

Dirichlet boundary control; approximating optimal functional feedback control gain, f_N.

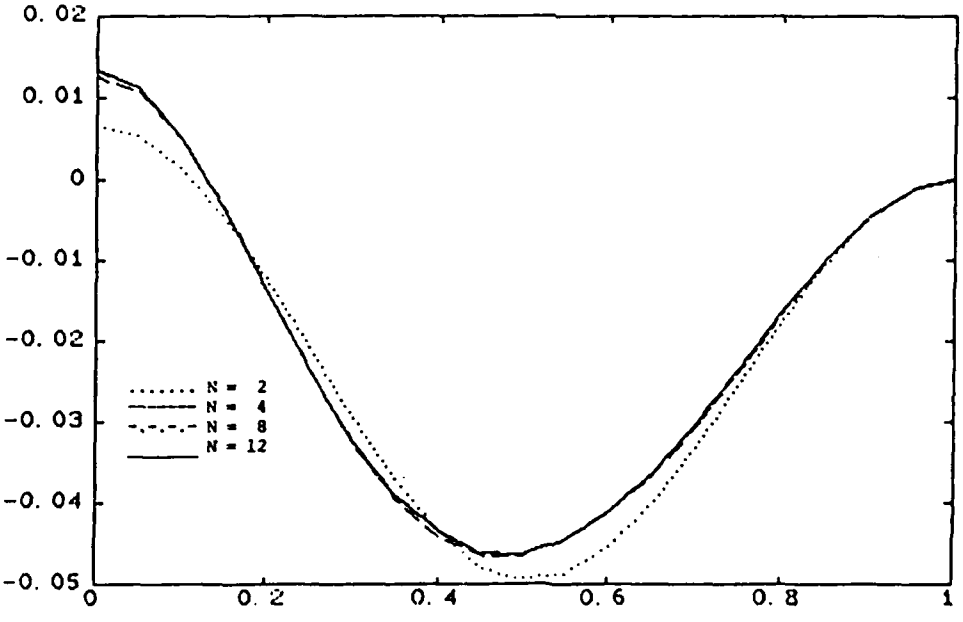

Dirichlet boundary control; first derivative of approximating optimal functional feedback control gain, Df_N.

Figure 4.3

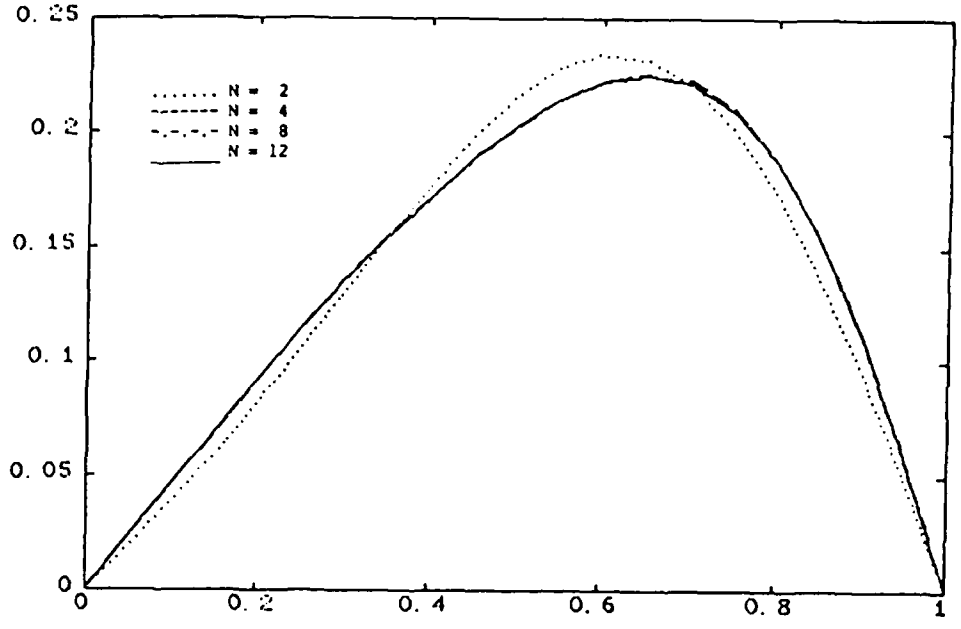

Dirichlet boundary control; approximating optimal functional observer gain, $\hat{f}_N$.

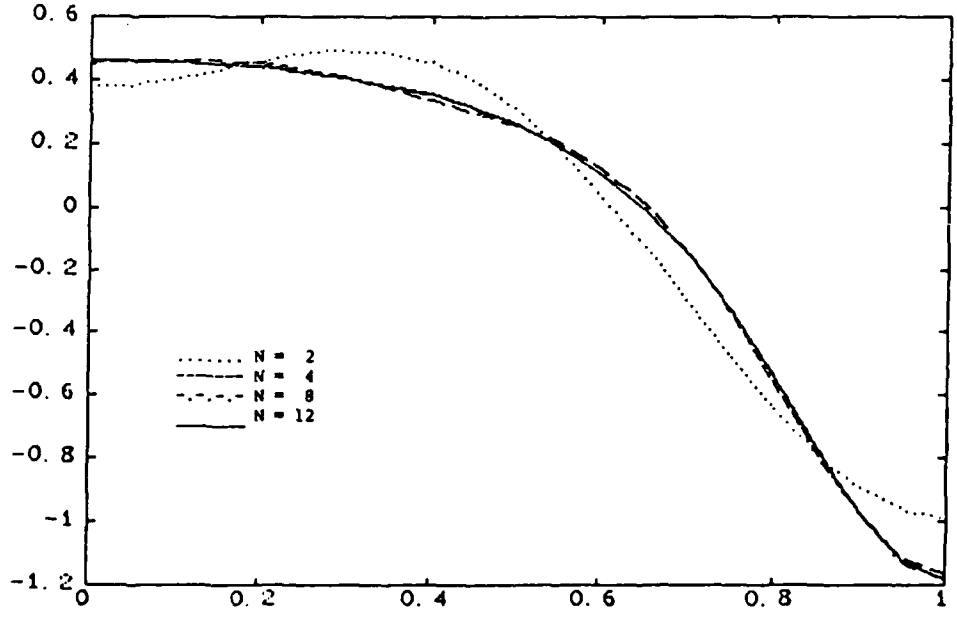

Dirichlet boundary control; first derivative of approximating optimal functional observer gain, $D\hat{f}_N$.
Figure 4.4

	Open-Loop	$\sigma(S_{12})$	$\sigma(\hat{S}_{12})$
1	.90601806	.90569591	.78573771
2	.67382545	.68243047	.57981918
3	.41136911	.40961171	.40082268
4	.20615299	.20758391	.20936323
5	.08480497	.08447005	.08636884
6	.02863695	.02873534	.02892353
7	.00793790	.00791793	.00792193
8	.00180617	.00180978	.00178763
9	.00033753	.00033682	.00033414
10	.00005172	.00005179	.00005162
11	.00000651	.00000650	.00000654
12	.00000067	.00000067	.00000068
13	——	.00000000	.00000000

Dirichlet boundary control; open and closed-loop spectrum

Table 4.2

References:

Curtain, R. F. (1984). Finite dimensional compensators for parabolic distributed systems with unbounded control and observation. SIAM J. Control and Opt., 22, pp. 255-276.

Curtain, R. F. and D. Salamon (1986). Finite dimensional compensators for infinite dimensional systems with unbounded input operators. SIAM J. Control and Opt., 24, pp. 797-816.

Gibson, J. S. and I. G. Rosen (1985). Numerical approximation for the infinite dimensional discrete-time optimal linear quadratic regulator problem. ICSAE Report No. 86-15, Institute for Computer Applications in Science and Engineering, NASA Langley Research Center, Hampton, VA, and SIAM J. Control and Opt., to appear.

Gibson, J. S. and I. G. Rosen (1986). Computational methods for optimal linear quadratic compensators for infinite dimensional discrete-time systems. ICASE Report No. 86-72, Institute for Computer Applications in Science and Engineering, NASA Langley Research Center, Hampton, VA, and Proceedings of Conf. on Control and Identification of Distributed Parameter Systems, Vorau, Austria, July, 1986, to appear as a volume in the Springer-Verlag Lecture Notes in Control and Information Sciences.

Gibson, J.S. and I.G. Rosen (1987). Approximation in discrete-time boundary control of flexible structures. Proceedings of The 26th IEEE Conference on Decision and Control, December 9-11, 1987, Los Angeles, California.

Harvey, C.A. and G. Stein (1978). Quadratic weights for asymptotic regulator properties. IEEE Trans. Auto. Control, AC-23, pp. 378-387.

Hille, E. and R.S. Phillips (1957). Functional Analysis and Semi-Groups. American Mathematical Society, Providence, RI.

Kato, T. (1966). Perturbation Theory for Linear Operators. Springer-Verlag, New York.

Kwakernaak, H. and R. Sivan (1972). Linear Optimal Control Systems. Wiley-Interscience, New York.

Lasiecka, I. and R. Triggiani (1983a). Dirichlet boundary control problem for parabolic equations with quadratic cost: analyticity and Riccati feedback synthesis. SIAM J. Control and Opt., 21, pp. 41-67.

Lasiecka, I. and R. Triggiani (1983b). An L_2 theory for the quadratic optimal cost problem of hyperbolic equations with control in the Dirichlet boundary conditions. In F. Kappel, K. Kunisch and W. Schappacher (Eds.), Control Theory for Distributed Parameter Systems and Applications, Lecture Notes in Control and Information Sciences 54, Springer-Verlag, Berlin, pp. 138-152.

Lasiecka, I. and R. Triggiani (1986). Riccati equations for hyperbolic partial differential equations with $L_2(0, T; L_2(\Gamma))$ - Dirichlet boundary terms. SIAM J. Control and Opt., 24, pp. 884-925.

Lasiecka, I. and R. Triggiani (1987a). The regulator problem for parabolic equations with Dirichlet boundary control Part I: Riccati's synthesis and regularity of optimal solution. J. Appl. Math. and Opt., to appear.

Lasiecka, I. and R. Triggiani (1987b). The regulator problem for parabolic equations with Dirichlet boundary control Part II: Galerkin approximation. J. Appl. Math. and Opt., to appear.

Pappas, T., A. J. Laub and N. R. Sandell, Jr. (1980). On the numerical solution of the discrete-time algebraic Riccati equation. IEEE Trans. Auto. Control, AC-25, pp. 631-641.

Pazy, A. (1983). Semigroups of Linear Operators and Applications to Partial Differential Equations, Springer-Verlag, New York.

Pritchard, A. J. and D. Salamon (1987). The linear quadratic control problem for infinite dimensional systems with unbounded input and output operators. SIAM J. Control and Opt., 25, pp. 121-144.

Schultz, M. (1971). Spline Analysis. Prentice-Hall, Englewood Cliffs, NJ.

Tolstov, G. P. (1962). Fourier Series. Prentice-Hall, Englewood Cliffs, NJ

APPROXIMATION IN DISCRETE-TIME BOUNDARY CONTROL OF FLEXIBLE STRUCTURES*

J.S. Gibson
Department of Mechanical, Aerospace and Nuclear Engineering
University of California
Los Angeles, CA 90024-1597

I.G. Rosen
Department of Mathematics
University of Southern California
Los Angeles, CA 90089

ABSTRACT

This paper treats discrete-time LQG optimal control of flexible structures with boundary control and what normally are unbounded measurement operators. The application of recently developed approximation theory for infinite dimensional discrete-time LQG problems to the problem here is discussed, and a numerical example is presented.

1. INTRODUCTION

Recently, approximation theory has been developed for the linear-quadratic-Guassian (LQG) control problem for infinite dimensional systems with bounded input and output operators, and the application for optimal digital control of flexible structures, diffusion processes and time-delay systems has been demonstrated in numerical examples (see [3,4,5]). In the corresponding continuous-time control problem, the requirement that the input operator be a bounded operator from the finite dimensional control space into the infinite dimensional state space almost always eliminates boundary control of distributed systems. However, in discrete-time control with piecewise constant inputs, the input operator representing a boundary control usually is bounded. This makes the theory developed in [3] and [4] applicable to boundary control of distributed models of flexible structures. An important feature of the approach in this paper is that we accommodate both boundary control and a normally unbounded measurement operator by working the problem in a Hilbert space (the space V in the following sections) with stronger topology than the natural energy space (the space X in the following sections). This trick appears to simplify many, though not all, problems whose continuous-time analogs are much more difficult.

In this paper we sketch the theory for transforming an abstract boundary control system with unbounded measurement operator into a discrete-time control system with bounded input and output operators. Also, we summarize the discrete-time LQG approximation theory in [3] and [4], and we give numerical results for control of a flexible beam.

2. THE ABSTRACT BOUNDARY CONTROL PROBLEM AND THE DISCRETE-TIME FORMULATION

We consider boundary control problems for flexible structures whose equations of motion, in first-order form, can be written abstractly as

$$\dot{x}(t) = Ax(t), \qquad t > 0, \tag{2.1}$$

$$\Gamma x(t) = u(t), \qquad t \geq 0, \tag{2.2}$$

$$x(0) = x_0, \tag{2.3}$$

$$y(t) = C\,x(t), \qquad t \geq 0, \tag{2.4}$$

where $A \in L(W,X)$, $\Gamma \in L(W,R^m)$, $C \in L(V,R^p)$ and $x_0 \in X$ with X, W and V Hilbert spaces. We assume that W and V are densely and continuously embedded in X; that the operator Γ is surjective and its null space, $N(\Gamma)$, is dense in X; and that the operator $A:Dom(A) \subset X \to X$, defined to be the restriction of A to $N(\Gamma)$, generates an C_0-semigroup $(T(t): t \geq 0)$ of bounded linear operators on X.

We treat the unbound input by rewriting the boundary control system (2.1)-(2.3) as an equivalent evolution system in a space Z, larger than X, and then considering weak, or mild, solutions (see [2] for this approach). To construct Z, we begin with the space $Dom(A^*)$ endowed with the graph Hilbert space norm associated with A^*. We then define the dual of $Dom(A^*)$ to be Z. It can be shown that X is densely and continuously embedded in Z and that $(T(t): t \geq 0)$ admits a unique extension to a C_0-semigroup on Z. The generator of this extended semigroup is an extension $\hat{A}$ of A, with $\hat{A}:X \subset Z \to Z$ given by $(\hat{A}\phi)\psi = \langle \phi, A^*\psi \rangle_X$ for $\phi \in X$ and $\psi \in Dom(A^*)$.

We recall that Γ was assumed to be onto and let $\Gamma^+ \in L(R^m,W)$ denote any right inverse of Γ. Then for $u \in R^m$, we define

$$Bu = A\Gamma^+u - \hat{A}\Gamma^+u. \tag{2.5}$$

It is not difficult to show that B is a well defined element of $L(R,Z)$, which does not depend on the partiuclar choice of Γ^+. For $u \in L_2(0,t_f; R^m)$ and $x_0 \in X$, it can be shown that the function

*This research was supported by AFOSR Grant 840309 and AFOSR Grant 840393.

$$x(t) = T(t)\,x_0 + \int_0^t T(t-s)\hat{B}u(s)ds \qquad (2.6)$$

is in $C([0,t_f];X) \cap H^2(0,t_f;Z)$, that $x(0) = x_0$ and

$$\dot{x}(t) = \hat{A}\,x(t) + \hat{B}u(t) \qquad (2.7)$$

in Z for almost every $t \in [0,t_f]$. The x-valued function x given by (2.6) is called a weak solution to the initial value problem with boundary input, (2.1)-(2.3).

We derive the discrete-time formulation of (2.1)-(2.3) by letting τ denote the length of the sampling interval and considering piecewise constant control inputs of the form $u(t) = u(k\tau)$, $k\tau \leq t < (k+1)\tau$, $k = 0, 1, 2, \ldots$. From (2.6) then, we obtain

$$x((k+1)\tau) = T\,x(k\tau) + B\,u(k\tau) \qquad (2.8)$$

where

$$T = T(k\tau) \in L(X),$$
$$B = (I - T(\tau))\Gamma^+ + \int_0^\tau T(t)\Delta\Gamma^+ dt \in L(R^m,X). \qquad (2.9)$$

Note that if Γ^+ can be chosen so that $R(\Gamma^+) \subset N(\Delta)$, then the discrete-time input operator B takes the simple form $B = (I - T)\Gamma^+$.

To simplify notation, we will assume henceforth that the time scale has been normalized to make $\tau = 1$. The discrete-time control system is then

$$x(k+1) = T\,x(k) + B\,u(k), \qquad (2.10)$$
$$k = 0, 1, 2, \ldots,$$
$$y(k) = C\,x(k). \qquad (2.11)$$

If the initial state $x(0) = x_0 \in X$ as we originally assumed, then each x(k) in (2.10) will be in X, so that the discrete-time control system does not involve the space Z.

From here on, we will assume that x(0) is in the stronger space V. The reason is that we will apply the approximation theory developed in [3] and [4] for optimal discrete-time LQG compensator synthesis for systems with bounded input and bounded output operators to boundary control systems with measurement operators that are unbounded on the space X. While the discrete-time input operator B is an element in L(R,X), in general the output operator C is not bounded from X to R. Consequently, we must consider the discrete-time control system (2.10)-(2.11) in the space V, where both the input and output operators are bounded. In addition to $x(0) \in V$, therefore, we require that $T = T(\tau) \in L(V)$ and $R(\Gamma) \subset V$, and we observe that these conditions imply $B \in L(R,V)$ and $x(k) \in V$, $k = 0, 1, 2, \ldots$. While not all boundary control problems for flexible structures satisfy these hypotheses, a large class of important problems do. This should be evident from the example in Section 4.

3. THE OPTIMIAL DISCRETE-TIME LQG COMPENSATOR AND APPROXIMATION

We present here a brief summary of the linear-quadratic theory and associated approximation results developed in [3], [4] and [5] for infinite dimensional discrete-time control systems having the form (2.10)-(2.11), with $T \in L(V)$, $B \in L(R^m, V)$ $C \in L(V, R^p)$ and $x(0) \in V$. The optimal compensator is an optimal feed back control law together with an optimal state estimator, or observer. We treat the control problem first.

The linear-quadratic optimal control problem is to find a control sequence $u(\cdot)$ to minimize the *performance index*

$$J(u) = \sum_{k=0}^{\infty} \langle Q\,x(k), x(k) \rangle + u(k)^T R\,u(k) \qquad (3.1)$$

where $x(0) \in V$, $x(k)$, $k = 1, 2, \ldots$, is given by (2.10), $Q \in L(V)$ is nonnegative and self adjoint, and R is an $m \times m$ positive definite symmetric matrix. For this problem the infinite dimensional theory closely parallels the finite dimensional case. A solution to the optimal control problem exists for each $x(0) \in V$ if and only if there exists a nonnegative, self adjoint operator $\Pi \in L(V)$ that satisfied the algebraic Riccati equation

$$\Pi = T^*(\Pi - \Pi B[R + B^*\Pi B]^{-1}B^*\Pi)T + Q. \qquad (3.2)$$

If for any control sequence that makes J(u) finite the state x(k) approaches 0 asymptotically, then there exists at most one nonnegative self adjoint solution to (3.2). When such a solution to (3.2) exists, the optimal control has the feedback form

$$u(k) = -F\,x(k), \qquad k = 0, 1, 2, \ldots, \qquad (3.3)$$

where $F \in L(V,R^m)$ is given by

$$F = [R + B^*\Pi B]^{-1}B^*\Pi T, \qquad (3.4)$$

the optimal trajectory satisfies

$$u(k) = S^k x(0), \qquad k = 0, 1, 2, \ldots, \qquad (3.5)$$

with $S = (T-BF) \in L(V)$ and $J_{min} = \langle \Pi x(0), x(0) \rangle_V$. A sufficient condition for the closed-loop system to be uniformly exponentially stable (i.e., for the spectral radius of S to be less than one) is that Q be coercive (i.e., $Q \geq \alpha > 0$).

Since $F \in L(V, R^m)$, there exists

$$f = (f_1\ f_2\ \ldots\ f_m) \in \overset{m}{\underset{j=1}{X}} V$$

such that the optimal control law in (3.3) can be written

$$u(k) = -\langle f, x(k) \rangle_V, \qquad k = 0, 1, 2, \ldots, \qquad (3.6)$$

or $[u(k)]_j = -\langle f_j, x(k) \rangle_V$, $j = 1, 2, \ldots m$. The vector f is called the optimal functional feedback control gain.

The optimal LQG state estimator, or observer, is

$$\hat{x}(k+1) = T\,\hat{x}(k) + B\,u(k) + \hat{F}\,[y(k) - C\,\hat{x}(k)], \qquad k = 0, 1, 2, \ldots \qquad (3.7)$$

Here, $\hat{x}(0) \in V$ and the estimator gain $\hat{F} \in L(R^p, V)$ is

$$\hat{F} = T\hat{\Pi}C^*[\hat{R} + C\hat{\Pi}C^*]^{-1} \qquad (3.8)$$

with $\hat{\Pi}$ in L(V) the minimal nonnegative self adjoint solution (if one exists) to the algebraic Riccati equation

$$\hat{\Pi} = T(\hat{\Pi} - \hat{\Pi}C^*[\hat{R} + C\hat{\Pi}C^*]^{-1}C\hat{\Pi})T^* + \hat{Q},$$

where $\hat{Q} \in L(V)$ is nonnegative and self adjoint and and $\hat{R}$ is a p x p positive definite symmetric matrix. If $\hat{Q}$ is trace-class, then (3.7) is an optimal Kalman-Bucy filter for (2.10)-(2.11) if a zero-mean, stationary white noise process with covariance operator $\hat{Q}$ is added to the right side of (2.10) and a similar noise process with covariance matrix $\hat{R}$ is added to the right side of (2.11) (see [1]. In compensator design, $\hat{Q}$ and $\hat{R}$ often are chosen to produce certain deterministic properties in the closed-loop system, such as stability margins and robustness; then, $\hat{Q}$ need not be trace-class. Conditions for existence and uniqueness of solutions to (3.9) are analogous to those for the control Ricatti equation (3.2).

Since $\hat{F} \in L(R^p, V)$, we can write

$$\hat{F}y = \hat{f}^T y, \qquad y \in R^p, \qquad (3.10)$$

where $\hat{f} = (\hat{f}_1\ \hat{f}_2\ \ldots\ \hat{f}_m)^T \in \overset{p}{\underset{j=1}{X}} V$ is known as the optimal functional estimator, or observer, gain.

The optimal compensator consists of the state estimator in (3.7) and the control law

$$u(k) = -F\,\hat{x}(k), \qquad k = 0, 1, 2, \ldots, \qquad (3.11)$$

with the control gain F given by (3.4) with the solution tc (3.2) and the estimator gain given by (3.8) with the solution to (3.9). The optimal closed-loop system then consists of (2.10)-(2.11), (3.7) and (3.11). It can be shown that the spectrum of this closed-loop system is $\sigma(T - BF)$ $\sigma(T - FC)$.

Our approximation of the infinite dimensional LQG problem and compensator is based on approximation of the operators T, B, C, Q and $\hat{Q}$ by operators on finite dimensional subspaces V_N of V. We denote by P_N the orthogonal projection of V onto V_N, and *we assume that* P_N *converges strongly* to the identity of operator on V. Also, we assume that there exist operators $\hat{T}_N$, $\hat{Q}_N$, $\hat{Q}_N \in L(V_N)$ and Q_N and $\hat{Q}_N$ nonnegative and self adjoint, $B_N \in L(R^m, V_N)$ and $C_N \in L(V_N, R^p)$ such that T_NP_N, $T_N^*P_N$, Q_NP_N and Q_NP_N converge strongly to T, T^*, Q and $\hat{Q}$, respectively, and B_N and C_NP_N converge in norm to B and C, respectively as $N \to \infty$.

For each N, we define a finite dimensional LQG problem for the open-loop system with the operators T_N, B_N and C_N and for the operators Q_N, R in the optimal control problem and the operators $\hat{Q}_N$ and R in the estimator problem.

The solution to this N^{th} LQG problem requires the solution of the two algebraic Riccati equations obtained by replacing the operators in (3.2) and (3.9) with their N^{th} approximations:

$$\Pi_N = T_N^*(\Pi_N - \Pi_N B_N[R+B^*\Pi_N B_N]^{-1}B^*\Pi_N)T_N + Q_N \qquad (3.12)$$

$$\hat{\Pi}_N = T_N(\hat{\Pi}_N - \Pi_N C_N^*[\hat{R}+C_N\hat{\Pi}_N C_N^*]^{-1}C_N\Pi_N)T_N^* + \hat{Q}_N \qquad (3.13)$$

The optimal control and estimator gains for the N^{th} problem are given by

$$F_N = [R + B_N^*\Pi_N B_N]^{-1}\ B_N^*\Pi_N T_N \qquad (3.14)$$

$$\hat{F}_N = T_N\hat{\Pi}_N[\hat{R}_N + C_N\hat{\Pi}_N C_N^*]^{-1} \tag{3.15}$$

If the pairs (T_N, B_N) and (T_N^*, C_N^*) are stabilizable, (3.12) and (3.13) have nonnegative, self adjoint solutions; if the pairs (Q_N, T_N) and $(\hat{Q}_N, T_N^*)$ are detectable, the nonnegative, self adjoint solutions to (3.12) and (3.13) are unique and positive definite.

As in the infinite dimensional problem, we have functional control gains $f^N = (f_1^N\ f_2^N\ \dots\ f_m^N)^T \in X\ V_N$ and functional estimator gains $\hat{f}^N = (\hat{f}_1^N\ \hat{f}_2^N\ \dots\ \hat{f}_m^N)^T \in X\ V_N$ corresponding to F_N and $\hat{F}_N$, respectively. We will give the formulas for computing the functional control and estimator gains for the single input/single output case ($m = p = 1$); the general case is a straightforward extension. When $m = 1$, B and B_N are elements of V and V_N, respectively, and when $p = 1$, C^* and C_N^* are elements of V and V_N, respectively. The following two formulas then follow from (3.14) and (3.15):

$$f^N = f_1^N = (R + B_N^*\Pi_N B_N)^{-1}\ T_N^*\Pi_N B_N, \tag{3.16}$$

$$\hat{f}^N = \hat{f}_1^N = (R + C_N\hat{\Pi}_N C_N^*)^{-1}\ T_N\hat{\Pi}_N C_N^*. \tag{3.17}$$

For the example in Section 4, it can be shown that the closed-loop operators for the approximating LQG problems are exponentially stable, uniformly in N; i.e., there exists constants $M > 0$ and $r < 1$, independent of N, such that

$$|(T_N - B_N F_N)^k| + |(\hat{T_N} - F_N C_N)^k| \le Mr^k, \quad \forall k \ge 0 \tag{3.18}$$

This condition and our assumptions about the strong convergence of the basic operators T_N, T_N^*, Q_N, $\hat{Q}_N$, B_N and C_N guarantee (see [3], [4]) that the functional control gains f_N and f_N converge in V to f and f, respectively. See [3], [4], [5] for more details on convergence analysis and numerical aspects of the compensator approximation discussed here, including results on convergence of the approximating compensators and closed-loop systems.

4. EXAMPLE

Consider the equation of motion for a clamped-free Euler-Bernoulli beam with Kelvin-Voight viscoelastic damping

$$\ddot{w}(t,s) + c_0\ D^4\ \dot{w}(t,s) + EI\ D^4\ w(t,s) = 0, \quad 0 < s < 1,\ t \ge 0 \tag{4.1}$$

$$w(t,0) = Dw(t,0) = 0, \qquad t \ge 0, \tag{4.2}$$

$$c_0\ D^2\ \dot{w}(t,1) + EI\ D^2\ w(t,1) = 0, \qquad t \ge 0, \tag{4.3}$$

$$c_0\ D^3\ \dot{w}(t,1) + EI\ D^3\ w(t,1) = -u(t), \quad t \ge 0, \tag{4.4}$$

The constants in (4.1)-(4.4) are

$$c_0 = .0001, \qquad EI = .01333.$$

As indicated by (4.4), the control force $u(t)$ is applied to the right end of the beam. For the setup in Section 2, the appropriate spaces are:

$$X = (\phi \in H^2(0,1):\ \phi(0) = D\phi(0) = 0) \times L_2(0,1) \tag{4.5}$$

$$V = (\phi \in H^3(0,1):\ \phi(0) = D\phi(0) = D^2\phi(1) = 0) \times (H^1(0,1):\ \phi(0)) = 0, \tag{4.6}$$

$$W = (\phi,\psi) \in X:\ c_0\psi + EI\phi \in H^4(0,1), \quad \phi(0) = D\phi(0) = 0,\ c_0D^2\psi(1) + EID^2\phi(1) = 0) \tag{4.7}$$

The state vector $x(t)$ is

$$x(t) = \begin{bmatrix} w(t) \\ \dot{w}(t) \end{bmatrix} \tag{4.8}$$

and the operators A, Γ and Γ^+ are

$$A = \begin{bmatrix} 0 & I \\ -EI\ D^4 - c_0\ D^4 & \end{bmatrix} \tag{4.9}$$

$$\Gamma:\ W \to R^1, \quad \Gamma(\phi,\psi) = -c_0D^3\psi(1) - EID^3\phi(1), \tag{4.10}$$

$$\Gamma^+:\ R^1 \to W, \quad \Gamma^+u = \phi_0 u, \tag{4.11}$$

where ϕ_0 is the third-degree polynomial that satisfies

$$\phi_0(0) = D\phi(0) = D^2\phi(1) = 0, \ D^3\phi(1) = -1/EI. \tag{4.12}$$

Hence

$$\Gamma\Gamma^+:\ R^1 \to R^1, \quad \Gamma\Gamma^+ = 1. \tag{4.13}$$

Now let

$$\mathrm{Dom}(A) = N(\Gamma), \qquad A = A|_{N(\Gamma)} \tag{4.14}$$

and let $(T(t):\ t \ge 0)$ be the semigroup generated on X by A. Then, as in (2.9),

$$T = T(\tau) \qquad B = (I - T(\tau))\phi_0. \tag{4.15}$$

Note that $R(\Gamma) \subset N(A)$.

For numerical solution of the LQG problem, we used two schemes to approximate the beam. The first method is a Galerkin scheme that uses cubic B-splines as basis vectors for the approximation subspaces V_N in the general approximation framework discussed in Section 3. The second approach is a modal approximation, which uses the natural mode shapes of undamped free vibrations of the beam as basis vectors in approximating the infinite dimensional control problem. We have not carried out all of the details of the convergence proofs, but it appears that methods similar to those in [5] will yield the required proofs.

For the optimal linear-quadratic regulator problem we take $\tau = .01$, $R = .01$ and Q such that

$$\langle Qx(t), x(t)\rangle_V = |x(t)|x^2. \qquad (4.15)$$

The functional control gain f in (3.6) has the form

$$f = (f_1, f_2) \in V. \qquad (4.16)$$

In the spline-based scheme, the function ϕ_0 is an element of each V_N, so that essentially we need only approximate the semigroup T(t) using the Galerkin method. For each N, we solve the finite dimensional Riccati equation (3.12) by standard numerical methods and compute the N^{th} approximation to f according to (3.16). Figures 1-3 show our approximations to f_1, f_1'' and f_2 for N = 2, 4, 6, 8 elements.

Some of the splines used in this scheme are in X but not in V, so we are not guaranteed V-convergence for the approximating functional gains. Figures 1-3 demonstrate that the approximations to f converge in X. It seems unlikely that these approximations converge in V; V-convergence would require that $f_1^{N''}(1)$ converge to zero, but it does not.

In the second approximation scheme, the natural mode shapes, which are used as basis vectors for the spaces V_N in Section 3, are elements of V, so we should get the functions f^N converging in V. It is straightforward to compute the operators T_N, B_N and Q_N for the finite dimensional Riccati equations. Figures 4 and 5 show the approximating functional control gains for N = 10, 14, 18, 20 modes, and the pointwise convergence of $f_1{}^{N''}$ is consistent with V-convergence of the approximations to the functional control gain f.

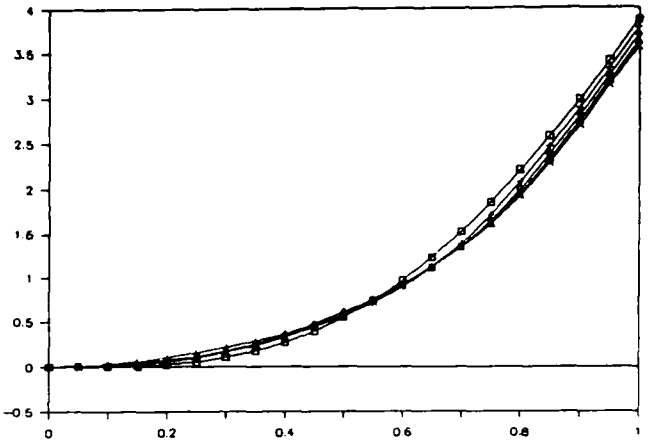

Figure 1. B-spline Approximations to f_1
N = 2, 3, 4, 5, 6 Elements

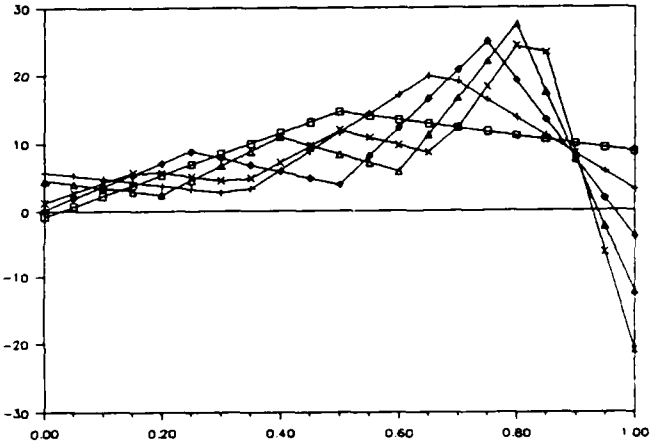

Figure 2. B-spline Approximations to f_1''
N = 2, 3, 4, 5, 6 Elements

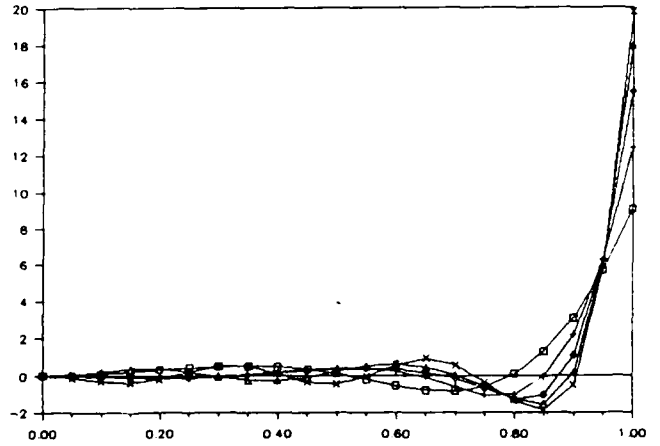

Figure 3. B-spline Approximations to f_2
N = 2, 3, 4, 5, 6 Elements

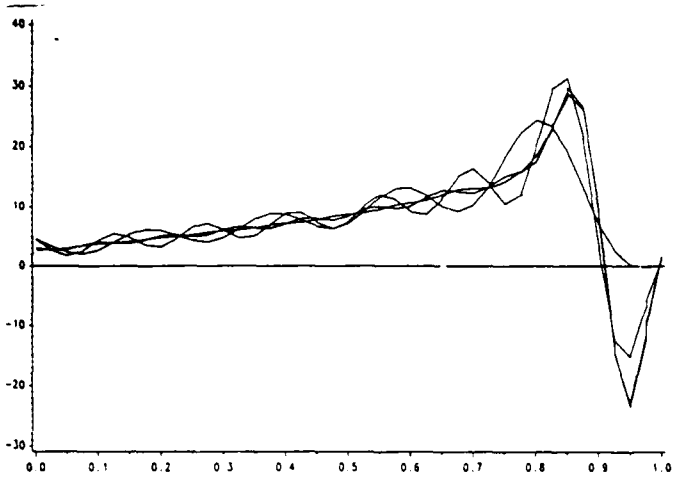

Figure 4. Modal Approximations to f_1''
N = 10, 14, 18, 20 Modes

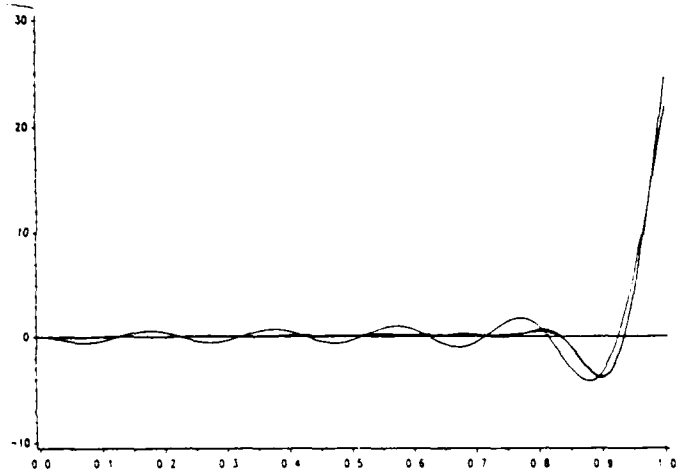

Figure 5. Modal Approximations to f_2
N = 10, 14, 18, 20 Modes

For state estimation, we take the measurement

$$y(t) = w(t,.5); \qquad (4.17)$$

i.e., we place a strain guage at the midpoint of the beam. We need the state vector to be in the space V in (4.6) so that a pointwise measurement of the second derivative of the displacement will be a continuous measurement of the state. In the estimation problem, we take R = 1 and Q = I.

We use only the modal approximation to solve for the estimator gains. For each N (number of modes), we solve the finite dimensional estimator Riccati equation (3.9) and then compute the approximating functional estimator gains $f_1^N = (f^N, f_2^N)$ according to (3.17). Figures 4-6 show F_1^{N-} and f_2^N. As expected, these functions converge uniformly pointwise. This is consistent with V-convergence of f^N.

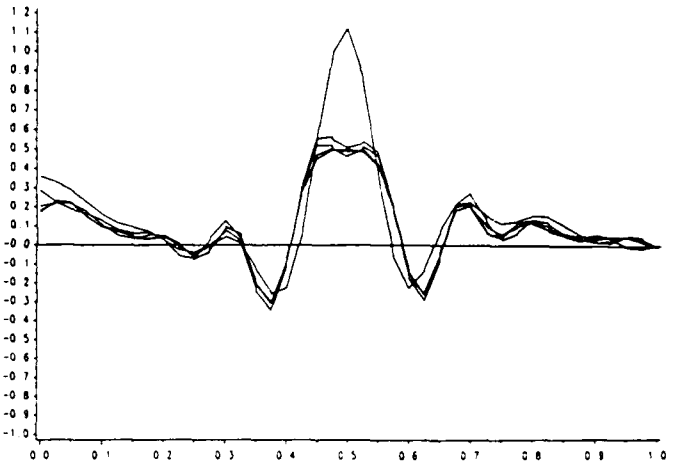

Figure 6. Modal Approximations to f_1''
N = 14, 18, 20, 22, 24 Modes

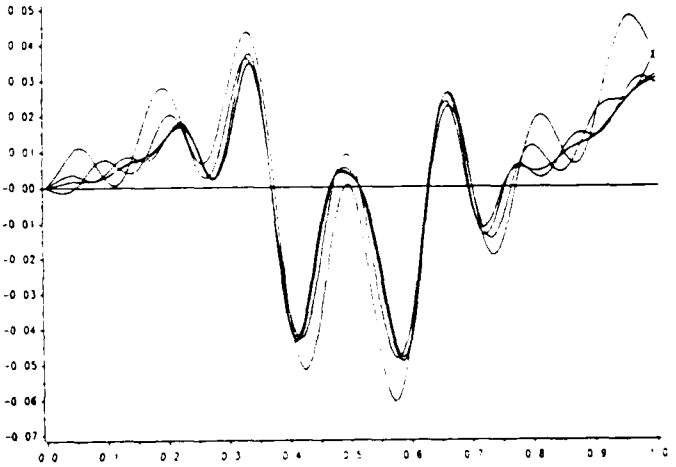

Figure 7. Modal Approximations to f_2
N = 14, 18, 20, 22, 24 Modes

ACKNOWLEDGMENT

The authors are indebted to Shiaw-Wu Chen, Seon-Myung Kim and Milton Lie for the numerical results in this paper.

REFERENCES

[1] A.V. Balakrishnan, Applied Functional Analysis, Springer Verlag, New York, 1981.

[2] R.F. Curtain and D. Salamon, "Finite Dimensional Compensators for Infinite Dimensional Systems with Unbounded Input Operators," SIAM J. Control and Opt., vol. 24, pp. 796-816, 1986.

[3] J.S. Gibson and I.G. Rosen, "Numerical Approximation for th Infinite-Dimensional Discrete-Time Optimal Linear-Quadratic Regulator Problem," ICASE Report 86-15, to appear in SIAM J. Control and Opt.

[4] J.S. Gibson and I.G. Rosen, "Computational Methods for Discrete-time Compensators for Distributed Systems," Conference on Control and Identification of Distributed Systems, Vorau, Austria, July 1986.

[5] J.S. Gibson and I.G. Rosen, "Approximation of Discrete-time LQG Compensators for Distributed Systems with Boundary Input and Unbounded Measurement," Submitted to Automatica.

VECTOR-CHANNEL LATTICE FILTERS AND IDENTIFICATION OF FLEXIBLE STRUCTURES

F. Jabbari*

Department of Mechanical Engineering

University of California, Irvine, 92717

J. S. Gibson*

Department of Mechanical, Aerospace and Nuclear Engineering

University of California, Los Angeles 90024

ABSTRACT

This paper presents a new derivation of a least-squares lattice filter and applies the filter to identification of flexible structures. The vector-channel lattice here -- derived in an infinite dimensional history space, without matrix manipulations or geometric arguments -- can constrain the AR coefficients for several outputs to be the same. Numerical results for a simulated flexible structure compare the vector-channel lattice with the standard lattice filter. These results show that the frequencies and damping ratios for the most significant modes can be identified adaptively with lattice filters.

---

* THIS RESEARCH WAS SUPPORTED BY THE UNITED STATES AIR FORCE, AFOSR Grant 840903.

1. INTRODUCTION

In recent years, adaptive lattice filters have been used increasingly in signal processing to implement least-squares algorithms and other estimation methods. One advantage of a least-squares lattice filter is that it is recursive in both time and order, while the classical least-squares algorithm is recursive in time only. Also, lattice filters have been shown to possess desirable numerical stability [1]. Lee, Morf and Friedlander [2,3] developed the time update equations needed for adaptive lattice filters and studied applications to speech processing and adaptive control. For derivations and discussions of lattice filters, see [4,5,6,7].

Potentially important new applications of lattice filters appear to lie in adaptive identification and control of large flexible structures. Because such sturctures have many, usually infinitely many modes of vibration, the problem of determining the order of a model to use for on-line identification and control is a major obstacle. A lattice filter, with its order-recursive property, can in principle identify the effective order of the structure and adaptively increase this order to accomodate new excitations to the structure or decrease the order as faster transients in the structure are damped out. Sundararajan and Montgomery [8,9] and Wiberg [10,11] were first to apply lattice filters to identification of flexible structures. Sundararajan and Montgomery used the lattice to estimate the number of excited modes of a flexible structure, while using fast Fourier transforms to identify the frequencies and damping ratios. Wiberg has studied identification of structural frequencies and damping with lattice filters. For structural identification from free-response data, Wiberg has developed a "vibration lattice", which enforces the constraint that each scalar measurement channel for the same structure have the same auto regressive (AR) coefficients.

To understand the motivation for Wiberg's vibration lattice and our vector-channel lattice, consider the usual linear AR (auto regressive) model

$$y(t) = \sum_{j=1}^{n} A_j y(t-j) + \varepsilon_n(t), \tag{1.1}$$

where $y(t)$ is an m-vector, each A_j is an m × m matrix of parameters to be estimated and $\varepsilon_n(t)$ is the error. The least-squares lattice filter yields a least-squares estimate for the A_j's that is recursive in both t and n. Now suppose that $y(t)$ represents m sensors on the same flexible structure and that N observable modes

of the structure are excited. Then the AR model above with n something less than 2N should fit the data. However, only in special circumstances, will the order of the minimum AR model that fits the data equal the order of the structural vibrations, since the AR model has nm eigenvalues while the structural response has 2N eigenvalues. In general, the minimal AR model will have extraneous eigenvalues. If modal frequencies and damping ratios are desired, their identification will be complicated severely by the extraneous eigenvalues of the AR model.

On the other hand, if the A_j 's in the ARMA model are constrained to be scalars, then the minimum n is always 2N. This constraint represents significant information about the system; it amounts to writing the scalar AR model for each component of the measurement vector and imposing the constraint that all m of these processes have the same AR coefficients because they are measurements of the same linear system. When the measurements are noisy, incorporating this information into the estimation algorithm is even more important than resolving the relation between the number of modes and the order of the AR model. Using all information about the system is especially important in on-line identification of distributed systems like flexible structures. Even if the sensor data is virtually free of random noise, the number of excited modes often is greater than the allowable order of the lattice filter, so that the higher frequency modes amount to unmodeled distrubance in the sensor data.

The lattice derived here solves the problem of constraining the AR coefficients for multiple outputs to be the same. We refer to this lattice as a vector-channel lattice because it treats several outputs as components of one vector measurement channel, as opposed to previous lattices, which treat each scalar output as a single channel. In general, there can be multiple vector measurement channels. When each channel contains only one component, the vector-channel lattice reduces to the standard multi-input-multi-output lattice, which we refer to as either the standard lattice or the scalar-channel lattice.

Although application of the classical recursive least-squares algorithm to the case where the measurements are vectors but the AR coefficients are scalars is straight forward and well known (see [7]), a lattice filter for this problem apparently was not derived until Wiberg introduced his vibration lattice for structural identification. The vector-channel lattice differs from the vibration lattice in two respects. First, one coefficient that is a scalar in Wiberg's and previous lattices is a matrix in the vector-channel lattice, the dimension of this matrix being determined by the dimension of he vector measurement channels.

Second, the vibration lattice does not accomodate an input, or control; i.e., the moving average part of an ARMA model. This capability is, of course, important in adaptive identificationl and control. As in previous lattices, a moving average must be treated as an additional measurement channel in the vector-channel lattice. The trick is to constrain the AR coefficients to be the same for all true measurement channels while allowing different coefficients for the input channels. Our method for including the MA terms in the vector-channel lattice is discussed in Section 3.3.

In Section 2, we derive the vector-channel lattice filter and the algorithm for generating the AR coefficients from the lattice data. This derivation differs from previous derivations of least-squares lattices in several importants respects, all of which stem from the fact that we work in a Hilbert space of infinitely long history vectors. Previous lattice derivations have dealt with finite history vectors of changing length and have relied heavily on matrix manipulation and/or geometric arguments, including nonorthogonal projections. We use neither type of argument; our derivation requires only elementary properties of orthogonal projections in Hilbert space.

The original motivation for the derivation here was not to develop a vector-channel lattice. In [12,13] we developed infinite dimensional ARMA models for certain classes of distributed systems, with one aim being to use these ARMA models as the basis for an approximation theory that will predict the behavior of lattices of increasing finite order in adaptive identification and control of infinite dimensional systems. In such analysis (which is continuing), infinite histories of inputs and outputs are used. Hence, the infinite dimensional history space in which we work.

In Section 3, we summarize the vector-channel lattice algorithm and discuss its implementation. From the derivation of the lattice, we deduce an algorithm for one-step-ahead prediction and show how to make copies of an input so that in a vector ARMA process the AR coefficients can be constrained to be the same for each channel but not the the MA coefficients.

In Section 4, we compare numerical results obtained with standard and vector-channel lattices for the simulated forced vibrations of a flexible structure with two position measurements. First, we use the standard lattice to treat the measuremets as two independent ARMA processes. Then we use the vector-channel lattice to treat the measurements as the two components of one vector process, thereby imposing the constraint that each measurement process have the same AR coefficients. We use the lattice

to identify both the number of significantly excited modes and the frequencies and damping ratios of those modes. We give results for simulations both with and without noisy measurements.

2. DERIVATION

Definitions and Order Updates

The history space in this paper is the following Hilbert space of infinite column vectors:

$$\ell_2(R^m, \lambda) = \left\{ \psi = [\, x_1^T \;\; x_2^T \;\; x_3^T \ldots \,]^T : \text{each } x_j \text{ is a real } m\text{-vector} \right. \\ \left. \text{and } \|\psi\|^2 = \langle \psi, \psi \rangle < \infty \right\}$$

where

$$\langle \psi, \hat{\psi} \rangle = \sum_{j=1}^{\infty} \lambda^{j-1} x_j^T \hat{x}_j \tag{2.1}$$

and λ (the forgetting factor) is a positive real number. Throughout this paper, $\langle \ldots \rangle$ means the inner product in (2.1).

The following derivation assumes a sampled process with p channels, each of which contains m scalar measurements. In other words, the measurement from channel i at time t is the m-vector

$$y^i(t) = [\; y_1^i(t) \;\; y_2^i(t) \ldots y_m^i(t) \;]^T, \quad i = 1, \ldots p. \tag{2.2}$$

The infinite history vector of channel i is

$$\psi^i(t) = [\; (y^i(t))^T \;\; (y^i(t-1))^T \;\; \ldots \;\; \ldots \;]^T . \tag{2.3}$$

In applications, all but a finite number of terms in $\psi^i(t)$ can be set to zero. The main advantage of the infinite dimensional history space for the lattice derivation is not that it allows histories of infinite length, but that it accomodates histories of all finite lengths in the same space.

The following definitions are necessary. For any integer t and nonnegative integer n:

$$S(t) = span\{\; \psi^1(t), \;\; \ldots, \; \psi^p(t) \;\} \tag{2.4}$$

$$H_0(t) = \{\, 0 \,\}, \qquad H_n(t) = S(t-1) \oplus S(t-2) \oplus \ldots \oplus S(t-n) \tag{2.5}$$

$$P_n(t) = \text{Orthogonal Projection onto } H_n(t) \tag{2.6}$$

$$E_0^f(t) = S(t), \qquad E_n^f(t) = [\ I - P_n(t)\ ]\ S(t), \quad \text{forward error space} \tag{2.7}$$

$$E_0^b(t) = S(t), \qquad E_n^b(t) = [\ I - P_n(t+1)\ ]\ S(t-n), \quad \text{fackward error space} \tag{2.8}$$

$$P_n^f(t) = \text{Orthogonal projection onto } E_n^f(t), \qquad P_n^b(t) = \text{Orthogonal projection onto } E_n^b(t) \tag{2.9}$$

Note that the definition of the backward error space $E_n^b(t-1)$ amounts to a Gram-Schmidt orthogonalization of the history spaces S(t-1), ... , S(t-n).

The rest of this section derives a number of recursions from the definitions given so far. Like (2.4)-(2.9), subsequent equations in this section are valid for any integer t and any nonnegative integer n, except where otherwise indicated. Of course, for implementation of the lattice algorithm, initialization at some finite initial time is necessary, and this is discussed in Section 3. In the current section, initialization need not be considered.

A first consequence of the foregoing definitions is

$$H_{n+1}(t) = H_n(t-1) \overset{\perp}{\oplus} E_n^f(t-1) = H_n(t) \overset{\perp}{\oplus} E_n^b(t-1) \tag{2.10}$$

where the notation $\overset{\perp}{\oplus}$ indicates the direct sum of orthogonal subspaces of $\ell_2(R^m, \lambda)$. Because of (2.10) and since $E_n^f(t)$ and $E_n^b(t-1)$ are orthogonal to $H_n(t)$, elementary properties of projection yield

$$P_{n+1}(t) = P_n(t-1) + P_n^f(t-1) = P_n(t) + P_n^b(t-1) \tag{2.11}$$

$$P_n^f(t)\ P_n(t) = P_n^b(t-1)\ P_n(t) = 0. \tag{2.12}$$

From (2.11) and (2.12), it follows that

$$[\ I - P_{n+1}(t+1)\ ] = [\ I - P_n^f(t)\ ]\ [\ I - P_n(t)\ ], \tag{2.13}$$

$$[\ I - P_{n+1}(t)\ ] = [\ I - P_n^b(t-1)\ ]\ [\ I - P_n(t)\ ]. \tag{2.14}$$

The definitions of the forward and backward error vectors are similar to (2.7) and (2.8):

$$f_0^i(t) = \psi^i(t), \qquad f_n^i(t) = [\ I - P_n(t)\ ]\ \psi^i(t), \quad i = 1, \ldots p \quad \text{Forward error} \tag{2.15}$$

$$b_0^i(t) = \psi^i(t), \qquad b_n^i(t) = [\ I - P_n(t+1)\ ]\ \psi^i(t-n), \quad i = 1, \ldots p \quad \text{Backward error} \tag{2.16}$$

Then,

$$E_n^f(t) = span\{ f_n^i(t) \} \quad \text{and} \quad E_n^b(t) = span\{ b_n^i(t) \}, \quad i = 1, \ldots p. \tag{2.17}$$

The order update formulas for the forward and backward error vectors follow from (2.13)-(2.16). Substituting (2.14) into (2.15) for n + 1 yields

$$f_{n+1}^i(t) = [\, I - P_{n+1}(t) \,]\, \psi^i(t) = [\, I - P_n^b(t-1) \,]\, [\, I - P_n(t) \,]\, \psi^i(t),$$

which in view of (2.7) becomes

$$f_{n+1}^i(t) = [\, I - P_n^b(t-1) \,]\, f_n^i(t) = f_n^i(t) - P_n^b(t-1) f_n^i(t) \tag{2.18}$$

for i = 1,2, ... p. Similarly, (2.13) and (2.16) with (2.8) yield

$$b_{n+1}^i(t) = b_n^i(t-1) - P_n^f(t)\, b_n^i(t-1). \tag{2.19}$$

To make these order update equations useful, the following elementary and standard result is required (see [14], page 56).

Lemma 2.1. Let H be a real Hilbert space, $E = span\{ h_1, h_2, \ldots, h_p \}$ a subspace of H and P_E the orthogonal projection of H onto E. Then for any $h \in H$,

$$P_E h = [\, h_1 \;\; h_2 \;\; \ldots \;\; h_p \,]\, a \qquad \left(= \sum_{i=1}^{p} a_i h_i \right) \tag{2.20}$$

where $a \in R^p$ satisfies

$$R_E\, a = d \tag{2.21}$$

with R_E the nonnegative symmetric matrix whose (i,j) element is $< h_i, h_j >_H$ and d the p-vector whose i^{th} element is $< h_i, h >_H$. For each $h \in H$, at least one solution to (2.21) exists. The matrix R_E is positive definite if and only if the vectors h_i are linearly independent.

The following matrices are useful for applying Lemma 2.1 in (2.18) and (2.19). For n = 0, 1, ... :

$$K_{n+1}(t) = p \times p \text{ matrix whose (i,j) element is } < f_n^i(t),\, b_n^j(t-1) >, \tag{2.22}$$

$$R_n^e(t) = p \times p \text{ matrix whose (i,j) element is } < f_n^i(t),\, f_n^j(t) >, \tag{2.23}$$

$$R_n^r(t) = p \times p \text{ matrix whose (i,j) element is } < b_n^i(t),\ b^j{}_n(t) > . \tag{2.24}$$

Also, we define

$$[\ f_n(t)\ ] = [\ f_n^1(t)\ \ f_n^2(t)\ \ \ldots\ f_n^p\ ],\qquad [\ b_n(t)\ ] = [\ b_n^1(t)\ \ b_n^2(t)\ \ \ldots\ b_n^p\ ]\ ; \tag{2.25}$$

i.e., $[\ f_n(t)\ ]$ is the matrix containing the p infinitely long columns $f_n^i(t)$, and $[\ b_n(t)\ ]$ is the corresponding matrix containing the $b_n(t)$'s. With these definitions and (2.17), Lemma 2.1 implies that (2.18) and (2.19) are equivalent to

$$[\ f_{n+1}(t)\ ] = [\ f_n(t)\ ] \ -\ [\ b_n(t-1)\ ]\ R_n^{-r}(t-1)\,K_{n+1}^T(t), \tag{2.26}$$

$$[\ b_{n+1}(t)\ ] = [\ b_n(t-1)\ ] \ -\ [\ f_n(t)\ ]\ R_n^{-e}(t)\,K_{n+1}(t). \tag{2.27}$$

Here, $R_{n+1}^{-e}(t)\,K_{n+1}(t)$ means any p×p matrix α such that $R_n^e(t)\ \alpha = K_{n+1}(t)$ and $R_{n+1}^{-r}(t-1)\,K_{n+1}^T(t)$ means any p×p matrix β such that $R_n^r(t-1)\ \beta = K_{n+1}^T(t)$. That at least one such α and one such β exist follows from Lemma 2.1 and the existence of the projections in (2.18) and (2.19).

While (2.26) and (2.27) are more explicit than (2.18) and (2.19), they still are not useful for computation because columns of the matrices $[\ f_n(t)\ ]$ and $[\ b_n(t)\ ]$ are infinitely long. It turns out that only the top m rows of (2.26) and (2.27) are used in the lattice filter. Hence, it is useful to define the following m×p matrices:

$$e_n(t) = \text{ Top } m \text{ rows of } [\ f_n(t)\ ],\qquad r_n(t) = \text{ Top } m \text{ rows of } [\ b_n(t)\ ]. \tag{2.28}$$

Then, the top m rows of (2.26) and (2.27) are

$$e_{n+1}(t) = e_n(t) \ -\ r_n(t-1)\,R_n^{-r}(t-1)\,K_{n+1}^T(t), \qquad \text{forward residual} \tag{2.29}$$

$$r_{n+1}(t) = r_n(t-1) \ -\ e_n(t)\,R_n^{-e}(t)\,K_{n+1}(t), \qquad \text{backward residual.} \tag{2.30}$$

These two equations are used in the lattice filter for order updates of the forward and backward residuals. For order updates of $R^e(t)$ and $R^r(t)$, substituting (2.29) and (2.30) into (2.23) and (2.24) yields

$$R_{n+1}^e(t) = R_n^e(t) \ -\ K_{n+1}(t)\,R_n^{-r}(t-1)\,K_{n+1}^T(t),$$

$$R^r_{n+1}(t) = R^r_n(t-1) - K^T_{n+1}(t)\, R^{-e}_n(t)\, K_{n+1}(t)\,.$$

Time Updates

The following vectors are elements of $\ell_2(R^m, \lambda)$:

$$\phi^i = [\ 0 \quad 0 \quad \ldots \quad \underset{\text{position i}}{1} \quad 0 \quad \ldots \quad 0 \quad \ldots \quad]^T, \qquad i = 1,2, \ldots m \tag{2.31}$$

$$\hat{\phi}^i_n(t+1) = [\ I - P_n(t+1)\ ]\ \phi^i\ , \qquad i = 1,2, \ldots, m\,; \tag{2.32}$$

where $P_n(t+1)$ is the projection onto $H_n(t+1)$, as before. The subspace

$$\hat{H}_n(t+1) = span\ \{\ \psi^1(t), \ldots, \psi^p(t), \ \ldots, \psi^1(t-n+1), \ \ldots, \psi^p(t-n+1), \ \ldots, \phi^1, \ldots, \phi^m\ \}$$

is useful in deriving the time update equations for the variables $K_n(t)$. From (2.3)-(2.5) it follows that

$$\hat{H}_n(t+1) = span \left\{ \begin{pmatrix} 0^{(m)} \\ \psi^1(t-1) \end{pmatrix}, \ \ldots \begin{pmatrix} 0^{(m)} \\ \psi^p(t-1) \end{pmatrix}, \ \ldots \right. \\ \left. \begin{pmatrix} 0^{(m)} \\ \psi^1(t-n) \end{pmatrix}, \ \ldots \begin{pmatrix} 0^{(m)} \\ \psi^p(t-n) \end{pmatrix}, \ \phi^1, \ \ldots, \ \phi^m \right\}, \tag{2.33}$$

$$\hat{H}_n(t+1) = H_n(t+1) \overset{\perp}{\oplus} span\ \{\ \hat{\phi}^1_n(t+1), \ \ldots, \ \hat{\phi}^m_n(t+1)\ \}\,, \tag{2.34}$$

where $0^{(m)}$ is the m×m zero matrix. If

$$\hat{P}_n(t+1) = \text{ Projection onto } \hat{H}_n(t+1) \quad \text{ and}$$

$$Q_n(t+1) = \text{ Projection onto } span\ \{\ \hat{\phi}^1_n(t+1), \ \ldots, \ \hat{\phi}^m_n(t+1)\ \}\,, \tag{2.35}$$

it follows from (2.34) that $\hat{P}_n(t+1) = P_n(t+1) + Q_n(t+1)$, so that

$$[\ I - P_n(t+1)\ ] = [\ I - \hat{P}_n(t+1)\ ] + Q_n(t+1)\,. \tag{2.36}$$

Substituting (2.36) into (2.16) yields

$$b_n^j(t) = \mathrm{II} + \Gamma \ , \tag{2.37}$$

where

$$\mathrm{II} = [\ I - \hat{P}_n(t+1)\ ]\ \psi^j(t-n)\,, \qquad \Gamma = Q_n(t+1)\ \psi^j(t-n)\,.$$

From (2.3) and (2.31) it follows that

$$\psi^j(t-n) = \begin{pmatrix} 0^{(m)} \\ \psi^j(t-n-1) \end{pmatrix} + \sum_{k=1}^{m} y_k^j(t-n)\,\phi^k \ .$$

As in (2.2), y_k^j is the k^{th} scalar measurement in channel j. Also, in view of (2.33),

$$\mathrm{II} = [\ I - \hat{P}_n(t+1)\ ] \begin{pmatrix} 0^{(m)} \\ \psi^j(t-n-1) \end{pmatrix} = \begin{pmatrix} 0^{(m)} \\ [I - P_n(t)]\,\psi^j(t-n-1) \end{pmatrix} = \begin{pmatrix} 0^{(m)} \\ b_n^j(t-1) \end{pmatrix}. \tag{2.38}$$

According to (2.35) and Lemma 2.1,

$$\Gamma = [\ \hat{\phi}_n(t+1)\ ]\ \ G_n^{-1}(t)\,d\,, \tag{2.39}$$

where

$$[\ \hat{\phi}_n(t+1)\ ] = [\ \hat{\phi}_n^1(t+1)\ \ \hat{\phi}_n^2(t+1)\ \ \ldots\ \ \hat{\phi}_n^m(t+1)\ ]\,, \tag{2.40}$$

$$G_n(t) = m \times m \text{ matrix whose (i,j) element is } < \hat{\phi}_n^i(t+1)\,,\ \hat{\phi}_n^j(t+1) > \ , \tag{2.41}$$

$$d = m\text{-vector whose k element is } < \hat{\phi}_n^k(t+1)\,,\ \psi^j(t-n) > \ . \tag{2.42}$$

The expression $G_n^{-1}(t)\,d$ means any m-vector α such that $G_n(t)\,\alpha = d$, and it follows from Lemma 2.1 that at least one such α exists. Since $[\ I - P_n(t+1)\ ]$ is self-adjoint (being an orthogonal projection),

$$\begin{aligned} \text{k element of } d &= < \hat{\phi}_n^k(t+1), \psi^j(t-n) > \\ &= < \phi^k, [\ I - P_n(t+1)\ ]\,\psi^j(t-n) > = < \phi^k\,,\ b_n^j(t) > = r_n^{kj}(t)\,; \end{aligned} \tag{2.43}$$

i.e., the vector d in (2.42) is the j^{th} column of the matrix $r_n(t)$.

Now, since $[\, I - P_n(t+1)\,]$ is an orthogonal projection, it is self-adjoint and equal to its square. Hence, from (2.37),

$$< f_n^i(t+1),\ b_n^j(t) > = < \psi^i(t+1),\ b_n^j(t) > = < \psi^i(t+1),\ \Pi > \ +\ < \psi^i(t+1),\ \Gamma > \ . \qquad (2.44)$$

According to (2.1) and (2.38),

$$< \psi^i(t+1),\ \Pi > = \lambda\ < \psi^i(t),\ b_n^j(t-1) > = \lambda\ < f_n^i(t),\ b_n^j(t-1) > \ . \qquad (2.45)$$

Since

$$\begin{aligned} < \psi^i(t+1),\ \hat{\phi}_n^k(t+1) > &= < \ [I - P_n(t+1)]\,\psi^i(t+1),\ \phi^k > \\ &= < f_n^i(t+1),\ \phi^k > = e_n^{i,k}(t+1), \end{aligned}$$

using Γ from (2.39)-(2.43) yields

$$< \psi^i(t+1),\ \Gamma > = [\ i^{th} \text{ column of } e_n(t+1)\ ]^T\ G_n^{-1}(t)\ [\ j^{th} \text{ column of } r_n(t)\ ]\ . \qquad (2.46)$$

Now, equations (2.44)-(2.46) show that the time update equation for $K_{n+1}(t)$ (defined by (2.22)) is

$$K_{n+1}(t+1) = \lambda\, K_{n+1}(t) + e_n^T(t+1)\, G_n^{-1}(t)\, r_n(t)\ .$$

The final equation needed to complete the residual error lattice is the order update equation for $G_n(t)$. From (2.32) and (2.41), the elements of this matrix are

$$\begin{aligned} G_n^{i,j}(t) &= < \hat{\phi}_n^i(t+1),\ \hat{\phi}_n^j(t+1) > = < \hat{\phi}_n^i(t+1),\ \phi^j > \\ &= < \phi^i,\ \phi^j > \ -\ < P_n(t+1)\phi^i,\ \phi^j > \ . \end{aligned} \qquad (2.47)$$

The subspace $H_n(t+1)$ can be written as the following direct sum of orthogonal subspaces:

$$H_n(t+1) = E_{n-1}^b(t) \overset{\perp}{\oplus} E_{n-2}^b(t) \overset{\perp}{\oplus} \ \ldots\ \overset{\perp}{\oplus} E_0^b(t)\ ,$$

so that

$$P_n(t+1) = P_{n-1}^b(t) \ +\ P_{n-2}^b(t) \ +\ \ \ldots\ \ +\ P_0^b(t)\ , \qquad (2.48)$$

According to (2.17), (2,28) and Lemma 2.1,

$$< P_k^b(t)\phi^i , \phi^j > = [\ r_k^{j,1}(t) \ \ldots \ r_k^{j,p}(t)\ ]\ R_k^{-r}(t) \begin{bmatrix} r_k^{i,1}(t) \\ \vdots \\ r_k^{i,p}(t) \end{bmatrix} .$$

Therefore, in view of (2.48), (2.47) becomes

$$G_n(t) = I - \sum_{k=0}^{n-1} r_k(t)\, R_k^{-r}(t)\, r_k^T(t) , \quad n = 1, 2, \ldots . \tag{2.49}$$

Since $P_0(t+1) = 0$ (recall (2.5), (2.6)), it follows from (2.32) and (2.41) that

$$G_0(t) = I . \tag{2.50}$$

Also, (2.49) and (2.50) yield

$$G_{n+1}(t) = G_n(t) - r_n(t)\, R_n^{-r}(t)\, r_n^T(t) , \qquad n = 0,1,2 \ldots . \tag{2.51}$$

It should be noted that in previous lattices, including the lattice in [10], the update equation corresponding to this last equation has a scalar $G_n(t)$ instead of the m×m matrix $G_n(t)$ here.

AR Coefficients

For each i = 1,...p, $P_n(t)\psi^i(t)$ can be written as a linear combination of the history vectors that span $H_n(t)$, and $P_n(t+1)\psi^i(t-n)$ can be written as a linear combination of the history vectors that span $H_n(t+1)$. This means that, with the notation in (2.25),

$$[\ f_n(t)\ ] = [\ \psi(t)\ ] - \sum_{j=1}^{n} [\ \psi(t-j)\ ]\ A_{nj}(t) , \quad n = 1,2,... \tag{2.52}$$

$$[\ b_n(t)\ ] = [\ \psi(t-n)\ ] - \sum_{j=1}^{n} [\ \psi(t-j+1)\ ]\ B_{nj}(t) , \quad n = 1,2,... \tag{2.53}$$

where $A_{nj}(t)$ and $B_{nj}(t)$ are p × p matrices and

$$[\ \psi(t)\ ] = [\ \psi^1(t) \ \ \psi^2(t) \ \ldots \ \psi^p(t)\ ] . \tag{2.54}$$

Since $[\, f_n(t)\,]$ is the error remaining after orthogonal projection of the data taken through time t (recall (2.2)-(2.3)) onto the history space $H_n(t)$, the coefficient matrices $A_{nj}(t)$ minimze the $\ell_2(R^m, \lambda)$ norm of $[\, f_n(t)\,]$ over all autoregressive models of order n. The matrices $A_{nj}(t)$ are called the AR coefficients at time t .

Substituting (2.52) and (2.53) into the order updates in (2.26) and (2.27) and matching coefficients of the history vectors $\psi^i(t-j)$ yields

$$A_{n+1\,j}(t) = A_{nj}(t) - B_{nj}(t-1)\,R_n^{-r}(t-1)\,K_{n+1}^T(t)\,, \qquad j = 1,2,\ldots,n, \quad n = 1,2,\ldots \tag{2.55}$$

$$A_{n+1,n+1}(t) = R_n^{-r}(t-1)\,K_{n+1}^T(t), \qquad n = 0,1,2,\ldots \tag{2.56}$$

$$B_{n+1\,j+1}(t) = B_{nj}(t-1) - A_{nj}(t)\,R_n^{-e}(t)\,K_{n+1}(t) \qquad j = 1,2,\ldots,n, \quad n = 1,2,\ldots \tag{2.57}$$

$$B_{n+1,1}(t) = R_n^{-e}(t)\,K_{n+1}(t), \qquad n = 0,1,2,\ldots. \tag{2.58}$$

The AR coefficients, $A_{n+1}(t)$, can be generated with (2.55)-(2.58); however, this algorithm requires that the AR coefficients be calculated at every sampling time because $B_{nj}(t-1)$ is needed to compute $A_{n+1}(t)$. The following derivation provides an algorithm for computing the AR coefficients at any time t without the values of $A_{nj}(t-1)$ and $B_{nj}(t-1)$.

Using (2.11) in (2.32) with the notation in (2.40) yields

$$\begin{aligned}\hat{\phi}^i_{n+1}(t+1) &= [\, I - P_{n+1}(t+1)\,]\,\phi^i = [\, I - P_n(t+1)\,]\,\phi^i - P_n^b(t)\,\phi^i \\ &= \hat{\phi}^i_n(t+1) - P_n^b(t)\,\phi^i = \hat{\phi}^i_n(t+1) - [\, b_n(t)\,]\,R_n^{-r}(t)\begin{bmatrix} r_n^{i,1}(t) \\ \vdots \\ r_n^{i,p}(t) \end{bmatrix}\end{aligned}$$

or

$$[\, \hat{\phi}_{n+1}(t+1)\,] = [\, \hat{\phi}_n(t+1)\,] - [\, b_n(t)\,]\,R_n^{-r}(t)\,r_n^T(t)\,. \tag{2.59}$$

Since $P_n(t+1)\,\phi^i \in H_n(t+1)$, it follows from (2.5) and (2.32) that there exist p × m matrices $C_{nj}(t)$ such that

$$[\,\hat{\phi}_{n+1}(t+1)\,] = [\,\phi\,] - \sum_{j=1}^{n} [\,\psi(t-j+1)\,]\; C_{nj}(t), \quad n = 1,2,... \tag{2.60}$$

where $[\,\phi\,] = [\,\phi^1 \quad \phi^2 \quad ... \quad \phi^m\,]$. Substituting (2.53) and (2.60) into (2.59) and matching coefficients of the history vectors yields

$$C_{n+1,j}(t) = C_{nj}(t) - B_{nj}(t)\, R_n^{-r}(t)\, r_n^T(t) \qquad j = 1,2,...,n, \quad n = 1,2,..., \tag{2.61}$$

$$C_{n+1,n+1}(t) = R_n^{-r}(t)\, r_n^T(t), \quad n = 0,1,2,.... \tag{2.62}$$

The expression $[\,\hat{b}_n(t)\,]$ will denote the part of $[\,b_n(t)\,]$ below the first m rows. Then, from (2.53)

$$[\,\hat{b}_n(t)\,] = [\,\psi(t-n-1)\,] - \sum_{j=1}^{n} [\,\psi(t-j)\,]\, B_{nj}(t), \quad n = 1,2,.... \tag{2.63}$$

Next, the developement in (2.37)-(2.43) yields

$$[\,b_n(t)\,] = \begin{bmatrix} 0^{(m)} \\ [\,b_n(t-1)\,] \end{bmatrix} + [\,\hat{\phi}_n(t+1)\,]\, G_n^{-1}(t)\, r_n(t). \tag{2.64}$$

After substitution of (2.60) into (2.64), the new equation from row (m + 1) down is

$$[\,\hat{b}_n(t)\,] = [\,b_n(t-1)\,] - \sum_{j=1}^{n} [\,\psi(t-j)\,]\, C_{nj}(t)\, G_n^{-1}(t)\, r_n(t), \quad n = 1,2,.... \tag{2.65}$$

Finally, equating the right sides of (2.63) and (2.65), using the right side of (2.53) for $b_n(t-1)$, and matching the coefficients of the history vectors yields

$$B_{nj}(t-1) = B_{nj}(t) - C_{nj}(t)\, G_n^{-1}(t)\, r_n(t), \qquad j = 1,2,...,n, \qquad n = 1,2,.... \tag{2.66}$$

The algorithm consisting of equations (2.55)-(2.58), (2.61), (2.62) and (2.66) can be started at any time to obtain the AR coefficients. The order of the AR coefficients need not remain the same from one time to another. In addition to this flexibility, this method is computationally attractive when the sampling rate is high but the plant and/or control parameters need not be updated at every sample time. The residual filter is the only part that must be computed at every time step.

3. IMPLEMENTATION

Summary of the Lattice Algorithms

Recall the definition (2.2) for the measurement vectors $y^i(t)$. We define the m · p matrix

$$y(t) = [\, y^1(t) \quad y^2(t) \quad \ldots \quad y^p(t) \,]$$

which contains the measurements at time t. We start the lattice filter at time t = 0 with the following initialization:

$$R_0^e(-1) = R_0^r(-1) = \sigma I \ , \qquad K_{n+1}(t) = 0 \ \text{ for } \ n+1 > t \geq 0 \ , \tag{3.1}$$

where σ is a small number. If $\sigma = 0$, this initialization corresponds to what commonly is called prewindowing, which means taking $y(t) = 0$ for all $t < 0$. We have found that taking σ on the order of 10^{-7} avoids numerical problems with inverting certain matrices in the filter, as discussed below.

Residual Error Lattice

For each t ≥ 0:

$$e_0(t) = r_0(t) = y(t) \ , \qquad R_0^e(t) = R_0^r(t) = y(t)^T y(t) + \lambda \, R_0^r(t-1) \ , \qquad G_0(t) = I. \tag{3.2}$$

For each t ≥ 1, for n = 0 to t-1:

$$K_{n+1}(t) = \lambda \, K_{n+1}(t-1) + e_n^T(t) \, G_n^{-1}(t-1) \, r_n(t-1) \tag{3.3}$$

$$e_{n+1}(t) = e_n(t) \ - \ r_n(t-1) \, R_n^{-r}(t-1) \, K_{n+1}^T(t) \tag{3.4}$$

$$r_{n+1}(t) = r_n(t-1) \ - \ e_n(t) \, R_n^{-e}(t) \, K_{n+1}(t) \tag{3.5}$$

$$R_{n+1}^e(t) = R_n^e(t) \ - \ K_{n+1}(t) \, R_n^{-r}(t-1) \, K_{n+1}^T(t) \tag{3.6}$$

$$R_{n+1}^r(t) = R_n^r(t-1) \ - \ K_{n+1}^T(t) \, R_n^{-e}(t) \, K_{n+1}(t) \tag{3.7}$$

$$G_{n+1}(t) = G_n(t) \ - \ r_n(t) \, R_n^{-r}(t) \, r_n^T(t) \qquad n = 0,1,2 \ldots \tag{3.8}$$

The maximum n can be increased by one with each successive time step. In practice, though, n is not increased past some fixed order, due to finite computational capacity.

AR Coefficients

The top m rows of (2.52) are

$$e_n(t) = y(t) - \sum_{j=1}^{n} y(t-j)\, A_{n,j}(t) \ , \quad n = 1,2, \ \ldots \ .$$

At any time t, the AR coefficients $A_{n,j}(t)$ can be generated from the residual filter data by the following:

For n = 1, t-1 and for i = 1,n

$$C_{n+1,i}(t) = C_{n,i}(t) - B_{n,i}(t)\, R_n^{-r}(t)\, r_n^T(t) \tag{3.9}$$

$$B_{n+1,i+1}(t) = [\ B_{n,i}(t) - C_{n,i}(t)\, G_n^{-1}(t)\, r_n(t)\ ] - A_{n,i}(t)\, R_n^{-e}(t)\, K_{n+1}(t) \tag{3.10}$$

$$A_{n+1,i}(t) = A_{n,i}(t) - [\ B_{n,i}(t) - C_{n,i}(t)\, G_n^{-1}(t)\, r_n(t)\ ]\ R_n^{-r}(t-1)\, K_{n+1}^T(t) \tag{3.11}$$

where equations (2.56), (2.58), and (2.62) are used as end conditions.

Matrix Inverses

If $R_n^e(t)$, $R_n^r(t)$ and $G_n(t)$ are nonsingular, then $R_n^{-e}(t)$, $R_n^{-r}(t)$ and $G_n^{-1}(t)$ are the respective inverses. If any of these matrices is singular, then the inverse should be interpreted as indicated after (2.27). If the measurements are independent, then $R_n^e(t)$, $R_n^r(t)$ and $G_n(t)$ are positive definite unless one of the channels (or a linear combination of the channels) fits the n^{th} order AR model exactly. We have found, however, that letting letting $R_0^e(-1) = R_0^r(-1) = \sigma\, I$ eliminates most numerical problems.

One Step Ahead Prediction

The n^{th} order least-squares prediction of $y(t)$, based on measurements up to and including time t-1, is

$$\hat{y}_n(t) = \sum_{j=1}^{n} y(t-j)\, A_{n,j}(t-1) \ , \quad n = 1,2, \ \ldots \ . \tag{3.12}$$

Equivalently, the least-squares prediction of $y(t)$ is the matrix $\hat{y}_n(t)$ that, if taken as the measurement at time t, yields $e_n(t) = 0$. This second interpretation of $\hat{y}_n(t)$ leads to an algorithm for its computation. Writing (2.15) in the notation of (2.25) and (2.54) yields

$$[\, f_n(t)\,] = [\, I - P_n(t)\,]\,[\,\psi(t)\,]$$
$$= [\, I - P_n(t)\,]\,[\,\phi\,]\, y(t) + [\, I - P_n(t)\,] \begin{bmatrix} 0^{(m\times p)} \\ \psi(t-1) \end{bmatrix} . \qquad (3.13)$$

The fact that the top m rows of $[\, f_n(t)\,]$ are $e_n(t)$ and an argument similar to the argument involving (2.47)-(2.50) show that the top m rows of (3.13) are

$$e_n(t) = G_n(t-1)\, y(t) + \hat{e}_n(t) ,$$

where $\hat{e}_n(t)$ is the value of $e_n(t)$ generated by the lattice for $y(t) = 0$. The prediction then is

$$\hat{y}_n(t) = - G_n^{-1}(t-1)\, \hat{e}_n(t) , \quad n = 1,2 \ldots . \qquad (3.14)$$

This prediction can be generated with only (3.2)-(3.4) of the residual error lattice algorithm.

Including Known Inputs

When there is only one measurement in each channel (i.e., m = 1), the algorithm presented in Section 2 reduces to the lattices derived in [2] and [3]. One of the major advantages of the algorithm in this paper, as mentioned before, is its capacity to accomodate an ARMA model in which all outputs have the same Auto Regressive structure. For such a model, the following imbedding accomodates an input that does not have the same MA coefficients for each channel.

Let there be m scalar outputs, $y_i^1(t)$, and one scalar input u(t). The first channel then is $[\, y_1^1(t), \ldots, y_m^1(t)\,]^T$. The second channel is the m-vector [u(t), 0,... 0]^T. The third channel is [0, u(t), 0,... 0]^T, and finally, the (m + 1) channel is the m-vector [0, 0, ...0, u(t)]^T.

It is easy to see that with these definitions, the desired model can be imbedded into a p-channel (p = m + 1) vector-channel Auto Regressive model. The extension to the case of more than one input is obvious. For m outputs and k inputs, the resulting vector-channel lattice has one channel for the outputs and mk channels for the inputs (and the corresponding copies).

4. EXAMPLE

Description of the Structure and Data Generation

A flexible beam is cantilivered to a rigid disc with fixed center, and a torsional spring is attached to the disc. In-plane motion, including the linear transverse vibration of the beam is modeled. The beam is modeled as an Euler-Bernoulli beam with the properties listed in Table 1. The system has one input, the torque applied to the hub, and two outputs, the elastic tip deflection η and hub rotation θ.

FIGURE 1. The Beam-Hub Model

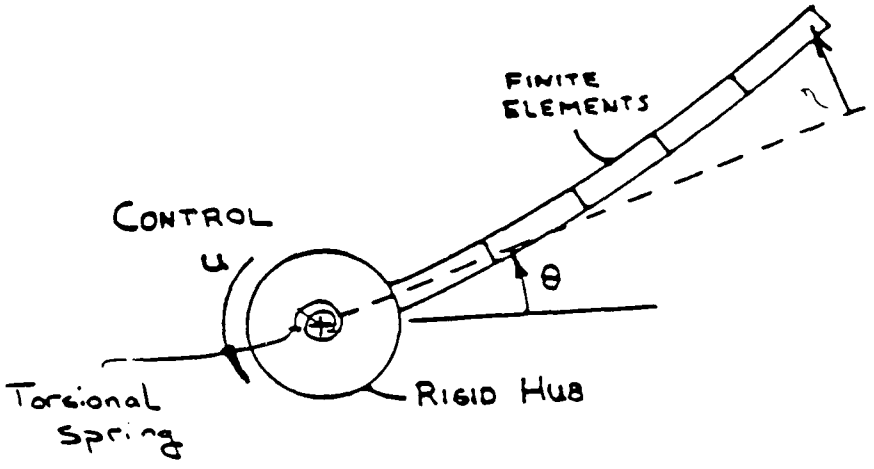

TABLE 1. Structural Characteristics

Mass per unit length	= .000288 slug/ inch
Hub moment of inertia	= 85.6 slg in^2
EI for the beam	= 40,506,000 slug in^3/sec^2
Torsional spring constant	= 85,600 lb-in
Beam length	= 1036.7 inches
Hub radius	= 46 inches
Modal Damping Ratio	= .005 (.5 % critical) in each mode

To generate input-output data, the state space representation of the first 12 modes of the structure was excited by a sequence of piecewise constant torques. A finite element model with 15 uniform beam elements (31 degrees of freedom) was used to compute the first 12 modes of the structure. The length of the sampling interval and the duration of the piecewise constant torques was .05 seconds (20 samples per

second). The input torque sequence was obtained from an IMSL subroutine that generates Gaussian random sequences with mean zero and variance 10,000.

Table 2 contains the true discrete-time system eigenvalues and their magnitudes, and the damping ratios (Zeta) and frequencies (Freq in rad/s) for the corresponding continuous-time eigenvalues. (From here on, *true system* means the first 12 modes of the finite element model.) The continuous-time frequencies and damping ratios were obtained from the logarithms of the discrete-time eigenvalues. The first five modes of the system are below the Nyquist frequency (10 Hz). For these modes, the frequencies and damping ratios in the first five rows of Table 2 are correct. For the modes above the Nyquist frequency, aliasing produces frequencies lower than the correct values and damping ratios higher than the correct values. (The aliased frequencies and damping ratios are listed in Table 2 for comparison with the subsequent eigenvalue estimates.) In Table 2, eigenvalues are ordered according to magnitudes.

TABLE 2. True System Eigenvalues (Discrete-Time)

	Real Part	Imaginary Part	Zeta	Freq	Magnitude
1	0.999390	0.034733	0.005000	0.694825	0.999827
2	0.961521	0.269716	0.005000	5.469626	0.998634
3	0.676489	0.730860	0.005000	16.480264	0.995888
4	-0.099991	0.986622	0.005000	33.435967	0.991676
5	-0.932683	0.319972	0.005000	56.222164	0.986043
6	-0.444545	0.872270	0.010383	40.842544	0.979018
7	0.924166	0.296545	0.095783	6.209997	0.970578
8	-0.164358	0.946500	0.023021	34.854594	0.960664
9	-0.515252	0.797210	0.024291	42.891594	0.949225
10	0.766445	0.537675	0.107091	12.234877	0.936233
11	-0.759660	0.521941	0.032095	50.791924	0.921686
12	0.503091	0.753000	0.100486	19.635824	0.905600

For studying the effects of measurement noise, small amounts of white noise were added to the outputs and the resulting noisy measurements were fed into the lattice filters. Note that three uncorrelated sequences of white noise were used. The first was the torque, which was an input known to the lattice; hence this sequence was white noise only in the sense of its statistics and the lattice saw it as a known deterministic input. The other two white noise sequences were scaled by various amounts and, in some cases, added to the data from the two sensors to produce the noisy measurement sequences that were fed into the lattice. This measurement noise was not known to the lattice.

It is well known that, in the presence of measurement noise, the least-squares method yields biased estimates for the AR coefficients. If it is essential to obtain accurate estimates for these parameters, other identification methods such as extended least squares (ELS) or instrumental variable (IV) methods can be used. The least-squares lattice can be modified easily for the ELS method. For lattice implementation of the IV method, see [15] or [16].

We processed input/output data with the lattice filters to estimate the number of excited modes (one half of the plant order) and the ARMA coefficients. From the AR coefficients, we obtained estimates for plant eigenvalues. We used a vector-channel lattice and two standard lattices for comparison. The vector-channel lattice had three channels, each with two components, (p = 3, m = 2). Channel 1 contained the two measurements (hub rotation and tip deflection); Channels 2 and 3 contained, as described at the end of section 3, the required copies of the input torque. We used the two standard lattices independently for the hub rotation measurement and for the tip deflection measurement. Each of these lattices had two one dimensional channels (p = 2, m = 1), Channel 1 for the measurement (hub or tip) and Channel 2 for the input torque. Due to the ambiguous relationship between minimal lattice order and the number of excited modes, mentioned in Section 1, and the possibility of extraneous eigenvalues, we did not use both measurements together in a standard multi-input-multi-output lattice. For all runs, the value of the forgetting factor λ was 0.95.

Order Determination

Recall the definition (2.23) for $R_n^e(t)$. Each diagonal element of this matrix is the square of the n^{th} order forward error norm for the corresponding channel. Figure 2, which was obtained from the vector-channel lattice after 300 steps, shows the behavior of the (1,1) element of $R_n^e(t)$ (the norm of the forwasr error for the first vector measurement channel) as n increases. Recall that the first channel of the vector-channel lattice contains the measurements from both sensors. The lowest curve corresponds to the no-noise case. The other curves correspond to successively increasing amounts of noise added to the measurements.

The effective order of the structure, which is twice the number of significantly excited modes, can be determined from how $R_n^e(t)$ varies with the lattice order n. The most important feature of the three curves

in Figure 2 is the drop as the lattice order goes from 10 to 12 (i.e., from 5 to 6 modes). This drop indicates that the effective order of structure is 12.

The behavior of the (1,1) element of $R_n^e(t)$ in the absence of measurement noise indicates that six modes are excited substantially by the input. The remaining six modes in the simulation model are excited minimally and contribute little to the output. The drastic drop in the graph between n = 10 and n = 12 occurs when the order of the filter matches the number of substantially excited modes. (The plant order must be even.) As n increases past 12, more and more of the output from the minimally excited modes is accounted for, until the forward error falls to zero at n = 24 because a 24^{th} order ARMA model fits all of the output.

When small amounts of noise are added to the measurements, the graph changes. The drop still occurs between 10 and 12, but its magnitude decreases as the amount of measurement noise increases. Furthermore, as n increases past 12, the (1,1) element of $R_n^e(t)$ hardly decreases at all. The excitation of the structure is the same with and without measurement noise, but the output from the minimally excited modes is lost in the measurement noise and the filter cannot distinguish these modes from the noise. With increasing measurement noise, the graph approaches a level straight line, indicating that the filter is distinguishing less and less data from the structure and noise.

The accuracy of the subsequent eigenvalue estimates indicates, as expected, that the five sub-Nyquist frequency modes are excited most and the first mode above the Nyquist frequency is excited substantially though lass than the first five. Different input sequences, including combinations of many sinewaves, produced the same behavior. In all cases, only the frequencies below Nyquist frequency are excited substantially. This is not surprizing, since the input is applied at the sampling frequency.

Several authors have suggested criteria to estimate the order of a system from input-output data, see [9,17]. Each of these criteria looks for a minimum of a scalar function of the form

$$F(n) = t \ \ln \left[\ 1/t \times R_n^e(t) \ \right] + n \times f(t) . \tag{4.1}$$

The major difference among these criteria is the choice of $f(t)$. For the systems studied here, a variety of these methods were attempted and none performed noticeably better than the (1,1) element of $R_n^e(t)$ alone, as used in Figure 2.

Figure 2. Norm of the Forward Error vs. Lattice Order

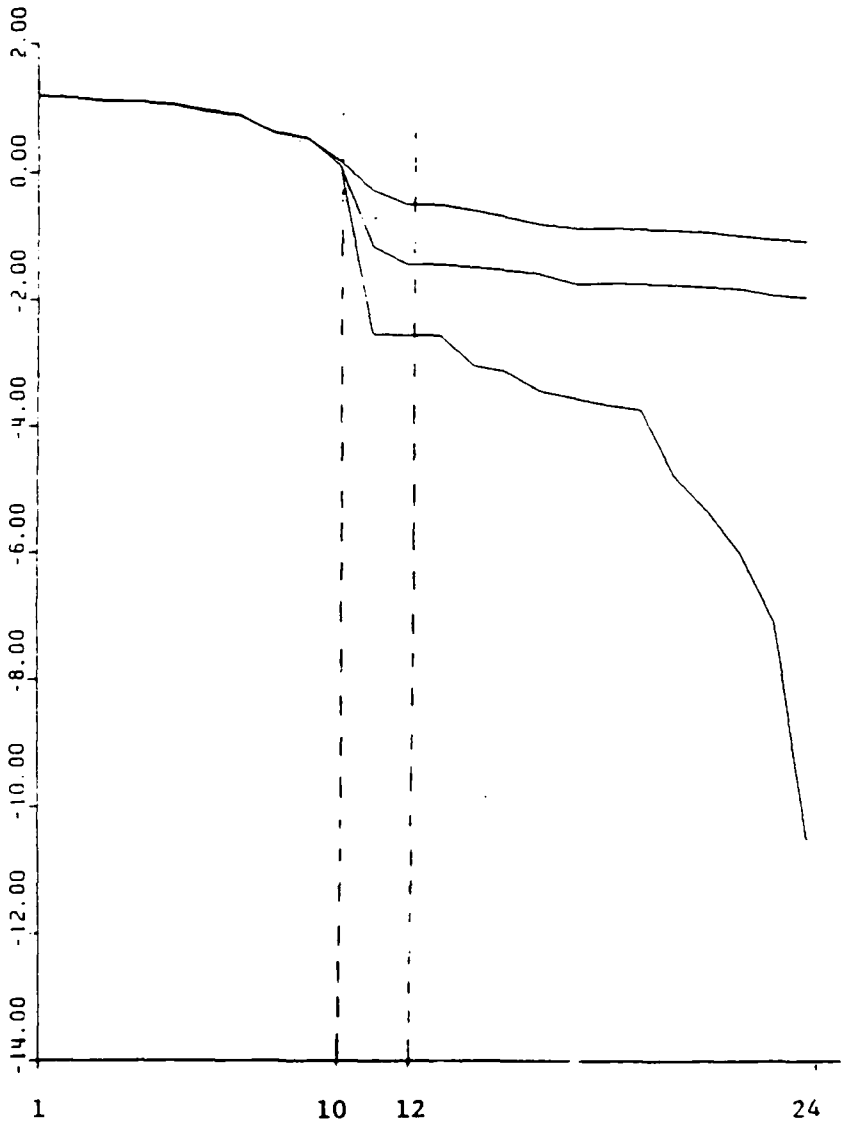

Top curve : 9% noise in each channel.
Middle curve : 3% noise in each channel.
Bottom curve : No noise.

Estimation of Eigenvalues, Frequencies and Damping Rations

To estimate the eigenvalues of the structure, we generated the estimates of the AR coefficients with the algorithm in Section 3, for various orders, and computed the eigenvalues of the AR model. The only case in which the estimated AR coefficients were correct was where there was no sensor noise and the lattice order was 24 (full order; i.e., the order of the true system), but the estimated eigenvalues for the sub-Nyquist modes are generally good for low measurement noise and lattice order 18 or greater. This is possible because most of the AR coefficients of a large order system are highly sensitive to perturbations in the eigenvalues and, conversely, the eigenvalues are relatively insensitive to perturbations in the AR coefficients. The relationship established by Cayley-Hamilton between the AR coefficients and the eigenvalues makes the high sensitivity of AR coefficients with respect to eigenvalues apparent.

In this section, we are interested primarily in the effects of measurement noise and unmodeled modes. In the absence of noise, all the eigenvalues corresponding to the higher modes were identified, given high enough filter order. The full-order vector-channel lattice (order 24) identified all of the system eigenvalues with four or more significant digits, except one of the faster modes, which had only three digit accuracy. The full-order standard lattice for either measurement produced eigenvalue estimates with 2 to 3 accurate significant digits. Table 3 compares standard and vector-channel lattices for the 18^{th}-order filter with no noise added to the measurements.

In Tables 3 and 4, complex eigenvalues are represented by their continuous-time damping ratio and frequency and discrete-time magnitude. The frequencies, damping ratios and magnitudes estimated for the first five modes are listed first. Then, the aliased frequencies and damping ratios estimated for the remaining modes are ordered according to the magnitude of the corresponding discrete-time eigenvalues. (These aliased frequencies and damping ratios are all that can be identified from the input/output data, without other knowledge of the true system.) In practice, the magnitudes of the eigenvalues are likely to be the only tool for proper ordering. It is common in structures, for example, that discrete-time eigenvalues corrsponding to higher modes have smaller magnitudes.

To study the effects of measurement noise, we added small amounts of noise, roughly 3% of the output on average, to the measurements. Table 4 compares the scalar and vector-channel lattices for this case.

TABLE 3. Lattice Comparisons : No Noise

Order = 18

After 1500 Steps

Zeta	Freq	Mag
Tip Displacement Lattice		
-0.1793	0.6866	1.0063
0.0057	5.4705	0.9984
0.0050	16.4786	0.9959
0.0051	33.4305	0.9914
0.0050	56.2204	0.9861
0.0122	40.7381	0.9754
0.0474	48.4888	0.8913
0.0785	34.8581	0.8717
positive real		0.2882
negative real		0.1907
Hub Rotation Lattice		
0.1301	0.6933	0.9955
0.0060	5.4721	0.9984
0.0050	16.4791	0.9959
0.0052	33.4310	0.9913
0.0050	56.2205	0.9861
0.0128	40.7135	0.9744
0.0487	48.6059	0.8882
0.0953	35.2980	0.8445
0.8384	31.6749	0.0875
Vector-Channel Lattice		
0.0809	0.6987	0.9972
0.0060	5.4696	0.9984
0.0050	16.4790	0.9959
0.0052	33.4304	0.9914
0.0050	56.2214	0.9861
0.0125	40.7320	0.9748
0.0470	48.6657	0.8919
0.0886	35.1743	0.8551
positine real		0.1289
negative real		0.0697

TABLE 4. Lattice Comparison: Noisy Measurements

Order = 24 (Full Order)

After 1200 Steps

Zeta	Freq	Mag
Tip Displacement Lattice		
-0.0813	0.7219	1.0029
0.0046	5.4668	0.9988
0.0052	16.4814	0.9957
0.0056	33.4273	0.9907
0.0056	56.2121	0.9845
0.0103	40.7798	0.9793
0.0129	44.9677	0.9714
0.0151	50.1422	0.9627
0.0676	22.8835	0.9254
0.0564	28.5524	0.9226
0.3655	15.4049	0.7390
negative real		0.9540
negative real		0.3509
Hub Rotation Lattice		
0.0593	0.6802	0.9980
0.0048	5.4703	0.9987
0.0051	16.4789	0.9958
0.0054	33.4057	0.9911
0.0052	56.2204	0.9854
0.0035	45.9140	0.9921
0.0123	40.6022	0.9754
0.0192	51.8548	0.9515
0.0668	27.8271	0.9110
0.0717	26.0990	0.9104
0.1526	15.2101	0.8892
negative real		0.9563
negative real		0.2579
Vector-Channel Lattice		
0.0133	0.6941	0.9995
0.0044	5.4658	0.9988
0.0051	16.4795	0.9958
0.0055	33.4165	0.9908
0.0054	56.2169	0.9850
0.0113	40.7037	0.9772
0.0118	45.4384	0.9735
0.0209	51.3041	0.9479
0.0677	27.9494	0.9096
0.0924	25.0789	0.8902
0.2028	15.6399	0.8505
negative real		0.9521
negative real		0.3142

Order = 20

After 1500 Steps

Zeta	Freq	Mag
Tip Displacement Lattice		
0.9710	0.2177	0.9567
0.0031	5.4718	0.9992
0.0040	16.4631	0.9967
0.0057	33.4298	0.9906
0.0039	56.3435	0.9890
0.0141	23.6348	0.9835
0.0119	40.8653	0.9760
0.0142	46.7545	0.9674
0.4058	24.7266	0.5776
negative real		0.9338
negative real		0.3413
Hub Rotation Lattice		
0.3404	0.7049	0.9873
0.0108	5.4909	0.9970
0.0049	16.4915	0.9960
0.0054	33.4236	0.9909
0.0059	56.2616	0.9835
-0.0057	48.1314	1.0138
0.0048	41.0987	0.9901
0.0951	21.7632	0.9013
0.1231	27.0668	0.8455
0.0909	58.5534	0.7655
Vector-Channel Lattice		
0.6853	0.5977	0.9723
0.0052	5.4792	0.9986
0.0044	16.4813	0.9964
0.0055	33.4307	0.9908
0.0055	56.2822	0.9848
0.0044	48.2454	0.9894
0.0074	40.9636	0.9849
0.0553	23.5206	0.9370
0.2774	26.0845	0.6863
negative real		0.8681
negative real		0.4307

Order = 18

After 1500 Steps

Zeta	Freq	Mag
Tip Displacement Lattice		
0.0031	5.459|	0.9991
0.0040	16.4651	0.9967
0.0057	33.4285	0.9905
0.0041	56.3500	0.9886
-0.0059	23.8576	1.0070
0.0133	40.8553	0.9731
0.0203	46.4778	0.9538
positive real		0.9759
negative real		0.9238
positive real		0.9001
positive real		0.0355
Hub Rotation Lattice		
0.0153	5.4965	0.9958
0.0044	16.4938	0.9964
0.0054	33.4298	0.9909
0.0064	56.2400	0.9821
0.0014	41.1753	0.9972
0.0527	24.0119	0.9386
0.0282	48.6725	0.9335
positive real		0.9648
positive real		0.9510
negative real		0.7082
negative real		0.1385
Vector-Channel Lattice		
0.9594	0.2498	0.9584
0.0065	5.4728	0.9982
0.0043	16.4825	0.9965
0.0056	33.4308	0.9907
0.0056	56.2721	0.9843
0.0080	40.9916	0.9837
0.0193	24.1705	0.9769
0.0174	48.0543	0.9591
negative real		0.8362
negative real		0.0488

Overall, the lattices produced good estimates for the modes below the Nyquist frequency. The eigenvalue corresponding to the first mode above the Nyquist frequency also was obtained with reasonable accuracy, although the frequency and the damping ratio for this mode are aliased. The lowest mode, corresponding to the hub rotation, is the hardest among the first five to identify. Longer data sets and higher-order filters are needed to obtain reasonable estimates for this mode. In general, the reduced-order lattices require more data points to obtain good estimates of frequencies and damping ratios.

Generally, lattices of order lower than 18 missed the lowest mode entirely, but identified the other four sub-Nyquist frequencies satisfatorily, although some of the damping ratios were quite inaccurate. If we only need small prediction error from the filter (say, for adaptive control), then Figure 2 indicates that 12 is a sufficient lattice order.

When we added sensor noise that was on average 5% of the sensor data, the results were almost as good as those in the tables for 3% noise. For noise levels of 9% and above, the filter identified only one or two of the higher sub-Nyquist frequencies and yielded poor estimates for damping ratios. This is consistent with Figure 2, which indicates that the lattice filter has trouble distinguishing between the structural dynamics and the greater sensor noise. We expect that the estimates of the lowest frequencies would improve with more samples, which would cover more periods of the lower frequencies.

Tables 3 and 4 indicate the advantages of the vector-channel lattice. The vector-channel estimates for the lowest mode are significantly better than those obtained by the independent standard lattices. For the rest of the modes, where standard lattices produced good estimates, the vector-channel produced estimates close to the average of the two independent standard lattices.

The ordering of the eigenvalues is also important. Often the standard lattices estimated erroneous eigenvalues whose magnitudes were greater than the magnitudes of the true eigenvalues. Sometimes these erroneous eigenvalues even had magnitudes greater than one (and negative damping ratios). This greatly complicates identifying the true modes below the Nyquist frequency.

We found that, in a large majority of comparisons, the vector-channel lattice estimates were at least as good as or better than the estimates from either standard lattice. However, since the vector-channel estimate is a kind of average of the individual standard lattice estimates, it is possible that one sufficiently

noisy measurement channel can cause the vector-channel estimate to be worse than another single channel estimate. This happened in Table 4, for example, where the standard lattice for the hub channel estimated a negative damping ratio, which caused the vector-channel lattice to estimate an incorrect mode with frequency 48.2 and damping ratio similar to that of the true modes.

5. CONCLUSIONS

We have developed a least-squares lattice filter that can constrain the coefficients in the AR model to be the same for some or all of the channels of a multi-output system. If this constraint is not imposed, the vector-channel lattice here reduces to the standard multi-input-multi-output least-squares lattice filter. Even in the standard lattice case, the derivation in Section 2 is needed for current research on the performance of lattice filters applied to distributed systems, which require infinite histories in the AR models. To handle forced-response data, as opposed to impulse response, the vector-channel lattice must accomodate scalar input (MA) channels as well as vector measurement channels. A method for this has been demonstrated, although the number of channels grows large fast with multiple inputs.

The primary motivation for the vector-channel lattice has been adaptive identification and control of flexible structures. Constraining all measurement channels to have the same AR model introduces information into the estimation algorithm that reduces the effect of sensor noise, as demonstrated by the numerical results in Section 4. The numerical results also show that the frequencies and damping ratios for the most significant modes can be identified with a lattice whose order is lower than the number of excited modes, even in the presence of noise.

REFERENCES

1. S. Ljung and L. Ljung, "Error Propagation of Recursive Least-squares Adaptation Algorithms", Automatica, vol 21., pp. 157-167, 1985.

2. D.T.L. Lee, M. Morf and B. Friedlander, "Recursive Least Squares Ladder Estimation Algorithms", IEEE Trans. on Acoustics, Speech, and Signal Processing , vol. 29, pp. 627-641, 1981.

3. D.T.L. Lee, B. Friedlander and M. Morf, "Recursive Ladder Algorithms For ARMA Modeling", IEEE Trans. on Automatic Control , vol. 27, pp. 753-764, 1982.

4. B. Freidlander, "Lattice Filters For Adaptive Processing", Proceedings of The IEEE, vol. 70, pp 828-867, 1982.

5. M.L. Honig and D.G. Messerschmitt, D. G., Adaptive Filters, Kluwer Academic Publishers, 1984.

6. L. Ljung and T. Soderstrom, Theory and Practice of Recursive Identification, The MIT press, 1983.

7. G.C. Goodwin and K.S. Sin, Adaptive Filtering, Prediction and Control, Prentice-Hall, 1984.

8. N. Sundararajan and R.C. Montgomery, "Identification of Structural Dynamics Systems Using Least-Squares Lattice Filters" , Lattice Filters" , AIAA Journal of Guidance, Control and Dynamics , vol. 6, pp 374-381, 1983.

9. N. Sundararajan and R.C. Montgomery, "Adaptive Modal Control of Structural Dynamics Systems Using Recursive Lattice Filters", AIAA Journal of Guidance, Control and Dynamics , vol. 8, pp. 223-229, 1985.

10. D.M. Wiberg, "Frequencies of Vibration Estimated by Lattices", J. of Astronautical Sciences , vol. 33, pp 35-47, 1985.

11. D.M. Wiberg and J.T. Gillis, "Estimation of Frequencies of Vibration Using Lattices", Proc. of 24th IEEE-CDC, Ft. Lauderdale, FL., Dec. 1985.

12. J.S. Gibson and F. Jabbari, "Discrete Time Optimal Control of Flexible Structures", Proc. of 22nd IEEE Conf. on Decision and control , San Antonio, Texas, pp. 286-290, Dec. 1983.

13. J.S. Gibson and F. Jabbari, "An ARMA Model For a Class of Distributed Systems", Proc. of 23rd CDC, Las Vegas, Nevade, pp. 1171-1175, Dec. 1984.

14. D.G. Luenberger, Optimization by Vector Space Methods, John Wiley, 1969.

15. F. Jabbari, "Lattice Filters and Adaptive Identification of Flexible Structures", Ph.D. Dissertation, Dept. of Mech., Aero. and Nucl. Engr., University of California, Los Angeles, 1986.

16. B. Friedlander, "Lattice Implementation of Some Recursive Parameter Estimation Algorithms", Int. J. of Control , vol. 37, pp. 661-681, 1983.

17. D.T.L. Lee, "System Order Estimation of ARMA Models by Ladder Canonical Forms", Proc. of ACC, pp. 1002-1007, 1983.

ADAPTIVE IDENTIFICATION OF FLEXIBLE STRUCTURES BY LATTICE FILTERS

Faryar Jabbari
Mechanical Engineering Department
University of California, Irvine 92717

J.S. Gibson [1]
Mechanical, Aerospace and Nuclear Engineering Department
University of California, Los Angeles 90024

Abstract

In this paper, we present our recent investigations on lattice filters and their applications to adaptive identification of flexible structures. Since the order of the systems can not be known –or the effective order may change– the order recursiveness of the lattices is of particular interest. Implementation of lattices would permit on-line order determination and would allow the order of the filter to be changed without the need to reprocess the previous data. Experimental data from the flexible grid structure at NASA-Langley are used to obtain results showing the feasibility of lattices and the advantages that result from their order recursive property. One-step-ahead prediction and estimates for natural frequencies are among the results shown. Of particular interest are the frequency estimates which agree closely with the frequency estimates obtained from off-line identification techniques. The one step-ahead-prediction results also show the advantages that lattices provide with their order-determination capability, which would be significant for adaptive control purposes.

1. Introduction

Adaptive identification of flexible systems is receiving increasing attention. Since flexible systems are often modeled as distributed systems, they provide major practical and theoretical challenges to the control community. Insufficient model fidelity, poor knowledge of structural damping, and the lack of feasibility for ground testing for many of the large space structures are some of the contributing factors to the recent interest in adaptive identification of these systems. Determination of an effective system order is one of the most important problems, since there is no fixed order that can be assigned to these systems a priori.

Recently, lattice filters are being studied for adaptive identification of flexible structures because they can identify the effective plant order as well as the parameters for the digital input/output model of a structure. The time-update equations needed for adaptive filtering were developed by Lee, Morf, and Freidlander who studied the applications of lattices to speech processing and adaptive control, see [LMF,LFM] among many.

Montgomery, Sundararajan [in SM1,SM2] and Wiberg [W1] were first to apply lattices to identification of flexible structures. Montgomery, et. al., have been using a variety of techniques –such as Discrete Fourier Tranforms– for the identication of these structures while the lattices were relied upon mostly for order determination. Wiberg has been emphasizing mainly the frequency estimation based on the free response (zero input) of the system. In our research [JG1,J1], we have expanded the scope and developed new approaches in the application of lattice filters for adaptive identification of flexible systems. Our approach uses the lattice filters as the only identification tool required. We also seek frequency (and damping ratio) estimates for a variety of input sequences with the eventual goal of adaptive control.

In this paper, we present results obtained from the application of lattice filters to the NASA-Langley grid, a flexible experimental structure used in research on control and identification of space structures. These results demonstrate the feasibility of lattice filters for on-line identification – and eventually adaptive control – of flexible structures.

2. State-space and ARMA representations

For numerical work, the linear motions of flexible structures are approximated by a finite dimensional differential equation of the form

$$\begin{cases} \dot{x}(t) = Ax(t) + B_c u(t) \\ y(t) = Cx(t) \end{cases} \tag{2.1}$$

where y is the output (measurements), u the input, etc. The discrete-time form of the above equation has the following well known representation:

$$\begin{cases} x(t+1) = Tx(t) + B_d u(t) \\ y(t) = Cx(t) \end{cases} \tag{2.2}$$

For digital adaptive control and identification, the input - output representation corresponding to (2.2) usually is used. This alternative representation is

$$y(t) = \sum_{i=1}^{N} a_i\, y(t-1) \; + \; \sum_{i=1}^{N} b_i\, u(t-i) \tag{2.3}$$

[1] This author was supported by AFOSR grant 840309

and is called an ARMA (Auto Regressive Moving Average) model.

Mass and stiffness properties of a system are, traditionally speaking, obtained from finite element analysis and extensive ground testing. The matrices in equations (2.1, 2.2) could then be formed by the standard methods. This approach, as mentioned in the previous section, is becoming less and less desirable, due to the properties and requirements associated with the modern applications of flexible systems.

Because of the difficulties associated with the identification of the matrices in (2.1) and (2.2) – such as the number of parameters involved and the lack of uniqueness – the ARMA representation of (2.3) is more useful for adaptive identification and control. In addition to the small number of parameters involved, this model uses only the measured inputs and outputs of the system (the state need not be estimated) and it can be used for a variety of adaptive control algorithms (see [GS1] among many). Furthermore, the AR coefficients contain the necessary information for natural frequency (and damping) determination. This can be seen easily by considering the single-input-single- output (SISO) case. There, the AR coefficients are the same as the coefficients of the characteristic polynomial of the state transition matrix of equation (2.2) (for details see [JG1 and C1]). In [JG1, J1] we have presented methods that extends this directly to the MIMO case, as well.

Adaptive (on-line) identification of these ARMA models has been studied extensively by many authors, see [LS1, GS1] for example. In most cases, however, the order of the system is assumed to be known and fixed. Such assumptions, clearly, are not applicable to the flexible systems of interest. Lattice filters, introduced in the next section, have the capability to identify the required parameters without such assumptions and can actually estimate the effective order of the system as well.

3. Adaptive Identification Using Lattice Filters

The most common method for the on-line estimation of the ARMA coefficients is the recursive least-squares algorithm. In most applications, the fact that N is finite is not a serious limitation because the dynamic behavior of the system can be approximated by the behavior of a finite dimensional approximation to the system. For flexible structures, which theoretically speaking are infinite dimensional, it is quite common to use an approximation model based on the few of the modes that are highly excited. The real problem is that, in the classical recursive least-squares algorithms, N must be fixed. Depending on the initial conditions and external excitation, the order of the finite dimensional model required to approximate the response of the system accurately can vary widely.

The least-squares lattice addresses this issue directly by providing an algorithm that can be variable-order. A lattice filter algorithm of order n, being recursive in time as well as order, results in filters of order one to n and allows the maximum order of the filter (n) to be increased gradually, without reprocessing of the previous data. Since all intermediate order filters are automatically obtained, *the effective order of the system can be estimated* so that the most appropriate set of coefficients (corresponding to the best estimated order) are used.

For n = 0 to t-1 :

$$K_{n+1}(t) = \lambda K_{n+1}(t-1) + e_n^T(t) G_n^{-1}(t-1) r_n(t-1)$$

$$G_{n+1}(t) = G_n(t) - r_n(t) R_n^{-r}(t) r_n^T(t) \qquad n = 0,1,2 \ldots$$

$$e_{n+1}(t) = e_n(t) - r_n(t-1) R_n^{-r}(t-1) K_{n+1}^T(t)$$

$$r_{n+1}(t) = r_n(t-1) - e_n(t) R_n^{-e}(t) K_{n+1}(t)$$

$$R_{n+1}^s(t) = R_n^e(t) - K_{n+1}(t) R_n^{-r}(t-1) K_{n+1}^T(t)$$

$$R_{n+1}^r(t) = R_n^r(t-1) - K_{n+1}^T(t) R_n^{-e}(t) K_{n+1}(t)$$

Table 1: The Residual Error Filter Algorithm

The order determination capability of lattices is the major reason for our interest. It should be noted, however, that other important features of lattices are their numerical stability [LL1] and their potential for VLSI implementation due to their special structure which consists of many similar modules.

In [JG1,J1], we have developed a novel derivation of the lattices that has two important features. The first one is the basic framework used, which lends itself nicely to some of the more theoretical aspects of these flexible systems. The second feature is the extension of the lattices to the case of many measurement channels (where each channel may contain many scalar measurements). This feature can be exploited easily to extend the many desirable properties of the SISO ARMA models to the MIMO systems and hence improve the estimates for the system natural frequencies, see [JG1,J1] for more detail.

The residual-error lattice algorithm is listed in Table 1. This algorithm must be performed at each time step to update the filter variables. The variable $R^e(t)$ is one of the crucial variables and is used to help determine the effective order of the system. Due to space limitation, the discussion concerning this issue is omitted. For details regarding the initialization and definitions of other variables see [JG1,J1].

The algorithm in Table 1, as mentioned before, calculates the residual error; i.e., the portion of the output y(t) that can not be fitted in a model based on all of the data including y(t). A more useful approach (for prediction and

For $n = 1, t-1$

For $i = 1, n$

$$C_{n+1,i}(t) = C_{n,i}(t) - B_{n,i}(t)\, R_n^{-r}(t)\, r_n^T(t)$$

$$B_{n+1,i+1}(t) = [\, B_{n,i}(t) - C_{n,i}(t)\, G_n^{-1}(t)\, r_n(t)\,] - A_{n,i}(t)\, R_n^{-e}(t)\, K_{n+1}(t)$$

$$A_{n+1,i}(t) = A_{n,i}(t) - [\, B_{n,i}(t) - C_{n,i}(t)\, G_n^{-1}(t)\, r_n(t)\,]\; R_n^{-r}(t-1)\, K_{n+1}^T(t)$$

Table 2: AR Coefficients Algorithm

eventually control purposes) would be the prediction error filter. By prediction error we mean the error between y(t) and its estimate using the data up to time (t-1). Simple modification of the above algorithm would yield a filter that calculates the prediction error (and eliminates the inversion of the G matrix in the process). Also, simple application of the matrix inversion formulas results in the elimination of another inversion (preferably R^r) and thus reduce the total number of inversions to one for each time step. Again, we omit the details for the sake of brevity. The prediction error lattice algorithm would be quite similar to the residual algorithm. Four of the above equations have to be modified as the following (with $\tilde{e}$ and $\tilde{r}$ as the prediction errors) :

$$K_{n+1}(t) = \lambda\; K_{n+1}(t-1) + \tilde{e}_n(t)\; G_n(t-1)\; \tilde{r}_n(t-1)$$

$$G_{n+1}(t) = G_n(t) + G_n(t)\; \tilde{r}_n(t)\; R_n^{-r}(t-1)\; \tilde{r}_n(t)\; G_n(t)$$

$$\tilde{e}_{n+1}(t) = \tilde{e}_n(t) - \tilde{r}_n(t-1)\; R_n^{-r}(t-2)\; K_{n+1}^T(t-1)$$

$$\tilde{r}_{n+1}(t) = \tilde{r}_n(t-1) - \tilde{e}_n(t)\; R_n^{-e}(t-1)\; K_{n+1}(t-1)$$

Table 2 consists of the algorithm that generates the ARMA coefficients for any desired order. For this, the ARMA of (2.3) is first converted to a two-channel AR form (using a simple embedding). This part is presented separately to underscore the point that these coefficients need not be updated at every time step. Rather, this algorithm is invoked at any time (and for any order) desired to generate the ARMA coefficients and will be turned off at other times.

Other technical issues (such as the required embedding, the reduced lattice structure to determine the input for the control applications, etc.) are discussed in [J1].

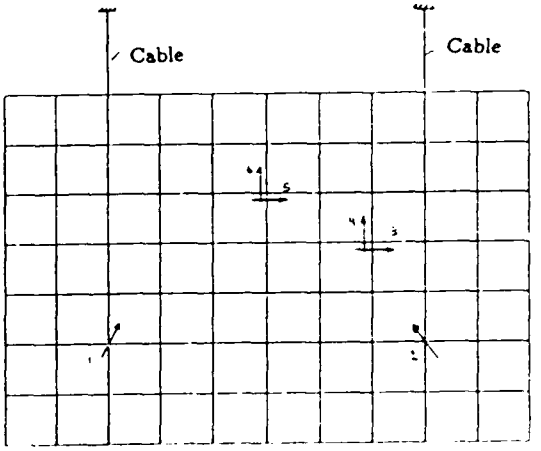

Figure 1: The Grid Schematic

4. The NASA-Langley Grid

This grid is an experimental structure at the NASA-Langley Research Center in Hampton, Virginia, designed for research on identification and control of flexible space structures. It is a 7 ft by 10 ft planar structure made of thin, flat aluminum bars with uniform spacing (8 vertical and 11 horizontal bars). The grid is suspended from the ceiling by two cables as shown in the schematic of Figure 1. Rate gyros are used to measure the rotational rate about an axis in the plane of the grid and the actuators are reaction wheels. The position of the actuators and sensors are marked on the diagram below.

This structure has been studied extensively by Montgomery, et al, [MWLN,SM1]. Sine wave sweeps have been used to determine the structural natural frequencies and the results show that the grid has as many as twenty modes below the frequency of 10 Hz. These closely packed natural frequencies (and their corresponding low damping ratios) are the main reasons for our interest in this structure for our research in adaptive identification and control of flexible systems.

5. Experimental Results

In this section, we present some of the results obtained from the grid by the lattice filter algorithms listed above. All of he results presented here are obtained from two test runs. In the first case the input consists of a sine-wave with a varying frequency. The second case has a square-wave as the input and is used to excite numerous modes of the structure. In each case, the aim is to identify the most important natural frequencies (and their corresponding damping) and study the behavior of the prediction error for different filter orders.

Figure 2 is a sample of the sensor measurements for the case of square input. The top plot is the first sensor, the second plot corresponds to sensor number 2, etc. It is clear that, although all sensors have certain amount of

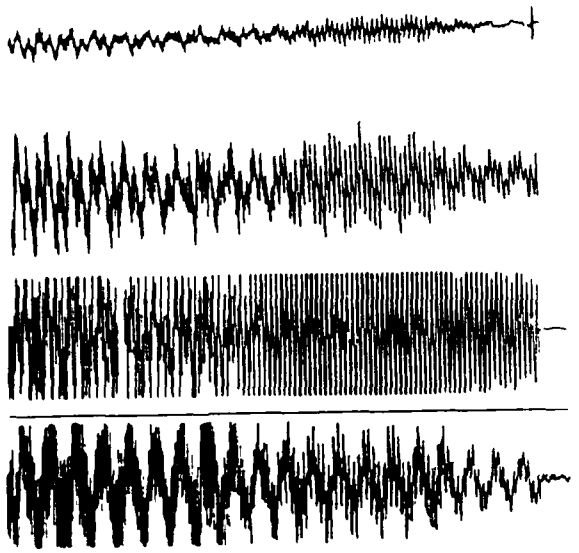

Figure 2: Sample of Sensor Measurements: Sensors 1-4

noise, sensor four is quite noisy and sensor three seems to be saturated most of the time. Overall, sensor two has the best measurements.

The first set of results concern the prediction error and its behavior as the order of the filter increases. Since most of the available adaptive control algorithm are based on some prediction for the future outputs (one or more steps ahead), this study is the first step toward the eventual adaptive control of these systems. Figue 4 shows the actual outputs (the first graph) and the (one step ahead) predicted value of the output for different order filters. The saw-tooth curve around the horizontal axis is the actual prediction error for that order filter. The error is plotted on the same scale so that it can be compared with the actual prediction. Also note the drop in the average magnitude of the error, as the filter order is increased.

As these graphs show, the general shape of the response (correponding to the dominant modes) is identified and predicted by relatively low order lattices. The high frequency content of the signal, however, requires filters of significantly larger order. This is evident in the peaks of the signal where the high frequencies are more distinguishable. The next graph (Figue 5) is the magnified version of Figure 4. There, the behavior of the prediction (and the corresponding error) is underscored more clearly.

Next, we will summarize some of results regarding the natural frequency estimates of the system. We have chosen to present the results from the case of sinewave input. The results obtained from this case show that the dominant frequencies can be identified with inputs that are not sufficiently rich to excite all of the frequencies (in the sense of [GS1,LS1]). Also, a few interesting issues that arise due to the specific nature of the input signal can be discussed. The frequency of the input sinewave was increased gradually according to Figure 3 (this graph was obtained from a simple single channel lattice).

All four sensors see these frequencies for both inputs.

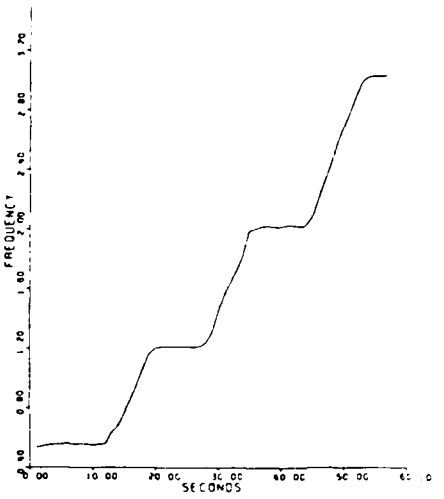

Figure 3: Frequency of Input Signal as Identified by Lattice

Naturally, the noisy sensor (four) gives the worst estimates and, in one exceptional case, can not identify one of the low modes. In all of our studies we have seen, consistently, that for a given input sequence and sensor, high order filters are needed to identify the frequency while good prediction can be obtained from much lower order lattices. The results below are all obtained from a lattice filter of order 48 using the sensor-two measurements.

Estimating the damping ratios is another topic of interest. The structure is widely believed to have non-linear, vibration-level dependent damping. The results here show that although a linear (and proportional) damping model does not fit the data, an approximate model with such properties would have the expected damping levels. Also, it was observed consistently that the quare wave input (which caused substantial vibration in the grid) results in higher damping for the modes of the structure.

Three sets of natural frequencies are identified. The first set is a group of three low frequencies (including the dominant one around .56 Hz). The behavior of these modes –the third one in particular– is quite interesting. The second and third modes are not quite identified by the lattice at the beginning. Once these modes receive substantial excitation (i.e., when the input frequency is close to the natural frequencies), the lattice results in good estimates for them. This can be seen by a simple comparison of the input frequencies (Figure 3) and the natural frequencies (Figure 6). Also the behavior of the damping ratio estimates is presented for one of the modes which is representative of the rest.

The second set of frequencies are those which the higher modes which are not as highly excited as the first three frequencies and require large order filters (generally speaking). Figure 7 shows the first three of these modes.

The third set of modes are a group of high frequency modes which have extremely low damping (typically less than one percent critical) which are present in all cases and are identified very quickly. Further investigation of

still data (i.e., data obtained when the structure is not vibrating) indicates that these modes are from the sensors and not from the structure, since all these modes were present when the sensors were observing the still grid. The plots in Figure 8 show the behavior of three of these modes.

6. Concluding Remarks

In this paper, we have investigated the application of lattice filters to the identification of flexible structures. The primary advantage of lattices, for such applications, is the flexibility they offer with respect to the system order. By being order recursive, lattices can be used to estimate an effective order for the system and, consequently, to change the order of the filter, on-line, without any loss of data. Experimental data from the NASA-Langley grid was used to show some of the results obtained. The behavior of the prediction for different order filters and the corresponding estimates for the system natural frequencies all point to the advantages that lattices provide for the on-line parameter identifiction of flexible structures.

The natural frequency estimates shown here agree with those obtained at NASA-Langley, see [MWLN], by using extensive off-line techniques. The following table shows a simple comparisons between [MWLN] and the results obtained here; i.e., [JG].

MWLN	JG
.3695	***
.58	.560
1.046	***
1.420	1.37
2.128	2.07

The lowest mode, at .3695 Hz, is the rigid body mode due to the cables connecting the grid to the ceiling. Since this mode was not excited in the experiments that data for this paper was collected from, this mode is not identified here. The third mode, at 1.046 Hz, has nodes at the sensor locations that were used here. This mode, therefore, could not be identified with the sensors used for the data presented here.

The accuracy of the results obtained here (less that 5% variation in frequencies shown above, for example) is indicative of the potential new applications of lattices for on-line identification (and adaptive control of) of flexible structures. We are currently investigating using white noise as the input (to excite all modes) and tracking of the changes in the parameters when the mass properties of the structure are altered singnificantly. Preliminary results have been quite encouraging. Such results will be presented in other publications in the near future.

References

C1— Chen, C.T., Linear System Theory and Design, HRW, 1984.

GS1- Goodwin, G.C., Sin, K.S., Adaptive Filtering, Prediction and Control, Prentice-Hall, 1984.

J1— Jabbari, F. "Lattice Filters and Adaptive Identification and of Flexible Structures". Ph.D. Dissertation, Dept. of Mech., Aero. and Nucl. Engr., UCLA, 1986.

JG1- Jabbari, F., Gibson, J.S., "Vector-Channel Lattice Filters And Identification of Flexible Structures", Submitted for publication.

LFM- Lee, D.T.L., Freidlander, B., Morf, M., "Recursive Ladder Algorithms For ARMA Modeling", IEEE Trans. on Automatic Control, Aug. 1981, pp 753-764.

LL1- Ljung, S., Ljung, L., "Error Propogation of Recursive Least-Squares Adaptation Algorithms", Automatica, vol 21, 1985, pp 157-167.

LMF Lee, D.T.L., Morf, M., Friedlander, B., "Recursive Least Squares Ladder Estimation Algorithms", IEEE Trans. on ASSP, June 1981, pp 627-641.

LS1- Ljung, L., Soderstrom, T., Theroy and Practice of Recursive Identification, The MIT Press, 1983.

MWLN Montgomery, R., C., Williams, J.P., Lazarus, T.L., Nelson, P.E., "Control Effectiveness Characterization For State Estimation And Control on A Highly Flexible Grid", AIAA Conference on Guidance, Navigation and Control, Williamsburg, VA, Aug. 1986.

SM1- Sundararajan, N., Montgomery, R.C., "Identification of Structural Dynamics Systems Using Least Squares Lattice Filters", AIAA J. Guidance, Control and Dynamics, vol 6, 1983, pp 374-381.

SM2- Sundararajan, N., Montgomery, R.C., "Adaptive Modal Control of Structural Dynamics Systems Using Recursive Lattice Filters", AIAA J. of Guidance, Control and Dynamics, vol 8, 1985, pp 223-229.

W1— Wiberg, D.M., "Frequencies of Vibration Estimated by Lattice", J. of Astro. Sciences, vol 33, 1985, pp 35-47.

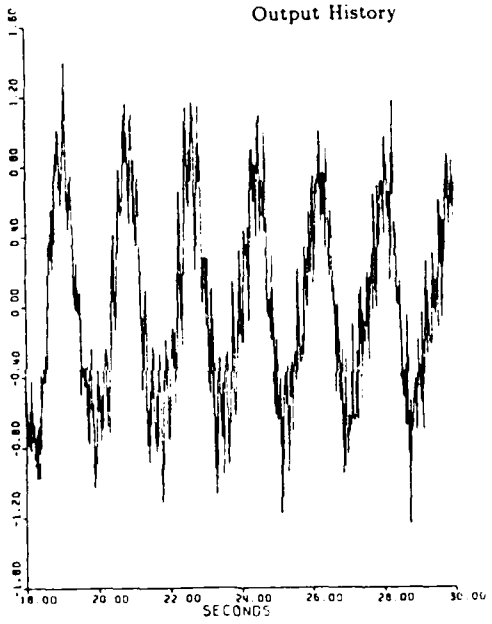

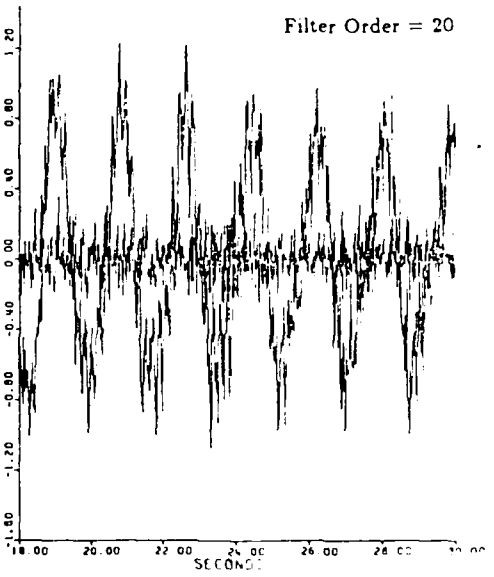

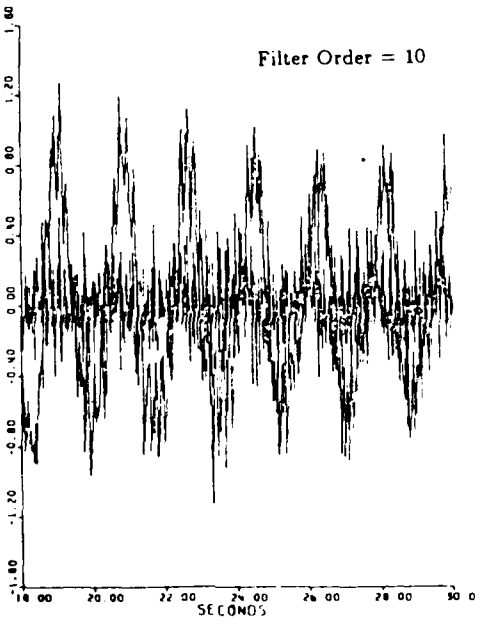

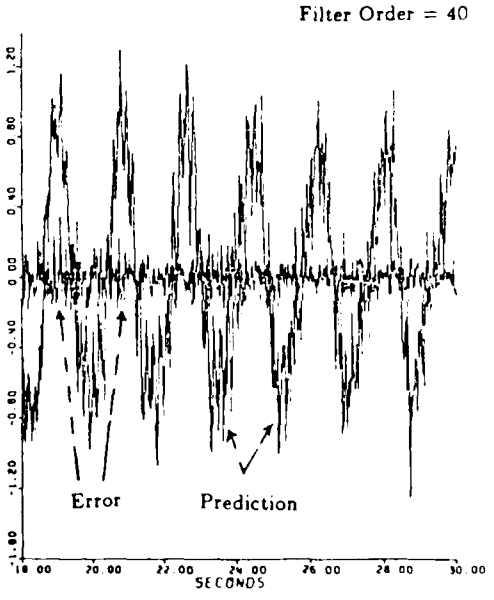

Figure 4: The Output and Prediction for Different Order Filters

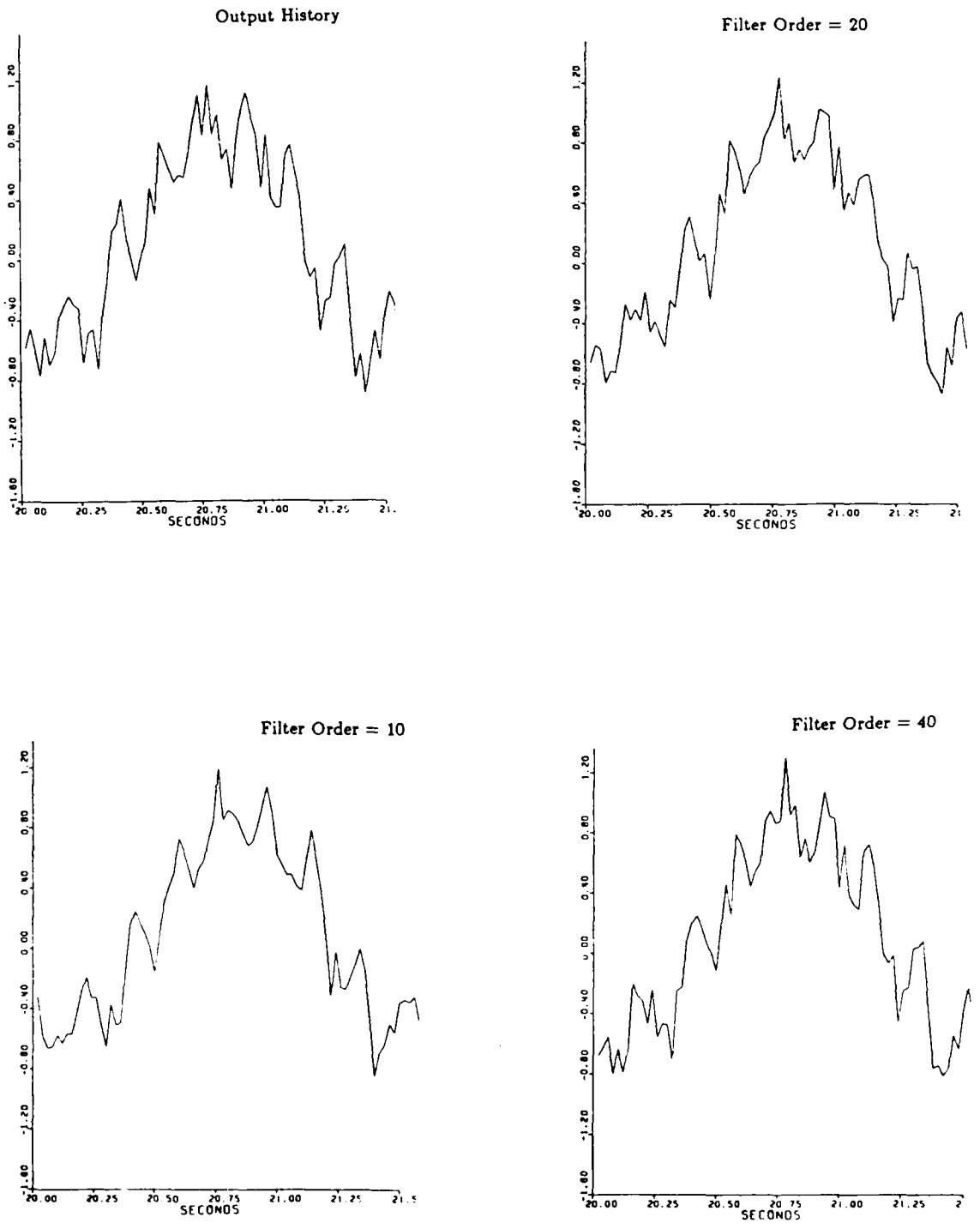

Figure 5: The Output and Prediction for Different Order Filters(Magnified)

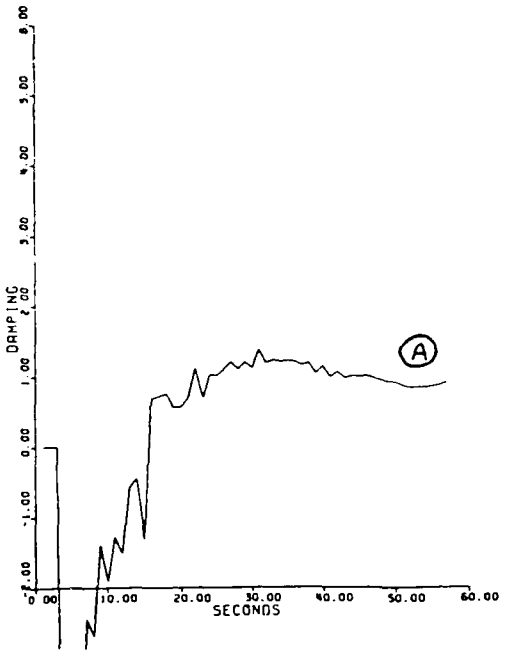

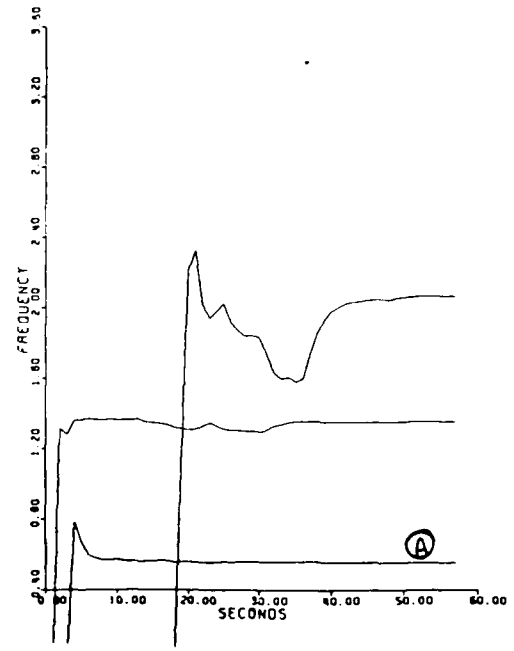

Figure 6: Sample of Low Frequencies and Damping Ratio (% critical) as Identified by Lattice

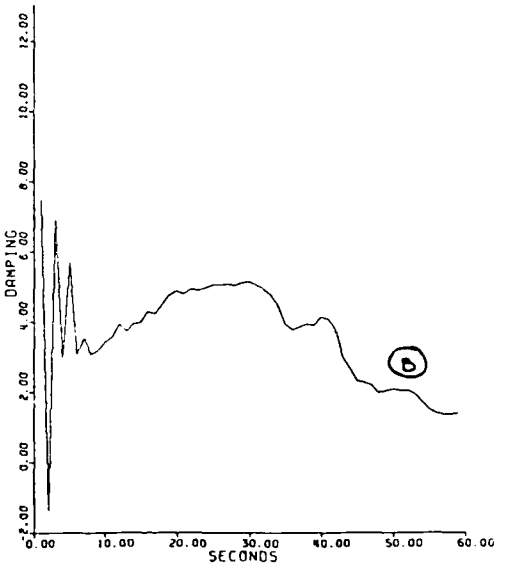

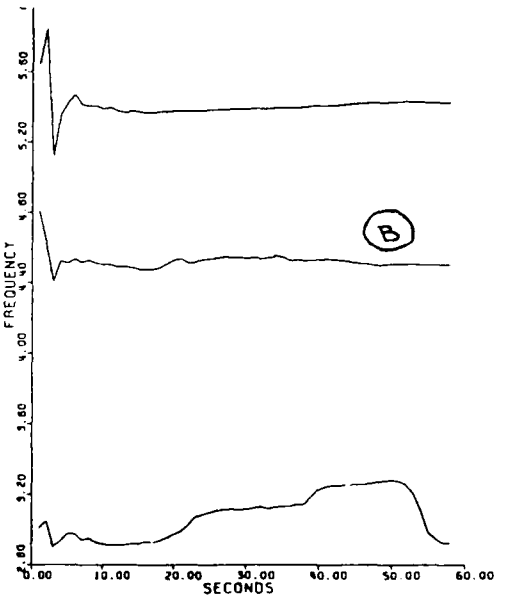

Figure 7: Sample of Intermediate Frequencies and Damping Ratio (% critical) as Identified by Lattice

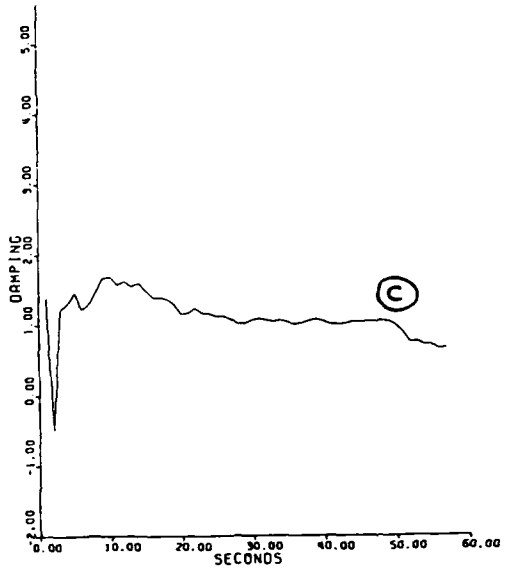

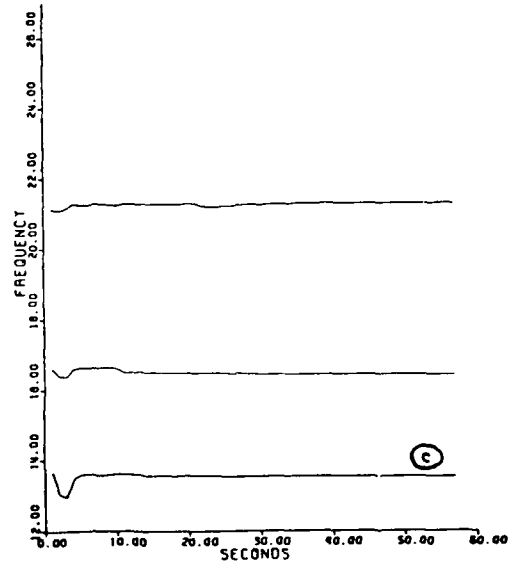

Figure 8: Sample of High Frequencies and Damping Ratio (% critical) as Identified by Lattice

END
DATE
FILMED
4-88
DTIC